Mechanical and Biologic Impact of Dynamic Loading on Bovine and Human Models of Osteoarthritis

by

Hannah Jacqueline Szapary

B.S. Applied Mathematics – Biology, Classics
Brown University, 2019

Submitted to the Department of Mechanical Engineering in Partial Fulfillment of the Requirements for the Degree of

Master of Science in Mechanical Engineering

at the

Massachusetts Institute of Technology

May 2022

Signature of Author: _____
Department of Mechanical Engineering
May 10, 2022

Certified by: _____
Alan J. Grodzinsky
Professor of Biological, Electrical and Mechanical Engineering
Thesis Advisor

Accepted by: _____
Nicolas Hadjiconstantinou
Professor of Mechanical Engineering
Graduate Officer

Mechanical and Biologic Impact of Dynamic Loading on Bovine and Human Models of Osteoarthritis

by
Hannah Jacqueline Szapary

Submitted to the Department of Mechanical Engineering on May 10, 2022 in Partial Fulfillment of the Requirements for the Degree of Master of Science in Mechanical Engineering

ABSTRACT

Both dexamethasone (Dex) and Insulin-like growth factor 1 (IGF-1) have shown promise as disease-modifying therapeutics for osteoarthritis (OA), a disease characterized by cartilage degradation. Additionally, dynamic loading has been demonstrated to affect chondrocyte metabolic activity, with mechanical stimuli acting as a therapeutic at specific amplitudes and frequencies. The goal of this thesis was to investigate the potential of these therapeutics and loading to be synergistic in preventing post-traumatic osteoarthritis (PTOA) disease initiation (e.g., after a traumatic joint injury) and in ameliorating progression of OA. We hypothesized that Dex and IGF-1 could help to maintain the mechanical properties and biochemical composition of cartilage in human osteochondral tissues when treated with exogenous inflammatory cytokines.

Bovine knee cartilage and human ankle cartilage-bone explants were used *in vitro* with a cytokine challenged to mimic an OA disease state. A load-controlled dynamic loading protocol was modeled after a physiologically relevant rehabilitation program and was tested in healthy tissue to optimize the applied stress magnitude and loading duration. The optimized protocol was then used for 7 days duration (at 0.33 Hz, 40% duty cycle for 1 hour per day) +/- Dex and IGF-1 to evaluate biochemical changes on the protein and gene expression levels. Stress-relaxation testing was utilized to calculate mechanical properties of human cartilage, both before and after one 1-hour loading session, at baseline and after treatment with cytokines and Dex.

It was found that a load-controlled protocol could mimic exercise with total strain in a physiologically relevant range. Loading after 7 days also increased the effects of Dex and IGF-1 on cell viability, and further increased GAG biosynthesis and decreased GAG loss seen with Dex alone. Notably, in human tissue there was donor-to-donor variability in this response to both loading on its own, and to Dex/IGF-1 with and without loading. While Dex preserved cell viability and decreased GAG loss and NO release from cartilage explants treated with cytokines, Dex did not alter mechanical properties (before or after loading) after 10 days. However, there was variation in these values between donor age groups at baseline. Taken together, these results suggest that a rehabilitative loading therapy in combination with Dex/IGF-1 could enhance certain disease-modifying effects of each of the two drugs, and that inherent tissue variability (between patients) could contribute to individual variation in responses and thus emphasize the need for a personalized medicine approach.

Thesis Supervisor: Alan J. Grodzinsky
Title: Professor of Biological, Electrical and Mechanical Engineering

ACKNOWLEDGEMENTS

I feel incredibly grateful for the people who I have met during my time at MIT over the past three years. My advisor, Al Grodzinsky, has been an incredible role model, as both a scientist and person. The way Al brings people together to solve scientific problems as a collaborative effort is inspiring. His expansive knowledge of the field, amazing teaching skills, and enthusiasm for solving hard questions has made him a well-loved leader. From lab lunches during the week to weekend experiments during winter snowstorms, he has never failed to make working hard a fun experience. He sets a wonderful tone for the lab, and I am so lucky to have been one of his final students.

Within the lab, I am indebted to Lisa Flaman, who trained me during my first year and continued to be a great help for my later experiments. Lisa works extremely hard, and I am very grateful for her support and laughs during the scientific process. Rebecca Black has worked alongside me for the past three years, and is an incredible scientist who has become my role model and friend. I would not have learned nearly as much without her presence, and her support, whether it be long conversations, walks across campus for coffee, or experimental advice in the lab, has been unbelieveable. I am also very thankful for the help received from other members of the lab, including Garima Dwivedi, Eliot Frank, Han-Hwa Hung, and Linda Bragman. They have all made the Grodzinsky lab a very fun and stimulating place to do science.

Outside of the lab, I am very thankful for the support of both of my programs, MechE and HST. Though I started out as an HST student, the MechE department allowed me to continue my research while diving deeper into engineering coursework, and this year has made me a much more independent scientist and budding engineer. I look forward to rejoining the HST community with these new skills and knowledge in my toolbox.

Finally, I am extremely fortunate to have wonderful friends and family who have supported me through everything. From daily phone conversations to weekend hikes, their love and endless laughs have made me happy, even after the longest days. I cannot imagine having gone through this journey without them.

TABLE OF CONTENTS

GLOSSARY

C-B MPS = Cartilage-bone microphysiological system
COX-2 = Cyclooxygenase-2
CYT = Cytokines
DAMP = Damage-associate molecular pattern
Dex = Dexamethasone
DMARDS = Disease modifying anti-rheumatic drugs
DMEM = Dulbecco's Modified Eagle Medium
DMMB = 1,9-Dimethylmethylene blue
DMOADS = Disease-modifying OA drugs
ECM = Extracellular matrix
E_d = Dynamic stiffness
ELISA = Enzyme-linked immunosorbent assay
EULAR = European League Against Rheumatism
E_y = Compressive equilibrium modulus
GAG = Glycosaminoglycan
GC = Glucocorticoid
IGF-1 = Insulin-like growth factor-1
IL = Interleukin
K_p = Hydraulic permeability
LGCCM = Low glucose complete control media
MMP = Matrix metalloproteinases
NO = Nitric oxide
NSAID = Non-steroidal anti-inflammatory drugs
OA = Osteoarthritis
PBS = Phosphate-buffered saline
PTOA = Post-traumatic osteoarthritis
TKA = Total knee arthroplasty
TNFα = Tumor necrosis factor α

LIST OF FIGURES

LIST OF TABLES

1 INTRODUCTION

1.1 Problem Statement

Osteoarthritis (OA) is a debilitating disease of the entire joint, eventually affecting all of its tissue components.[1,2] This complex process affects hundreds of millions of people worldwide, leading to loss of joint function and a reduction in quality of life - specific subtypes of OA accompany varying risk factors that mediate OA initiation and progression.[3,4] Post-traumatic OA (PTOA), which develops after joint injury, accounts for 12% of the total OA population, and is particularly encumbering with an earlier onset than traditional OA and a manifestation in the young and more active.[5] It has been reported that 50 to 80% of young active individuals who suffer joint injuries (e.g., tears of the anterior cruciate ligament or meniscus) progress to PTOA within 10 to 20 years.[6-8] Within 24 hours of an acute joint injury, inflammatory cytokines (e.g., IL-1, IL-6 and TNFα) primarily secreted by the synovial membrane into the synovial fluid can diffuse into cartilage and rapidly initiate proteolysis and cartilage matrix degradation and loss.[9,10] With this, degradation and loss of subchondral bone may occur, exacerbating progression of disease, and by the time of clinical (radiographic) diagnosis of PTOA, irreversible changes to these tissues have occurred. However, an understanding of this systematic progression timeline allows for the chance to prevent PTOA development after injury.[7]

While disease modifying anti-rheumatic drugs (DMARDS) for rheumatoid arthritis and related rheumatic diseases exist, there are no efficacious disease-modifying OA drugs (DMOADS) available, and current therapies only provide short term pain and inflammation relief.[1,11] Short-term therapeutics, such as non-steroidal anti-inflammatory drugs (NSAIDs), corticosteroids and hyaluronic acid, do not protect against further cartilage degeneration, the hallmark of end stage OA that necessitates joint replacement.[9,12] However, the potent synthetic glucocorticoid dexamethasone (Dex), which is typically used for pain management in OA patients and is given as an intra-articular injection into the joint, has shown promise as a preventative therapy. Previous work has shown that low dose Dex is chondroprotective in animal models of OA with anti-catabolic effects, inhibiting cytokine induced matrix loss and cell death via glucocorticoid receptor pathways.[13-16] More recently, studies using a combination of the anti-catabolic drug Dex

with insulin-like growth factor-1 (IGF-1), a pro-anabolic growth factor that upregulates cartilage matrix synthesis, have suggested that using both Dex and IGF-1 together has greater benefits than each molecule by itself in preventing cartilage degradation in disease.[17]

Separate from pharmacologic therapy, dynamic loading has been studied as a potential modulator of chondrocyte metabolic activity. In cell culture, loading can alleviate chondrocyte catabolic responses to inflammatory cytokines, and in normal bovine cartilage explants, loading can enhance matrix biosynthesis and increase drug transport into tissue, depending strongly on the frequency, amplitude and duty cycle of compressions.[18-23] Mechanically, stimulation of chondrocyte-mediated biosynthesis has been localized to regions of high interstitial fluid flow induced by compression, with signal transduction pathways involving MAPK activation, cyclic AMP, and intracellular calcium.[24-28] However, these chondroprotective effects have a limit - in bovine models of OA, it has been shown that moderate dynamic compression, modeled directly after the amplitudes and duty cycles of *in vivo* human patient studies, can inhibit bovine cartilage degradation and TNFα/IL-6 release in explants up until a particular dynamic strain threshold.[29-31] Further, studies in mouse, human, and bovine cartilage models demonstrate that dynamic loads can change mechanical properties of cartilage after a single loading session, impacting the tissue's ability to support future loading within the range representing daily joint motion.[32,33] Thus, loading has structural effects that are just as important to disease progression as its biological impacts.

Taken together, these studies suggest that a combination of pharmacologic molecules and dynamic compression within a rehabilitative range could maximize therapeutic action in preventing cartilage degradation and even promoting anabolism in OA development. While much work has been done on the effects of compression and Dex/IGF-1 separately, most of this research has been conducted on bovine tissue rather than human, and little is known about the impact these therapies have together, at a physiologically relevant compression frequency that represents realistic exercise regimens. Understanding whether an optimized mechanical joint loading protocol has pro-anabolic, anti-catabolic, and/or

structural effects on osteochondral tissues could greatly help clinicians integrate rehabilitation exercises with drug therapy in preventing OA disease progression.

1.2 Specific Aims

The primary aim of this work was both to determine the loading stress and frequency that best mimics a physiologically relevant rehabilitation program in healthy cartilage, and to test the biologic effects of the molecules dexamethasone and Insulin-like growth factor-1 in an OA disease model. Further, this work sought to assess the effects of Dex on human cartilage mechanical properties in the disease model for different donors, to better understand the variability at baseline and in response to treatments that may contribute to individual-dependent responses to dynamic loading.

1.3 Scope of Report

The first set of experiments addressed the need to optimize a loading protocol by testing loading magnitudes over 2 days from 100 kPa to 1 MPa on human osteochondral plugs (25 kPa to 200 kPa in bovine chondral explants), which reflects the load range experienced by articular cartilage in daily activities[34,35], keeping the duration and frequency of loading constant. For human experiments, osteochondral plugs were harvested from the condyles/trochlear grooves and talar dome of cadaveric human distal femurs and ankles, respectively, while chondral plugs were harvested from the femoropatellar grooves of 1-2 week old calves for bovine experiments. This study also assessed the impact of loading duration (1 vs. 2 one-hour sessions a day) over 7 days.

Additional experiments utilized an osteochondral (cartilage-bone) microphysiological system (CB MPS) that simulates the human joint response to injury and inflammation and early phases of progression to PTOA.[36] Osteochondral and chondral plugs were subjected to the cytokines TNFα, IL-6 and IL-6R, and either were unloaded or underwent a loading program for 7 days that accurately models physiologic rehabilitation established with the first aim. This protocol was approximately a 1-hour session per day that includes 6 repeats of 4 sets of 8 compressions at a frequency of 0.33 Hz, with 1 minute of rest between sets and 5 minutes of rest between repeats. Both loaded and unloaded plugs were also subjected

to treatments with dexamethasone and Insulin-like growth factor-1. Biologic metrics were obtained at the end of 7 days, assess cell viability, cartilage glycosaminoglycan (GAG) loss and biosynthesis, collagen content, and inflammatory cytokine and nitric oxide (NO) release.

Finally, the structural changes in human osteochondral plugs after 10 days with cytokines or cytokines with dexamethasone were evaluated with biomechanical assessment of transient stress-relaxation testing and dynamic loading, both before and after one 1-hour loading session. For testing, cylindrical disks of cartilage were loaded with unconfined compression to ramps of a specified strain over time, while continuously collecting stress measurements. Exponential curves were fit to this data in order to determine the mechanical properties of cartilage. Sinusoidal tests were then carried out over a frequency range of 0.005 to 2 Hz, using a previously published protocol.[34] These experiments attempted to assess the variability of biomechanical properties between donors at baseline, in a disease state alone and with drug treatment, both before and after a session of cyclic loading.

1.4 Summary of Results

Experiments that optimized a loading protocol tested different physiologically relevant dynamic loading amplitudes (25 – 200 kPa for bovine tissue, 100 kPa – 1 MPa for human tissue) on both bovine cartilage and human cartilage-bone explants, in a polysulfone chamber within an incubator-housed compression apparatus. Load-controlled compression successfully imitated exercise with total strain in a physiologically relevant range found in human patient studies (15-30%). Studies looking at loading duration (1 vs. 2 one-hour sessions per day) on human tissue demonstrated no differences between these time-scales. For further experiments, the optimized protocol was used (at 0.33 Hz for 1 hour per day), and bovine and human tissue subjected to cytokines and Dex/IGF-1 were either loaded or allowed to free-swell for 7 days. Loading increased the effects of Dex and IGF-1 on cell viability, and further increased GAG biosynthesis and decreased GAG loss seen with Dex in the disease model, with donor variability in responses in human tissue.

Stress-relaxation and sinusoidal testing (in unconfined compression) was used to calculate equilibrium compressive modulus (E_y), dynamic stiffness (E_d) and hydraulic permeability (k_p), both before and after one 1-hour loading session, for human tissue at baseline and after treatment with cytokines and Dex. There was variation in dynamic stiffness between donors grouped by age at baseline. After 10 days of treatment with either cytokines, or cytokines with Dex, Dex preserved cell viability and decreased GAG loss and NO release in cartilage treated from cytokines, but it did not alter mechanical properties (before or after loading). In the two treated groups, GAG content exhibited a correlation with E_y and E_d that was weaker than that seen at baseline.

2 BACKGROUND

2.1 Synovial Joint and Hyaline Cartilage Anatomy

Permitting the most mobility in the body, the synovial joint is the most common joint in mammals and allows for multiple planes of motion between bones. Synovial joints anatomically consist of a fibrous articular capsule that encloses the space underneath ligaments, the joint cavity itself lined with a synovial membrane and filled with synovial fluid, and articular cartilage on adjacent bone ends (Figure 1a). The lubricated cartilage surface primarily functions to allow for minimal friction and shock absorption with load transmission encountered during movement.[37] Synovial fluid is an ultrafiltrate of blood plasma, and is concentrated through filtration by macrophages and fibroblasts in the synovial membrane.[38] It normally acts as a lubricant for cartilage, with a high concentration of hyaluronic acid giving the fluid an appropriate viscosity for this function.[38] The fluid also circulates nutrients and regulatory cytokines through the joint space, and is rapidly cleared by the lymphatic system (with a turnover time of around 1 hour in a healthy knee).[39]

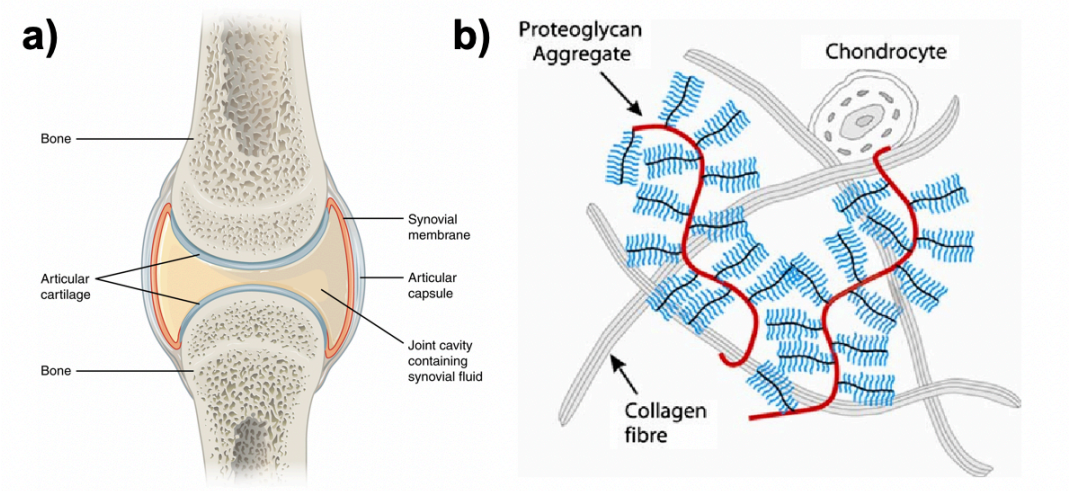

Figure 1. Configurations of the Synovial Joint and Hyaline Cartilage. (a) Important anatomy of the synovial joint includes the articular capsule, joint cavity with synovial fluid secreted by synoviocytes, and articular cartilage. (b) Articular cartilage consists of hyaline cartilage, which is made of cells (chondrocytes), extracellular matrix, and water with dissolved ions. Image credit: OpenStax[40], Schulz et al 2007[41]

One of the three main forms of cartilage is hyaline cartilage (Figure 1b), which consists of chondrocytes, the sole cellular component of this type of connective tissue derived from mesenchymal stem cells, surrounded by a complex matrix. Hyaline cartilage makes up parts of the nose, lines the tips of the ribs, and surrounds the respiratory tract in addition to its role as articular cartilage in the synovial joint. Articular cartilage is a specialized form of hyaline cartilage, particularly notable for its simple structure and smooth, slippery, milky appearance. It is 2-4 mm thick and has a sparse number of chondrocytes, which make up around 10% of its wet weight, embedded within the dense extracellular matrix (ECM) that they synthesize (10-25%) and water (65-80%).[42] Containing dissolved inorganic ions such as sodium, calcium, chloride and potassium, this fluid flows through its thickness and across its surface to distribute nutrients and provide lubrication - around 30% of this water associates with the intrafibrillar space of collagen while the remainder settles inside the matrix pores.[43]

Collagen makes up 60% of the dry weight of articular cartilage, consisting of type II collagen fibrils intertwined with aggrecan proteoglycans and stabilized by minor amounts of type I, IV, V, VI, IX, and XI collagens.[43] The molecules of collagen fibrils generally consist of 3 polypeptide alpha chains (containing mostly glycine and proline) wound into a triple helix, providing a stabile structure strong enough to endure shear and tensile stress.[44] The second main matrix component contributing to 30-35% of the dry weight are proteoglycans, which are made of a protein core with covalently attached glycosaminoglycan chains extending outward, repelled from one another due to negative charges. In articular cartilage the most common proteoglycan is aggrecan, which aggregates by noncovalent connections to hyaluronic acid with link proteins.[45] Aggrecan-hyaluronic acid aggregates fill the spaces between collagen fibrils, and are filled with water molecules associated with electrostatic repulsions between GAG chains that provide compressive resistance without causing excess intratissue swelling (Figure 1b).[46] The small remaining weight of cartilage consists of glycoproteins, lipids, phospholipids, and noncollagenous proteins, which aid in the organization and maintenance of the ECM structure.[43]

Articular cartilage can be divided into zones that differ in relative composition of ECM and chondrocytes (Figure 2). The superficial zone is thinnest and is covered by synovial fluid. This layer contains flattened ellipsoid chondrocytes that make less proteoglycans and more collagen fibrils, the latter of which are arranged parallel to the surface to provide the greatest tensile and shear resistance. The transitional or middle zone is below the superficial and contains spherical shaped cells, in lower density with a large amount of ECM. There is a higher concentration of proteoglycans here, and collagen fibrils are randomly arranged. Under this is the deep zone, in which proteoglycan content is highest and the cell density is lowest. Collagen fibrils are arranged perpendicular to the cartilage surface, allowing for the greatest compressive resistance. The tidemark marks the line between the deep zone and the calcified cartilage zone, in which there are very few cells that produce a calcified matrix with type X collagen to act as a shock absorber with the subchondral bone layer below it. These are the final two zones protecting the cancellous bone containing bone marrow underneath.[47] Notably, articular cartilage is avascular, aneural and alymphatic, receiving nutrients by diffusion from blood vessels of subchondral bone along with the synovial fluid. This, along with an overall minimal cell to matrix ratio (5%) and low metabolic activity of mature chondrocytes limits its ability to be repaired or heal with injurious damage, and its preservation is crucial to overall joint condition.[42]

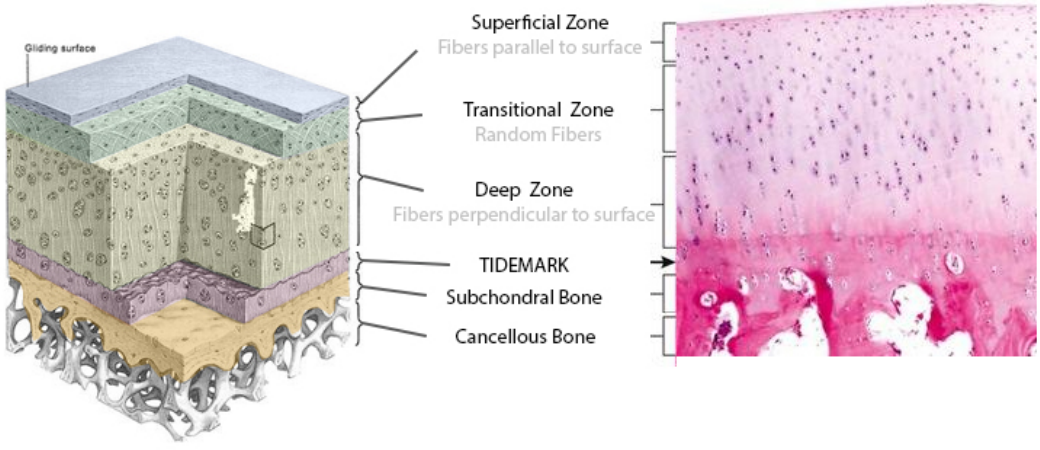

Figure 2. Zones of Articular Cartilage. A 3D rendering and histological specimen representing the multiple layers that make up articular cartilage. The most thin section resides at the cartilage surface and is the superficial zone, in which collagen fibrils lay parallel to the surface and chondrocytes are flattened in an

ellipsoid shape. Deeper into cartilage, chondrocytes become less dense with larger amounts of ECM produced. The tidemark is the border between the deepest cartilage zone and calcified cartilage with subchondral bone. Image credit: Orthobullets[48]

2.2 Etiology and Pathophysiology of Osteoarthritis

Osteoarthritis (OA) is a debilitating disease of the entire synovial joint, eventually affecting all of its tissue components, including cartilage, bone, synovium, ligaments, menisci, muscles, and neural tissue.[1,2] The disease is characterized primarily by cartilage erosion, remodeling of subchondral bone, and bone projections called osteophytes.[49] These changes can further cause joint space narrowing, bone pieces in the joint space (termed "joint mice"), and subchondral bone cysts and sclerosis, all of which can be discovered with radiographical imaging (Figure 3), which is used in conjunction with symptoms to diagnose OA.[50] These degradative transformations cause immense pain, morning stiffness and reduced joint function, all of which are the clinical criteria for OA diagnosis by the European League Against Rheumatism (EULAR).[51] This combination can greatly alter an individual's quality of life: OA is the most common articular disease in the developed world, and one of the leading causes of chronic disability.[52] The burden of OA is financial in addition to physical, as there are costs for both disease treatment and livelihood adaptions for many who cannot work due to their disability.[53]

Figure 3. Comparative Radiographs of Non-OA and OA Knee. While the image on the left is an X-ray of a normal knee, the image on the right is that of a knee with Kellgren-Lawrence grade 2 OA. The knee with OA has two characteristic radiograph findings, joint space narrowing and a medial tibial osteophyte (bony projection). These, along with other findings on imaging can be used to diagnose OA. Image credit: Altman et al 2007[54]

As of 2020, it is estimated that 302 million people worldwide have OA, with a very high prevalence of knee OA in particular.[55] OA affects individuals of all ages, and genetics have shown to play some role in its etiology – heritability estimates are site specific, measured at 40% for knee, 60% for hip, 65% for hand, and 70% for spine.[56] Current genetic research has focused on candidate genes relating to cartilage structure, bone density, inflammatory cytokines, and chondrocyte cell signaling.[57,58] However, there are many other risk factors for OA, such as obesity, female sex, joint laxity, poor muscular strength, and repetitive joint use or injury.[51] Occupation has also been shown to play a role especially for knee OA, as manual labor occupations such as construction, agriculture and mining increase risk of developing disease, likely due to biomechanical stressors with a heavy physical work load.[59-60]

The pathophysiology of OA is complex and dependent on the interplay between biological processes in both cartilage and bone. Triggering factors initially cause small amounts of

aggrecan and collagen degradation by matrix aggrecanases (ADAMTS4,5) and matrix metalloproteinase collagenases (MMP-1,13), respectively, in the cartilage ECM.[61,62] This destruction leads to matric and chondrocyte swelling and reduced shock absorption of the articular cartilage, and continual load-bearing in these conditions causes chondrocyte death.[63] Cell death has two consequences – a spillage of more matrix proteases and inflammatory cytokines that activate them into the synovial cavity, as well as fewer chondrocytes left behind to build new matrix - leading to further erosion and that outpaces matrix synthesis, inevitably creating irreversible damage that exposes the subchondral bone.[64,65] Thus, the transfer of load-bearing causes subchondral bone remodeling that results in the formation of thicker bone (sclerosis), cysts, and osteophytes.[63]

As mentioned above, traumatic joint injury - which may be a fracture, cartilage damage, acute ligament tear, or chronic ligament instability - can lead to disease development, and OA that progresses from injury is termed post-traumatic osteoarthritis (PTOA).[66] PTOA accounts for around 12% of OA cases, and is especially debilitating due to an earlier onset and predisposition to affect younger and more active individuals.[67] Clinical studies have shown that 50% of patients with rupture of the anterior cruciate ligament develop OA within 5-15 years,[68-70] and up to 90% of OA in the ankle joint is post-traumatic.[71] The mechanism of PTOA development is not well understood, but it is thought that momentary extreme forces to the synovial joint causes stress fractures through the cartilage and potentially subchondral bone, activating further matrix destruction as described in traditional OA.[72] Even in the absence of overt fractures or cracks of cartilage, acute ACL and meniscus tears along with mechanical impact to the cartilage surface can cause chondrocyte death and the released of inflammatory cytokines such as IL-1, IL-6, and TNFα into the synovial fluid (e.g., from synovium) which can promote metabolic pathways behind PTOA development such as protease activation and apoptotic initiation.[73-77] More research has suggested that oxygen free radicals released from chondrocytes,[78] ECM debris acting as damage-associate molecular patterns (DAMPs),[79] mechanical activation of MMPs,[75] and abnormal forces and torques after injury altering cytoskeletal proteins could all play a role.[75,80]

Nevertheless, PTOA is often diagnosed late in the disease process as symptoms do not appear until that time point, even if there are radiographic changes earlier on.[2,81,82] Biomarkers of blood, urine and synovial fluid have been proposed as a method to detected cartilage degeneration after injury, and type II cartilage metabolites as well as cytokines have been studied targets, though these markers need to be further researched in connection with patient outcomes to provide a predictive value that is useful clinically.[67,83,84] Regardless, PTOA provides a unique role for treatment because of a known "time zero" point at which injury occurs, and an understanding of this systematic progression timeline allows for the chance to slow or prevent matrix loss and chondrocyte death after trauma.

2.3 Pharmacologic Treatments for OA

While disease modifying anti-rheumatic drugs (DMARDS) for rheumatoid arthritis and related rheumatic diseases exist, there are no efficacious disease-modifying OA drugs (DMOADS) available.[11,85] In addition to lifestyle changes such as weight loss, blood sugar control and stress minimization, current drug treatments for OA only provide short term pain and inflammation relief. Medicines currently used include analgesics to relieve pain, non-steroidal anti-inflammatory drugs (NSAIDs) and corticosteroids to reduce inflammation and pain, and hyaluronic acid to lubricate the joint to alleviate discomfort.[86] Other drugs such as the anti-depressant duloxetine and anti-seizure medication pregabalin are also FDA-approved to treat OA pain.[12] However, use of only temporary relief is becoming more of a concern regarding disease burden with an aging OA population and an especially young group affected in the case of PTOA.[87] Furthermore, there are concerns about the significant side effects associated with long term use of relief therapeutics such as NSAIDs.[88] If symptoms persist after appropriate nonsurgical treatment, surgery is considered for patients – options include arthroscopic debridement, osteotomy, and unicompartmental or total knee arthroplasty (TKA) for advanced OA. Though TKA is effective for these patients, component durability is only 10-15 years, and postoperative pain still occurs for 1 of every 8 individuals.[89,90] Taken together, there is an unmet need for therapeutics that will control or prevent the development of OA, which would greatly benefit millions of patients worldwide.

For many years, researchers have tried to find solutions to this dilemma, using approaches targeting cartilage, subchondral bone, and the inflammatory pathways involved with disease. Cartilage targets have included MMP inhibitors,[91,92] synthetic growth factors,[93,94] mesenchymal stem cell injection,[95-97] and Cathepsin K (a protease involved in cartilage degradation) inhibitors.[98,99] Bisphosphonates,[100,101] calcitonin,[102] and strontium ranelate[103,104] have been examined as therapies to prevent subchondral bone remodeling. Finally, inhibitors of inflammatory mediators have targeted GM-CSF,[105] iNOS,[106,107] IL-1β,[108,109] and TNFα.[110,111] Some of these therapeutics have shown promise, but most clinical trials have failed to produced desired results, likely due to flawed design, insensitive outcome measures, inadequate delivery to target tissues, or side effects. The complex nature of OA makes it difficult to assess drug success, and work is ongoing to plan high-quality clinical trials for the future.[85]

The development of intraarticular injections has been greatly advantageous to OA treatment – currently, both corticosteroid and hyaluronic acid therapies are FDA-approved for injection into the synovial cavity. Local administration increases bioavailability of the drug, limits systemic exposure, and prevents off-target and adverse events.[112] Since cartilage is avascular, intraarticular injections improve drug delivery, but there are costs to this approach. Chondrocytes are exposed to a higher drug concentration, so chondrotoxicity must be taken into account when designing these therapeutics.[113-115] Further, synovial fluid within the joint space drains into the lymphatic system quickly,[116] so protein dwell time is on the order of hours and is independent of macromolecule size.[117] Research in the Grodzinsky lab has focused on methods to increase cartilage-targeting and joint retention time of intraarticular drugs, most notably with dexamethasone.[118]

2.4 Dexamethasone

Dexamethasone (Dex) is a synthetic glucocorticoid (GC) (a class of biologically active corticosteroids) that has a 20-30 times greater potency than hydrocortisone, a naturally occurring GC (Figure 4).[119] GCs diffuse across plasma membranes and bind to GC receptors intracellularly, which directly or indirectly regulate gene expression as transcription factors. GC receptors, when activated, have an anti-inflammatory effect,

upregulating IL-1 antagonist and IL-10[120] while repressing IL-1β, IL-6, TNFα and cyclooxygenase-2.[121-124] Because many cell types contain GC receptors, systemic GCs have been long used to treat inflammatory and autoimmune conditions. However, this use comes with adverse effects such as loss of bone density, avascular necrosis, weight gain, insulin resistance and risk of infection. As human chondrocytes express GC receptors,[125] GCs have been an established treatment for chronic OA as well as rheumatoid arthritis, with intra-articular administration to minimize systemic risks.[126,127] Because of Dex's high potency due to greater receptor affinity,[128] orthopedists are hesitant to use it clinically as an intra-articular injection, due to concerns regarding cartilage damage.[113] However, studies have shown that low dose Dex reduces the release of proteoglycans and collagen from the extracellular matrix of bovine articular cartilage exposed to mechanical injury and/or inflammatory cytokines as an *in vitro* model of PTOA,[13] a finding confirmed with rabbit[14,15] and human[36] models as well. Under these conditions, chondrocyte viability is preserved and matrix synthesis is maintained,[16] suggesting that short term exposure (such as a single injection) to a low dose concentration of the drug could have disease modifying benefits with minimal toxicity to chondrocytes.

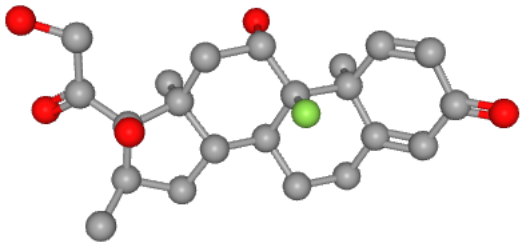

Figure 4. Chemical Structure of the Corticosteroid Dexamethasone. As a steroid derivative consisting of a four-ringed structure, dexamethasone binds intracellular receptors that normally bind endogenous cortisol with 20-30 times greater affinity. This allows it to be used a potent drug with an anti-inflammatory effect, though systemic circulation has its risks. Recent studies have suggested that low doses of the molecule have a protective anti-catabolic effect against cartilage in inflammatory conditions. Green = fluorine; red = oxygen; grey = carbon. Image credit: PubChem[129]

2.5 Insulin-like Growth Factor 1

Insulin-like growth factor 1 (IGF-1) is a 70 amino acid polypeptide hormone that is mainly (~70%) produced by the liver in response to growth hormone and insulin stimulation (Figure 5).[130] This protein binds to the IGF-1 receptor or insulin receptor (with less affinity) on cellular plasma membranes, which have tyrosine kinase activity and activate IRS-1/PI3K/Akt signaling. IGF-1 affects many biochemical pathways, but most notably increases cellular glucose uptake and upregulates lipid and protein synthesis to promote tissue growth and development.[131] It is also thought that IGF-1 has anti-aging protective effect by reducing free radical production in mitochondrial, but this mechanism is less well understood.[132-134] Because of these anabolic effects, IGF-1 has been studied as a potential modulator of chondrocyte damage in PTOA disease models. *In vitro* bovine and human models have shown that IGF-1 rescues chondrocyte apoptosis induced by mechanical injury and inflammatory cytokines, and upregulates cartilage matrix biosynthesis.[135-137] Building on the idea that the pro-anabolic IGF-1 with the anti-catabolic Dex might complement each other, the work of Li et al[17] further illustrated that combined treatment more significantly reduces proteoglycan loss and increases biosynthesis than either drug alone while maintaining chondrocyte viability in a human PTOA model. These results form the basis for the use of combination drug therapy in this thesis in order to maximize the pharmacologic effects targeting cartilage degradation.

Figure 5. Ribbon Structure of the IGF-1 Protein. Insulin-like growth factor 1 is a polypeptide consisting of 70 amino acids, and gets its name from its downstream effects that are similar to that of insulin, binding the IGF-1 or insulin receptors on plasma membranes. Its main biological effects include increasing glucose uptake and upregulating lipid and protein synthesis. Image credit: Protein Data Bank[138]

2.6 Mechanical Properties of Cartilage

Through the variety of activities that synovial joints experience throughout the day, articular cartilage undergoes a wide range of compressive force magnitudes and frequencies with weight bearing. Compressive loads on the joint range from 1 to 6 MPa with light to moderate activities and up to 12 MPa in strenuous activities,[139-141] with reports of 20 to 30% cartilage strain.[31,142,143] The frequency of daily loading varies from <1 Hz with weightlifting and walking to >10 Hz for movements such as running and jumping.[144-146] In addition to the glycoprotein lubricin that lines the joint surface to reduce friction levels,[147,148] the closely-spaced negatively charged GAG side chains of aggrecan in the ECM help by resisting the flow of intra-tissue fluid, resulting in greatly increased pressurization inside cartilage that distributes forces during compression.[149] Cartilage also displays the phenomenon of creep, meaning that it deforms over time with a constant compressive stress until it reaches an equilibrium value.[43,150] It is also both viscoelastic and poroelastic, behaving differently over time when subjected to a compressive force, due to frictional drag with interstitial fluid flow, increased pressure in fluid-filled pores within the ECM, and motion intrinsic to the macromolecules within the matrix.[32,43,151,152] These properties, determined by the collagen network and aggrecan molecules, allow for energy dissipation in cartilage and self-stiffening in response to increased compression frequency, both crucial to the joint load-bearing response over the described range of activity.[149,153,154,155]

In terms of material properties, articular cartilage has a compressive equilibrium modulus that can be described as the ratio of stress to strain - the material stiffness in response to constant force. The stress-relaxation test can determine this – the tissue undergoes fixed increases in strain, with continual detection of stress during these ramps. When the fixed value of strain is reached, it is maintained for a certain period of time, and stress on the tissue then decreased exponentially to an equilibrium stress value to maintain this deformation. The poroelastic nature of cartilage helps govern when this stress equilibrium occurs, as fluid flow within and through the matrix causes delays in stress relaxation in

response to fixed strain.[156] Experimentally, an exponential decay curve is fit to stress relaxation data using the following equation:

$$\sigma = a + be^{-t/\tau} \quad (1)$$

where a is the equilibrium stress and τ is the characteristic relaxation time. The values of a are then plotted against each specified strain, and the resulting slope returns the compressive equilibrium modulus (E_y). Using unconfined compression, E_y is called the Young's modulus.

Physiologically, many movements have frequency, and are better represented by dynamic compression. The dynamic stiffness, a property of viscoelastic materials such as cartilage, is the stiffness under vibratory conditions, where:

$$\text{axial strain: } \varepsilon = \varepsilon_0 \cos(\omega t) \quad \text{and} \quad \text{axial stress: } \sigma = \sigma_0 \cos(\omega t + \delta) \quad (2)$$

with $\omega = 2\pi f$ where f is the frequency of strain oscillation, t is time, and δ is the phase angle between axial stress and axial strain. The dynamic stiffness E_d is then calculated as:

$$E_d = (\sigma_0/\varepsilon_0)e^{j\delta} \quad (3)$$

where j is the complex number defined by $j^2 = -1$.[156] Hydraulic permeability is another significant property of the poroelastic cartilage, and measures the ease with which fluid moves through its spaces, and for tissue is represented as the approximation:

$$k_p \sim r^2/[(3.4)(2)(E_d)(\tau)] \quad (4)$$

where r is the tissue radius, and τ is the time constant fit from the end of the final stress-relaxation data.[157] Experimental protocols evaluating these parameters are the basis for the work used in thesis to capture the structural changes that occur with biologic alterations of cartilage in a disease state (cytokine-challenged).

2.7 Dynamic Loading and the Metabolic Activity of Cartilage

Regular exercise has long been considered significant in maintaining overall physical and mental health, balance and posture, but more recently has been illustrated to have an anti-inflammatory effect on the development of chronic disease.[158] Exercise therapy for patients already diagnosed with OA showed significant improvement in pain and disability compared with a non-exercise group.[159] With the thought that movement might play then

a role in the prevention of cartilage degradation, clinical trials have been initiated for patients after joint injury and have yet to release results.[160,161] In animal and tissue explant studies of healthy cartilage, loading without a time-varying component tended to decrease ECM synthesis and deposition,[162-164] while studies looking at loading with time variation saw an increase in these parameters.[165-167] In line with these findings, dynamic loading, which models repeated sequences of weight bearing on a joint, has been studied separate from pharmacologic therapies as a potential modulator of chondrocyte metabolic activity in diseased tissue. In cell culture, loading can alleviate chondrocyte catabolic responses to inflammatory cytokines, and in normal bovine cartilage explants, loading can enhance matrix biosynthesis and increase drug transport into tissue, depending strongly on the frequency, amplitude and duty cycle of compressions.[18-23] Further work has shown that human osteoarthritic chondrocytes upregulate amino acid synthesis in response to cyclic compressions.[168] Mechanically, stimulation of chondrocyte-mediated biosynthesis has been localized to regions of high interstitial fluid flow induced by compression, with signal transduction pathways involving MAPK activation, cyclic AMP, and intracellular calcium.[24-28] More recently, loading has also been shown to post-transcriptionally modulate the microtubule protein tubulin, blocking cilia elongation in bovine chondrocytes incubated with IL-1β.[169]

However, these chondroprotective effects have a limit even within the physiologically relevant range of knee loading stress - in bovine models of PTOA, it has been shown that moderate dynamic compression post-injury can inhibit cartilage degradation and TNFα/IL-6 release in explants up until a particular dynamic strain threshold.[29] These *in vitro* loading studies were modeled directly after the amplitudes and duty cycles of *in vivo* studies conducted at the Massachusetts General Hospital, which used dual fluoroscopic imaging with magnetic resonance imaging during static loading of both healthy human knees and those with prior anterior cruciate ligament rupture.[30,31]

Further, studies in mouse, human and bovine cartilage models illustrate that loading has structural effects that are just as important to disease progression as its biological impacts. Bovine cartilage with GAG loss modeling early stages of osteoarthritis shows a dramatic

increase in hydraulic permeability and a concomitant decrease in dynamic stiffness at higher frequencies, suggesting that early OA-like changes to cartilage render the tissue unable to support dynamic loads within the range representing daily joint motion.[170] This mechanical fatigue was replicated in a study with human articular cartilage explants, which also found a decrease in specimen thickness at higher frequencies attributed to ECM disruption.[35] Thus, loading rate is extremely important in addition to loading magnitude in potentially contributing to or alleviating disease progression. It has also been demonstrated that the mechanical properties of cartilage tissue are fluid to a certain extent – in mouse models, dynamic loads can change these properties after a single loading session,[33] and in human knee tissue, cartilage can optimize its compressive modulus over time to minimize strains, impacting the tissue's ability to support future loading within the range representing daily joint motion.[32]

These studies suggest that a combination of pharmacologic molecules and dynamic compression within a rehabilitative range could maximize therapeutic action in preventing cartilage degradation and even promoting anabolism in OA development. While much work has been done on the effects of compression and Dex/IGF-1 separately, most of this research has been conducted on bovine tissue rather than human, and little is known about the impact these therapies have together, at a physiologically relevant compression rate that represents realistic exercise regimens. Additionally, there are few studies that simultaneously look at changes in mechanical properties with biological measures in response to dynamic loading, especially as a potential therapeutic in a disease model. The work of this thesis aimed to fill this gap in current knowledge, investigating whether an optimized mechanical joint loading protocol has pro-anabolic and anti-catabolic effects on osteochondral tissues under inflammatory conditions, as well as an effect on cartilage mechanical properties suggesting either structural preservation or continued vulnerability as expected in a disease state.

3 METHODS

3.1 Harvest of Cartilage and Cartilage-Bone Explants

3.1.1 *Bovine*

Tissue was harvested from the femoropatellar grooves of 1-2 week old calves (Research 87, Boylston, MA, USA) (Figure 6). A biopsy corer (Smith & Nephew, Andover, MA) was placed at a 90-degree angle to the cartilage to ensure a straight surface for the cartilage explant, and only unfibrillated cartilage was used. A hammer (Smith & Nephew) was then used to apply pressure to the corer to isolate full-thickness cartilage tissue at a diameter of 3.5 mm. An ejector (Smith & Nephew) accessory was used to pull the tissue out of the joint and eject it from the corer by applying pressure on the bottom end to avoid damaging the cartilage surface. Cartilage was then sliced with a blade to obtain the top 1 mm disk containing the intact superficial zone. Explants were rinsed in cold PBS, and then placed to equilibrate in low glucose DMEM (1 g/L) supplemented with 10 mM HEPES buffer, 0.1 mM nonessential amino acids, 0.4 mM proline, 20 ug/ml ascorbic acid, 100 units/ml penicillin G, 100 ug/ml streptomycin, 0.25 ug.ml amphotericin B, and 1% ITS (10 ug/ml insulin, 5.5 ug/ml transferrin, 5 ng/ml selenium) (all products from Sigma-Aldrich, St. Louis, MO, USA) at 5% CO2, 37°C for 2 days. For gene expression studies, ITS-free conditions were used to isolate the specific effects of exogenous IGF-1.

Figure 6. Harvest of a Bovine Knee Joint. Once muscle and fat around the knee joint are removed, the cartilage is exposed and a biopsy corer was used to obtain 3.5 mm diameter cylindrical cartilage explants. Image credit: Garima Dwivedi and Lisa Flaman.

3.1.2 *Human*

Tissue was harvested from postmortem knee and ankle joints obtained from adult human donors with either Collins Grade 0 or Grade 1 cartilage (Figure 7). Joints were obtained from the Gift of Hope Organ and Tissue Donor Network (Itasca, IL, USA), National Disease Research Interchange (Philadelphia, PA, USA), and LifeNet Health (Virginia Beach, VA, USA), and all procedures for obtaining osteochondral (OC) tissue were approved by the Committee on Use of Humans as Experimental Subjects at MIT. Joint cartilage was graded by a forensic pathologist using the modified Collins grading system. Joints were rinsed with high-glucose DMEM (4.5 g/L) after obtainment, and were inspected for signs of degeneration and damage before harvest. A biopsy corer with hammer and ejector was used on unfibrillated cartilage at the femoropatellar and condylar regions of the knee or talar dome of the ankle in the same method employed for obtaining bovine explants, to isolate OC tissue at a width of 3.5 mm and a depth of 7-10 mm. This process was repeated until all healthy cartilage regions were utilized on the knee or ankle joint, and all explants were rinsed in sterile cold PBS for 10-15 minutes. All OC tissues were sliced on the bone end using a bone cutter (Fine Science Tools, Foster City, CA, USA) to ensure a uniform length of 5 mm for all explants, and equilibrated in high-glucose DMEM containing the same supplements as in the bovine culture medium for 2 days (each with 1 mL of media) at 5% CO2, 37°C.

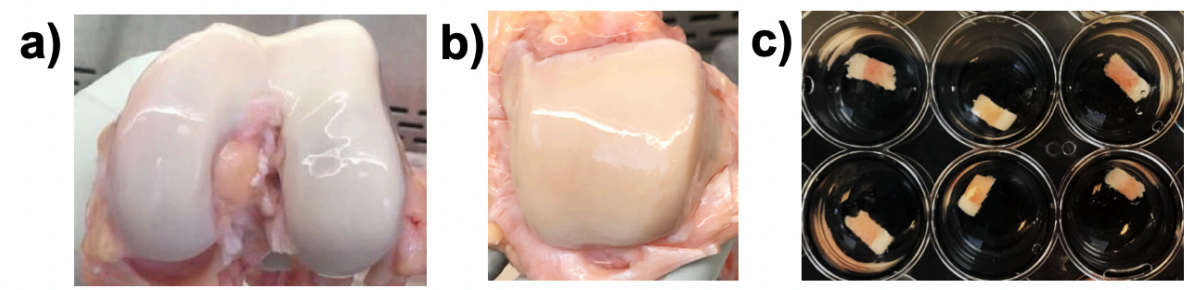

Figure 7. Harvest of Human Knee and Ankle Joints. Both knee (a) and ankle (b) joints were used for human studies. The same biopsy corer as used for bovine joints was used to obtain 3.5 mm diameter cylindrical osteochondral explants (c). Image credit: Garima Dwivedi and Lisa Flaman.

3.2 Experimental Timeline and Dynamic Loading

Motivated by the need to model inter-tissue interactions that lead to a disease state, the Grodzinsky lab has developed a cartilage-bone microphysiological system (MPS) that simulates the human joint response to injury and inflammation and early phases of progression to OA, used for the work in this thesis. To model disease, the cartilage (bovine) or cartilage-bone tissue was cultured in media containing the pro-inflammatory cytokines TNFα, IL-6 and sIL-6R.

3.2.1 *Bovine*

On the 2nd day after harvesting, two cartilage explants were taken for day 0 viability testing described in 3.3.1. At the start of experiments (day 0), each explant was placed in 0.5 ml of low glucose DMEM with supplements described in 3.1.1, labeled low glucose complete control media (LGCCM). Media was collected and changed every 2 days, except on day 6 when [^{35}S]-sulfate was added into media for 24 hours only as described in 3.3.2. Four treatment groups were studied in both unloaded and loaded conditions: (1) C – cartilage explant controls, (2) C + CYT – cartilage explants treated with exogenous cytokines as a PTOA disease model (25 ng/mL TNFα, 50 ng/mL IL-6, 250 ng/mL sIL-6R; PeproTech, East Windsor, NJ, USA), (3) C + DEX alone (100 nM; Sigma-Aldrich) and (4) C + CYT + DEX (100 nM) as a disease + treatment group. For dynamic loading, disks were placed in a 12-well polysulfone chamber with the superficial zone facing upwards, and compressed in a custom-designed, incubator-housed loading apparatus.[171] A load-controlled program was developed using a haversine waveform (0.33 Hz, 40% duty cycle) and a dynamic stress amplitude of 25 kPa, superimposed on a 25 kPa static offset stress, for 1 hour in every 24-hour period. For gene expression studies, six treatment groups were studied in both unloaded and loaded conditions: (1) C – cartilage explant controls, (2) C + CYT – cartilage explants treated with exogenous cytokines (25 ng/mL TNFα, 50 ng/mL IL-6, 250 ng/mL sIL-6R), (3) C + DEX alone (100 nM), (4) C + IGF alone (100 ng/ml; PeproTech), (5) C + CYT + DEX (100 nM) and (6) C + CYT + IGF (100 ng/ml) as disease + treatment groups. All explants were placed in 0.5 ml serum-free LGCCM for 23 hours, at which point loaded groups were placed in a 1 hour loading program as used for the 7 day study,

and unloaded groups were left to free swell for 1 hour. Explants were immediately flash frozen after loading or free-swelling, and placed at -80°C.

3.2.2 *Human*

On the 2nd day after harvesting, two cartilage-bone explants were taken for day 0 viability testing described in 3.3.1. At the start of experiments (day 0), each explant was placed in 1.5 ml of LGCCM, and media was collected and changed every 2 days, except on the final day of experiments when [^{35}S]-sulfate was added into media for 24 hours only as described in 3.3.2. The number of treatment groups varied between donors, but included: (1) CB – cartilage-bone explant controls, (2) CB + CYT – explants treated with exogenous cytokines as a PTOA disease model (100 ng/mL TNFα, 50 ng/mL IL-6, 250 ng/mL sIL-6R), as well as (3) CB + CYT + DEX (100 nM), (4) CB + CYT + IGF (100 ng/ml), and (5) CB + CYT + DEX (100 nM) + IGF (100 ng/ml) as a disease + treatment groups. For dynamic loading, disks were placed in a 16-well polysulfone chamber with cartilage facing upwards held by two metal rings allowing media circulation, and compressed in the same incubator-housed loading apparatus used for bovine studies.[171] A load-controlled program using a haversine waveform (0.33 Hz, 40% duty cycle) at a dynamic stress amplitude of 100 kPa amplitude, superimposed on an initial 10% static offset strain, for 1 hour in every 24-hour period.

3.3 Tissue and Biochemical Assays

3.3.1 *Cell Viability*

At day 0 and on the final experimental day, human and bovine chondrocyte viability was estimated using fluorescein diacetate (4 ug/ml in PBS, Sigma-Aldrich) to stain viable cells and propidium iodide (40 ug/ml in PBS, Sigma-Aldrich) to stain non-viable cells. Cartilage tissue was removed from its attached bone and cut into 100-200 um thick slices. Two slices from each explant were stained for 2 minutes in the dark, and then were washed twice with PBS for 2 minutes each time. The PBS solution was removed and tissues were visualized using a fluorescence microscope (Nikon, Melville, NY, USA) with a 4x magnification.

3.3.2 *Cartilage Matrix GAG Biosynthesis and GAG Loss*

On the day before experiment termination, 20 uCi/ml (human) or 5 uCi/ml (bovine) [^{35}S]-sulfate (PerkinElmer, Waltham, MA, USA) was added to the LGCCM for each explant, along with a control media sample. After 24 hours of radiolabeling, all cultures were washed 4 times with Rx-PBS wash for 30 minutes each, to completely remove any free label. The cartilage of each explant was sliced off of the bone, and each tissue was weighed for every culture. Tissues were separated into different tubes and then each was digested with proteinase K (Roche Life Sciences, Indianapolis, IN, USA) in Tris buffer at 2 mg/ml for 18 hours in a water bath set at 60°C. Digested samples were transferred to a -20°C freezer until needed. If mechanical testing was being conducted, this would occur before weighing and tissue digestion.

To measure cartilage GAG biosynthesis through sGAG incorporation, control media along with undiluted cartilage tissue digests were combined with scintillation fluid and placed in a liquid scintillation counter to measure [^{35}S]-sulfate radioactivity as described previously.[18] Control media had an inherent radioactivity equivalent to 814000 pmol/ml, and 1 hr sGAG incorporation for each sample was calculated as R_1 = (sample reading*814000)/(control reading*24). These readings were normalized to cartilage wet weight and reported as pmol/hr/mg.

To measure cartilage sGAG loss into the media over the experiment duration, a 1,9-dimethylmethylene blue (DMMB) dye binding spectrophotometric assay was used as previously described.[172] Media samples were undiluted, cartilage tissue samples were prepared at 1:10 dilution, and chondroitin-6 –sulfate was used as the standard, as it is the most prevalent GAG in articular cartilage. All samples and standards were prepared with DMMB dye solution, and read at a 520 nm absorbance in a spectrophotometer. All plate data was normalized to the blank wells, a standard curve was formed by fitting a linear trend to standard absorbance data. From this curve, the GAG concentration of all samples was determined and normalized to wet weight (or media amount). Total media GAG ($m_2 + m_4 + \ldots + m_n$) was added to cartilage GAG (c_n) to get the GAG amount at the experiment day 0, and GAG loss

was calculated at each time point *x* as $L_x = (m_2 + \ldots + m_x)/(m_2 + m_4 + \ldots + m_n + c_n)$.

3.3.3 *DNA Content*

To measure DNA content in bovine samples, an assay utilizing bisbenzimidazole fluorescent dye Hoechst 33258 was used as previously described.[173] Hoechst 33258 dye solution was made by dissolving dye powder with a buffer containing 10 mM Tris, 1 mM Na_2EDTA, and 0.1 M NaCl at pH 7.4, for a final dye concentration of 0.1 ug/ml. Cartilage tissue samples were prepared at 1:10 dilution, and a DNA standard curve was made from a 1 mg/ml stock solution. All samples were prepared with Hoechst 33258 dye solution, and read at a 520 nm absorbance in a spectrophotometer. All plate data was normalized to the blank wells, a standard curve was formed by fitting a linear trend to standard absorbance data. From this curve, the DNA content of all samples was determined in ug using the equation DNA content = [Concentration]*0.5*10 and normalized to wet weight.

A PicoGreen DNA assay was used for human cartilage samples, as it is 400x more sensitive than the Hoechst assay, which is more useful for detecting human cartilage DNA with less cellular cartilage compared to bovine. Cartilage tissue samples were prepared at 1:10 dilution, and a DNA standard curve was made from a 1 mg/ml stock solution. All samples and standards were prepared with PicoGreen reagent (Thermo Fisher Scientific, Waltham, MA, USA) and a 10 mM Tris-HCl, 1 mM EDTA buffer solution, and read at a 260 nm absorbance in a spectrophotometer. All plate data was normalized to the blank wells, a standard curve was formed by fitting a linear trend to standard absorbance data. From this curve, the DNA content of all samples was determined in ug using the equation DNA content = [Concentration]*5*0.5*10/1000 and normalized to wet weight.

3.3.4 *Collagen Content*

Collagen content in both human and bovine samples was measured using the hydroxyproline assay as previously described.[174,175] Undiluted cartilage tissue samples were prepared with 12 N HCl, and dried at 80°C. Digests were reconstituted with a buffer containing citric acid, glacial acetic acid, sodium acetate

trihydrate and sodium hydroxide, and placed at 4°C for 18 hours. Samples were plated with a collagen standard made from a 1 mg/ml stock solution. All samples and standards were incubated with Chloramine T and then 4-(Dimethylamino)benzaldehyde (DMAB) (Sigma-Aldrich), and read at a 560 nm absorbance in a spectrophotometer. All plate data was normalized to the blank wells, a standard curve was formed by fitting a linear trend to standard absorbance data. From this curve, the collagen content of all samples was determined in ug using the equation Coll Content = [Concentration]*5*7.143 and normalized to wet weight.

3.3.5 *Nitric Oxide*

Nitric oxide (NO) levels in human media samples were determined using a nitrite detection assay (Promega, Madison, WI, USA). Media samples, as well as a nitrite standard reference curve made from diluting 0.1 M sodium nitrite stock in low glucose DMEM, were incubated with sulfanilamide, and then N-1-napthylethylenediamine dihydrochloride. Samples were then read at a 520 nm absorbance in a spectrophotometer. All plate data was normalized to the blank wells, a standard curve was formed by fitting a linear trend to standard absorbance data. From this curve, the NO content of all media samples was determined in uM.

3.3.6 *Cytokine Enzyme-Linked Immunosorbent Assay*

The concentrations of the pro-inflammatory cytokines IFN-y, IL-1B, IL-2, IL-4. IL-6, IL-8, IL-10, IL-12p70, IL-13 and TNF-a were determined in human media samples using a sandwich ELISA (Meso Scale Discovery, Rockville MD, USA). Samples were prepared according to the manufacturer's instructions, and calibration curves were used to calculate cytokine concentrations in pg/ml.

3.3.7 *Gene Expression*

Bovine cartilage disks that were flash frozen were pooled for each group, pulverized and homogenized in TRIzol reagent (Thermo Fisher Scientific), and then separated using phase-gel tubes (Qiagen, Hilden, Germany). The RNeasy kit protocol (Qiagen) was used to purify the supernatant. Equal amounts of mRNA from each treatment group were reverse transcribed into cDNA (Promega; Therma Fisher Scientific; AB Sciex, Foster City, CA, USA).

Real-time PCR was performed using the LightCycler 480 Instrument (Roche Life Sciences) with SYBR Green Master Mix (Applied Biosystems, Waltham, MA, USA). Primer pairs and sequences are listed in Table S1. Briefly, these included markers of inflammation (iNOS, COX-2, NFkB), apoptosis (caspase-3), cellular mechanotransduction (MAPK1), major extracellular matrix proteins (collagen II, aggrecan) and matrix degradation (ADAMTS-4, ADAMTS-5). Expression data for each gene were calculated from the threshold cycle (Ct) value, and normalized to the internal housekeeping gene beta-actin, which was determined to be an appropriate reference for analysis of gene expression in bovine cartilage tissue based on pilot studies in the lab.

3.3.8 *Data Analysis*

Bovine and human GAG loss and biosynthesis, collagen content, DNA content, wet weight, and gene expression were analyzed using a non-parametric Kruskal-Wallis test with Dunn's multiple comparison testing for treatment groups within each animal donor. These statistical tests were performed using Prism (Graphpad Software, San Diego, CA, USA). For experiments in 5.3 where multiple donors were analyzed together, GAG loss, collagen content, DNA content, wet weight, and media NO concentration were analyzed using a linear mixed effects model with human donor as a random factor, followed by the least-squares means for pairwise comparisons. Correlation was tested by calculating Pearson's correlation coefficient. These statistical tests were performed using R v3.6.1 (RStudio, Boston, MA, USA). P values of less than 0.05 were considered statistically significant.

3.4 Functional Assay: Mechanical Testing

Macroscale stress-relaxation testing was used to determine the large-scale mechanical properties of human cartilage plugs, E_y and k_p. Sinusoidal testing in unconfined compression was used to measure E_d.

3.4.1 *Sample Preparation*

Explants were thawed at room temperature in a solution of PBS with protease inhibitor (PBS-PI) (Roche Life Sciences). The height of each cartilage plug was

determined using a micrometer, and this thickness was used to determine strain percentages in mechanical testing.

3.4.2 *Protocol*

Unconfined compression testing was performed using a Dynastat mechanical spectrometer (IMASS, Hingham, MA, USA) (Figure 8). A cartilage plug was loaded into an unconfined compression chamber (10 x 32.4 x 14.5 mm (w x l x h)) and a 9.5 mm diameter platen was lowered to the top of the plug height. 2 ml of PBS-PI was added to the chamber. Cartilage plugs were subjected to one ramp of 4% strain and four ramps of 2% strain for a total compression of 12%. Strain ramps were applied over 60 seconds and held for 5 minutes each. Following the final strain ramp and relaxation, a 0.5% dynamic strain-amplitude sinusoidal frequency sweep spanning from 0.005–2.0 Hz was applied. These values were chosen based on previous studies with human cartilage.[176] Stress was measured with displacement throughout the experimental protocol. At the end of the protocol, the cartilage plugs were digested with proteinase K in Tris buffer at 2 mg/ml for 18 hours in a water bath set at 60°C, and tissue biochemical tests were conducted as described in 3.3.

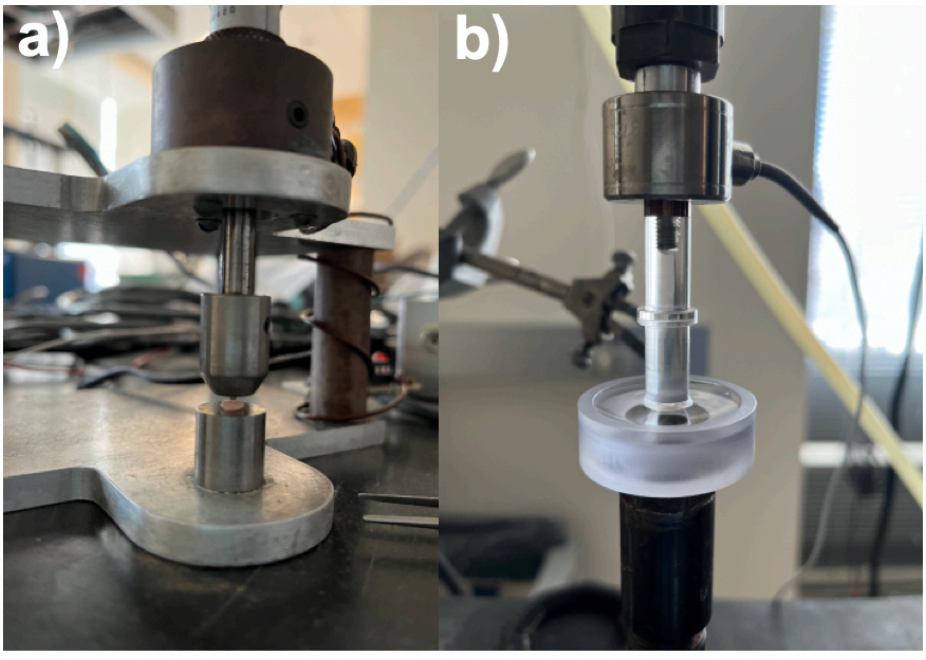

Figure 8. Setup of Mechanical Stress-Relaxation Test. Cartilage plugs sliced from osteochrondral explants were measured with a micrometer to determine thickness for strain ramp calculations (a).

Plugs were then placed in a chamber and underwent unconfined compression (b), allowing fluid (PBS-PI) to flow around the sides of the plug while undergoing loading. Strain ramps of 4%, followed by 2%, were applied over 60 seconds and held for 5 minutes each. At the final strain ramp, a 0.5% dynamic strain-amplitude sinusoidal frequency sweep was applied.

3.4.3 *Data Analysis*

Load data for each plug was converted to stress using the following equation:

$$\sigma = [\text{load (kg)} / \text{area (m}^2\text{)}] * (9.8 \text{ N} / 1 \text{ kg}) \quad (5)$$

where σ is stress in pascals. An exponential decay model (equation 1) was fit to the stress data for each strain ramp. Model values for $\lim_{t \to \infty}$ were plotted against strain to obtain the compressive equilibrium modulus (E_y) as the slope of the linear fit to the equilibrium stress-strain points. Equations 2 and 3 were used on dynamic data to obtain the dynamic stiffness (E_d), and equation 4 was used to calculate the hydraulic permeability (k_p). The compressive equilibrium modulus, dynamic stiffness, and hydraulic permeability were analyzed using a linear mixed effects model with human donor as a random factor, followed by the least-squares means for pairwise comparisons. Correlation was determined by calculating Pearson's correlation coefficients. These statistical tests were performed using R v3.6.1 (RStudio). P values of less than 0.05 were considered statistically significant.

4 RESULTS

4.1 Loading Optimization

To determine the loading stress and frequency that best mimics a physiologically relevant loading rehabilitation program, bovine (cartilage only) and human (cartilage-bone) explants were used to test the mechanical effects of varying contact and dynamic loading amplitudes, as well as loading duration. Bovine cartilage came from the knee joint and human cartilage came from both the knee and ankle joints (Table 1). The general framework for the loading protocol was a 1 hour session in every 24 hour period, consisting of an initial static compression for 5 minutes to ensure contact, followed by dynamic compression with a load-controlled haversine waveform (0.33 Hz, 40% duty cycle), with 8 waveform repetitions in each of 4 sets, in each of 6 exercises (Figure 9). The results below demonstrate the effect of variations in contact and dynamic loading stress amplitude

on cartilage strain and viability, as well as the effect of loading duration (1 vs 2 times per day) on cell viability, wet weight, DNA content, GAG loss, GAG biosynthesis, collagen content, and media NO levels.

Animal	ID	Tissue	Date of arrival	Sex/Age	Collin's Grade	BMI	Experiment Length (Days)
Bovine	Donor 1	Knee	07/07/20	-	-	-	2
Bovine	Donor 2	Knee	07/21/20	-	-	-	7
Human	Donor 1	Knee	01/31/20	F/69	1	24.9	2
Human	Donor 2	Knee	03/12/20	F/58	1	19.8	2
Human	Donor 3	Ankle	10/11/20	M/59	1	30.4	2
Human	Donor 4	Ankle	12/01/20	M/60	1	37.6	7

Table 1. Bovine and Human Donor Characteristics for Loading Optimization Studies. Cartilage-only plugs were taken from two bovine donor knees, while cartilage-bone explants were taken from two human donor knees and ankles, each. For human donors, this table outlines the sex, age, BMI and Collin's grade of each joint.

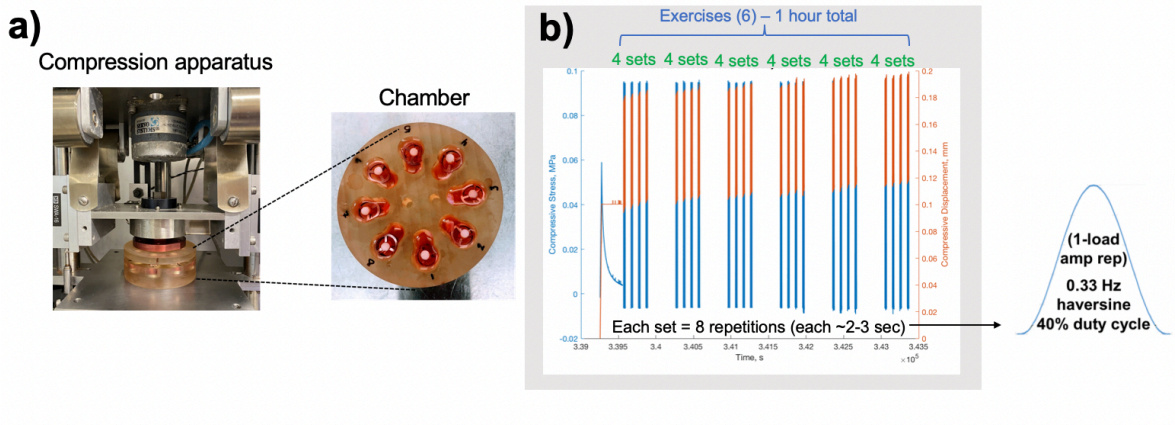

Figure 9. Dynamic Loading Apparatus, Chamber and Protocol. A polysulfone chamber was used to hold plugs undergoing dynamic loading in a custom-designed compression apparatus[171] (a). The chamber was 12-well for bovine plugs and 16-well for human plugs. The dynamic compression protocol was based on the exercise regimen given to astronauts on the ISS,[177] and consisted of a 1 hour session with a static ramp to make contact with plugs, and then 6 exercises of 4 sets of 8 repetitions each (b). Each repetition was a load-controlled haversine waveform of 0.33 Hz and 40% duty cycle to best replicate the movement of a rehabilitative exercise.[178] Parameters that could be altered were the contact and dynamic loading amplitudes, as well as the number of times the protocol was run in every 24 hour period.

4.1.1 *Bovine Knee*

Knee joints from two bovine donors were studied to better understand the effect of varying contact and dynamic loading amplitudes for the same loading protocol described above. Based on pilot studies looking at the corresponding strain for different magnitudes of stress in cartilage tissue as well as published Young's modulus values of bovine cartilage[34], two contact loads were chosen (25 and 50 kPa), and paired with three dynamic load amplitudes each. After a single session of loading, compressive strain was higher in plugs with a 50 kPa contact load as compared to those with 25 kPa (0.30-0.35 vs. 0.16-0.33, Figure 10). Additionally, compressive strain increased non-linearly with increases in dynamic loading amplitude, for both the 25 kPa (0.16, 0.27, 0.33 for 25 kPa, 50 kPa, 100 kPa) and 50 kPa (0.30, 0.33, 0.35 for 50 kPa, 100 kPa, 200 kPa) contact load groups. Based on the study by Li et. al. which demonstrated an optimal total strain (contact + dynamic loading) of 20-30%[29], in which GAG biosynthesis and cell viability are maximized and GAG loss is minimized, it was decided that for bovine cartilage, a 25 kPa dynamic load superimposed on a 25 kPa contact load would best allow for strains in this range, especially given that multiple loading sessions over 7 days would only increase total strain, and this study was 2 days long.

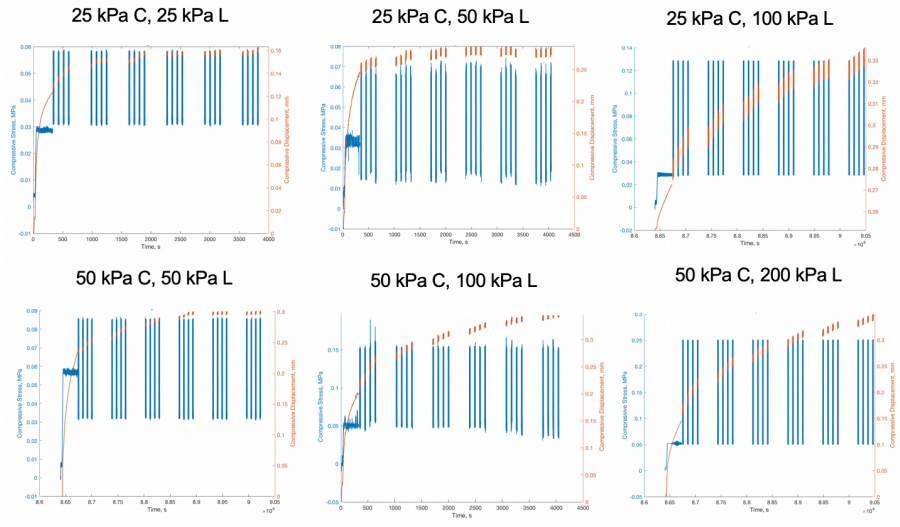

Figure 10. Representative Loading Stress/Strain Curves for Varying Contact and Dynamic Loading Amplitudes (Bovine Tissue). Contact (C) and dynamic loading (L) amplitudes were varied for the same loading protocol. Two contact loads (25 and 50 kPa) were chosen, and paired with three dynamic loading values each. Orange curve represents compressive displacement, and blue curve represents compressive stress. Compressive displacement increased with increased

contact load, as well as with increased dynamic loading amplitude for a fixed contact load. There were N=12 plugs in each group, though the stress/strain curve is calculated for the entire chamber undergoing loading.

To study whether different loading combinations had an effect on cartilage cell viability, live/dead cell staining was used at the end of 7 days for two plugs in each group (Figure 11). Staining demonstrated no changes in cell viability at the macroscale between different contact and dynamic loading amplitude groups.

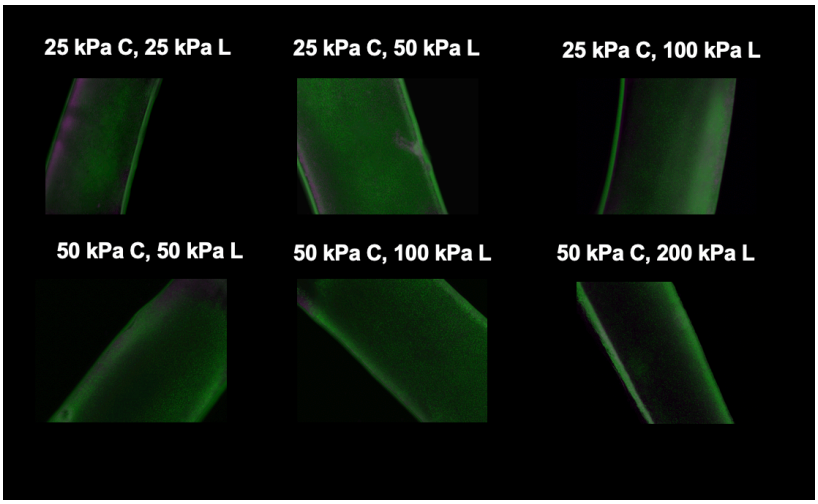

Figure 11. Cell Viability for Varying Contact and Dynamic Loading Amplitudes (Bovine Tissue). Green: live cells; magenta: dead cells; C: contact load; L: dynamic load. Cell viability did not decrease as both contact load and dynamic load amplitude increased after 7 days. There were N=2 plugs taken for staining from each condition, and figure is a representative image taken from each group.

4.1.2 *Human Knee and Ankle*

With the understanding that human and bovine cartilage differ in terms of mechanical properties[179], and that an ideal system for studying OA would include bone attached to cartilage, the contact and dynamic loads used on bovine cartilage are likely to produce a strain that is different when placed on human cartilage. Knee joints from two human donors were first utilized to apply similar experimental testing used on bovine joints in order to determine the effect of varying load amplitudes on human tissue. Due to the difficulty in achieving cartilage contact of all explants with cartilage-bone plugs of varying heights (due to crumbling bone), a displacement-controlled contact strain was fixed at 10%, and four dynamic amplitude loads were tested (100 kPa, 200 kPa, 500 kPa, 1 MPa). After a single

session of loading, compressive displacement increased non-linearly with increases in dynamic loading amplitude (0.18 mm, 0.55 mm, 1.25 mm, 1.53 mm for 100 kPa, 200 kPa, 500 kPa and 1 MPa, Figure 12). Based on these results, it was decided that in order to have loading fall within the 20-30% strain range studied by Li et. al. and shown to be reflective of physiologically relevant daily loading[29-31], a 10% contact strain with a 100 kPa dynamic load would be optimal for human cartilage-bone explants. The consideration of multiple loading session over a 7 day experiment described in 4.1.1 was also considered for human tissue.

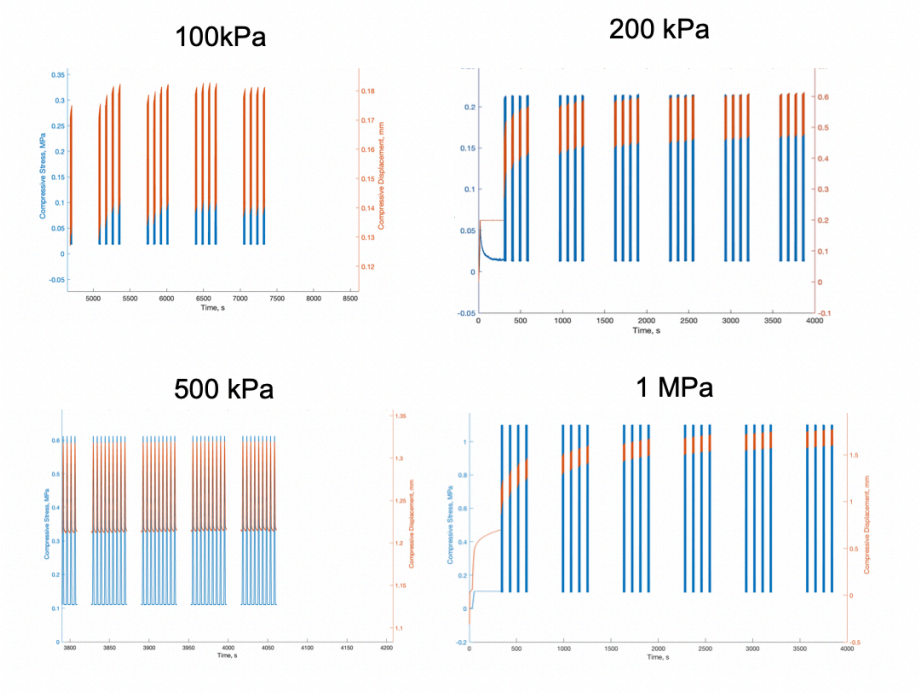

Figure 12. Representative Loading Stress/Strain Curves for Varying Dynamic Loading Amplitudes (Human Tissue). Contact was fixed at 10% and displacement-controlled, due to the difficulty in achieving complete contact of all plugs with varying heights of bone. Four dynamic loading amplitudes were superimposed on this contact strain for the same loading protocol. Orange curve represents compressive displacement, and blue curve represents compressive stress. Compressive displacement increased with increased dynamic load, with 100 kPa amplitude closest to the 25 kPa contact, 25 kPa dynamic load effects on total strain in bovine cartilage. There were N=16 plugs in each group, though the stress/strain curve is calculated for the entire chamber undergoing loading.

Cartilage cell viability was also studied in human tissue for three different dynamic loading amplitudes (100 kPa, 200 kPa, 500 kPa) at the end of 7 days. Human

cartilage has decreased chondrocyte cellularity as compared to bovine tissue, and thus macroscale viability changes may be easier to see for a given time period. Staining demonstrated slight decreases in cell viability as dynamic load increased, cementing the decision to use the 100 kPa loading amplitude to maximize cartilage tissue health in future experiments.

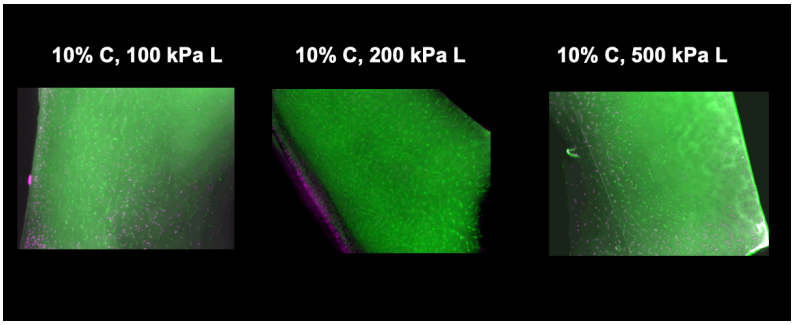

Figure 13. Cell Viability for Varying Dynamic Loading Amplitudes (Human Tissue). Green: live cells; magenta: dead cells; C: contact load; L: dynamic load. Cell viability decreased slightly at the macroscale as dynamic load amplitude increased after 7 days. There were N=2 plugs taken for staining from each condition, and figure is a representative image taken from each group.

Having decided upon an optimal contact strain and dynamic loading amplitude for human cartilage-bone explants, the effect of loading session frequency was tested. Human cartilage-bone explants from the ankle joint were placed in LGCCM with either cytokines (100 ng/mL TNFα, 50 ng/mL IL-6, and 250 ng/mL sIL-6R) to model a disease state or media alone, and both groups were either unloaded, loaded for one session a day (1 hour total), or loaded for two sessions a day (2 hours total), for 7 days. Loading for all groups was a 10% contact and 100 kPa load, and total loading strain was within the 20-30% for all plugs (Figure S1). Live/dead cell staining revealed greatly increased cell death in response to cytokines in the unloaded condition (Figure 14). Loading appeared to rescue cytokine-induced cell death in both the 1X and 2X per day loading groups, with no significant differences between the two.

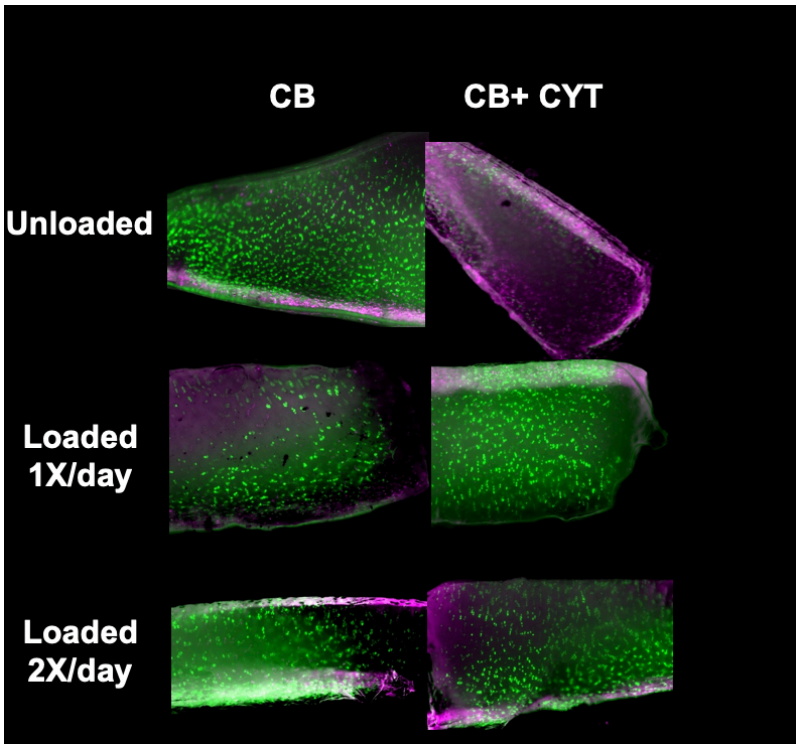

Figure 14. Loading Frequency Study: Unloaded and Loaded Cell Viability. Green: live cells; magenta: dead cells; CB: cartilage-bone explant; CYT: cytokines. Cell viability was greatly decreased in the unloaded condition for the CB + CYT group, which was rescued in both loaded groups. There was no significant differences in cell death between the 1X and 2X per day loaded groups. There were N=2 plugs taken for staining from each condition, and figure is a representative image taken from each group.

In terms of biochemistry, there were no significant differences in DNA content or wet weight between any groups (unloaded and loaded, with and without cytokines) after 7 days (Figure S2). [S^{35}] incorporation demonstrated a decrease in GAG biosynthesis with the addition of cytokines for both loaded and unloaded conditions to the same extent, without any differences between the once and twice per day loading groups (Figure 15). Notably, biosynthesis was increased in the loaded 1X CB condition without cytokines, which was further increased in the loaded 2X CB group in a linear fashion. Though there were no significant differences in GAG loss detected in the media, the addition of cytokines did slightly increase GAG loss for both loaded and unloaded groups. Loading at both 1X and 2X per day did not appear to affect GAG loss within the media-alone and cytokine groups.

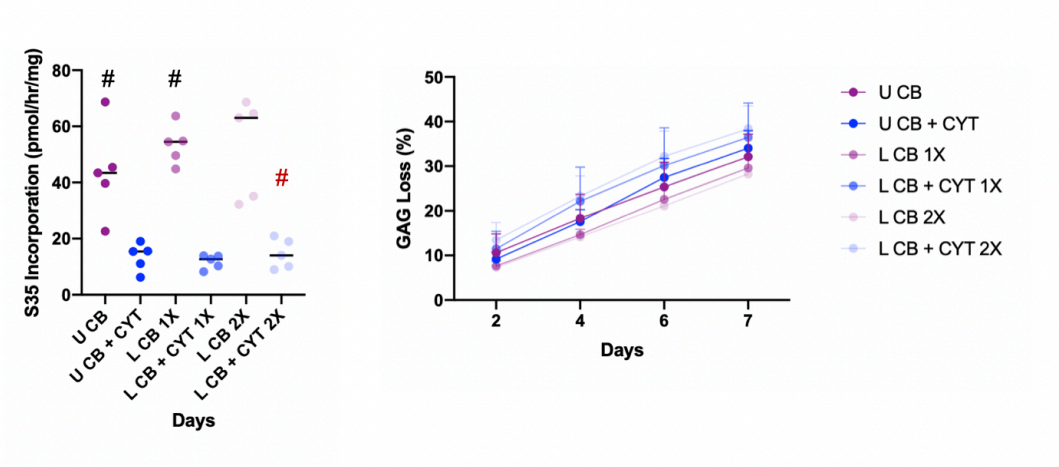

Figure 15. Loading Frequency Study: Biosynthesis and GAG Loss. U: unloaded; L: loaded; CB: cartilage-bone explant; CYT: cytokines. # $p<0.05$ as compared to L CB + CYT 1X; # $p<0.05$ as compared to L CB 1X using Kruskal-Wallis test. GAG biosynthesis was decreased in both loaded and unloaded CB + CYT groups, and was increased in both loaded CB groups from their unloaded equivalent. There were no significant differences in GAG loss between groups, though the addition of cytokines slightly increased GAG loss for both loaded and unloaded conditions.

While an effect on GAG biosynthesis and GAG loss was present, there were no significant differences in both cartilage and bone content between unloaded and loaded groups (Figure 16). In general, collagen content in bone was around a quarter to half that found in cartilage. Additionally, NO concentration released by cells into the media was determined for pooled media samples for each group at each time point (Figure 17). Media NO concentration was slightly increased with the addition of cytokines for all groups on days 2, 4 and 6, though concentrations became equal to their non-cytokine counterpart groups by day 7. Loading appeared to slightly decrease media NO concentration on days 2-6 for CB + CYT groups, but not for CB groups. There were no differences in media NO concentration for CB and CB + CYT groups between loading 1X vs. 2X per day.

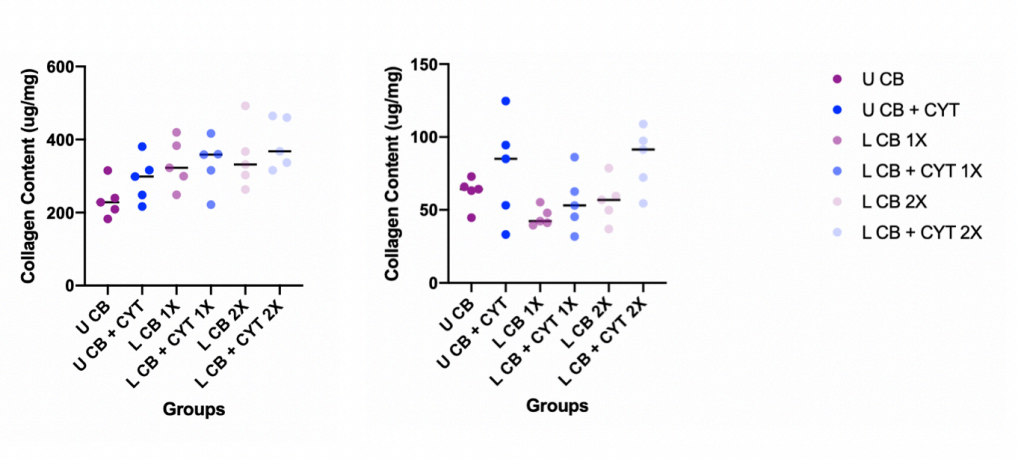

Figure 16. Loading Frequency Study: Cartilage and Bone Collagen Content. U: unloaded; L: loaded; CB: cartilage-bone explant; CYT: cytokines. There were no significant differences in cartilage or bone collagen content between all groups, though collagen content in bone was about a quarter to half that in cartilage, in general.

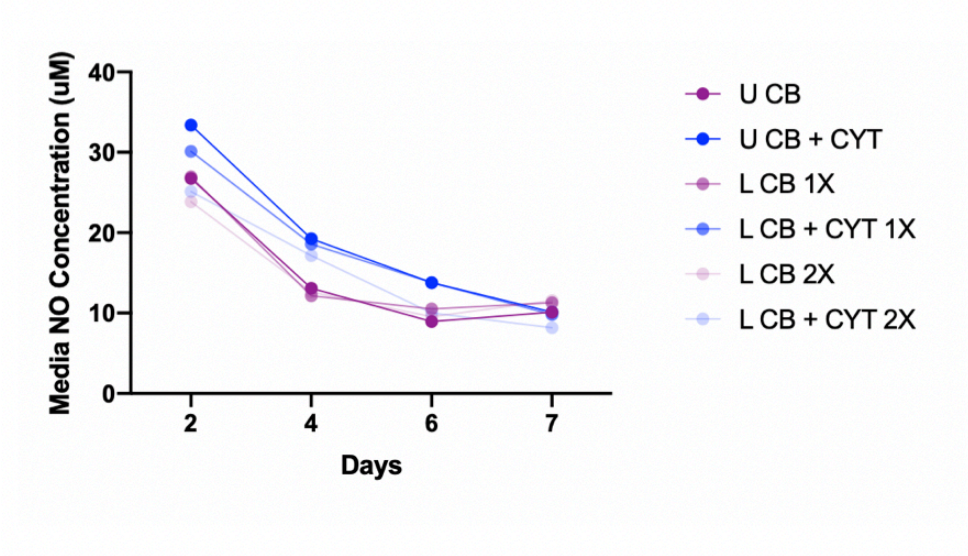

Figure 17. Loading Frequency Study: Media NO Content. U: unloaded; L: loaded; CB: cartilage-bone explant; CYT: cytokines. Pooled media for all plugs in each group at each time point created an inability to perform statistical testing on results. Media NO concentration was slightly increased with the addition of cytokines for all groups on days 2-6, though concentrations became equal to their non-cytokine counterpart groups by day 7. Loading appeared to slightly decrease media NO concentration on days 2-6 for CB + CYT groups.

Overall, the loading frequency study demonstrated that the addition of cytokines to human ankle tissue caused decreases in cell viability and GAG biosynthesis, as well as increases in GAG loss and NO release, and that loading the tissue once and twice per day had similar effects on explants with no “dose-dependent” results. With this

in mind, it was decided that for future biological and mechanical experiments described in 4.2 and 4.3, loading would be kept to one session per day, with the additional benefit of keeping the loading protocol as physiologically relevant as possible.

4.2 Biologic Effect of Loading with Dexamethasone and IGF-1

Both bovine (cartilage only) and human (cartilage-bone) explants were used to test the effects of dexamethasone and IGF-1 with dynamic loading on an OA disease model using exogenous cytokines. Bovine cartilage came from the knee joint and human cartilage came from the ankle joint, each from three donors (Table 2). Experiments for biochemistry and cell viability lasted 7 days (one human donor lasted 13 days), and experiments for gene expression (PCR) lasted one day (Figure 18). Based on previous studies, the cytokine concentrations used for the bovine disease model were 25 ng/mL TNFα, 50 ng/mL IL-6, and 250 ng/mL sIL-6R, while that used for the human model were 100 ng/mL TNFα, 50 ng/mL IL-6, and 250 ng/mL sIL-6R, based on concentrations used successfully to create a disease model from previous studies in the lab.[13,17] For both models, Dex and IGF-1 concentrations remained the same at 100 nM[17,137,180] and 100 ng/ml[13,17], respectively. The results below demonstrate the effect of dynamic loading, Dex, and IGF-1 on cell viability, wet weight, DNA content, GAG loss, GAG biosynthesis, collagen content, media cytokine/NO levels, and gene expression.

Animal	ID	Tissue	Date of arrival	Sex/Age	Collin's Grade	BMI	Experiment Length (Days)
Bovine	Donor 1	Knee	08/05/20	-	-	-	7
Bovine	Donor 2	Knee	08/18/20	-	-	-	7
Bovine	Donor 3	Knee	09/01/20	-	-	-	7
Bovine	Donor 4	Knee	11/15/20	-	-	-	1 (PCR)
Bovine	Donor 5	Knee	08/03/21	-	-	-	1 (PCR)
Bovine	Donor 6	Knee	08/03/21	-	-	-	1 (PCR)
Human	Donor 1	Ankle	10/11/20	M/59	1	30.4	7
Human	Donor 2	Ankle	11/05/20	F/54	1	25.7	7
Human	Donor 3	Ankle	12/01/20	M/60	1	37.6	13

Table 2. Bovine and Human Donor Characteristics for Biological Studies. Cartilage-only plugs were taken from six bovine donor knees (three for 7-day experiments, three for 1-day PCR), while cartilage-bone

explants were taken from three human donor ankles. For human donors, this table outlines the sex, age, BMI and Collin's grade of each joint.

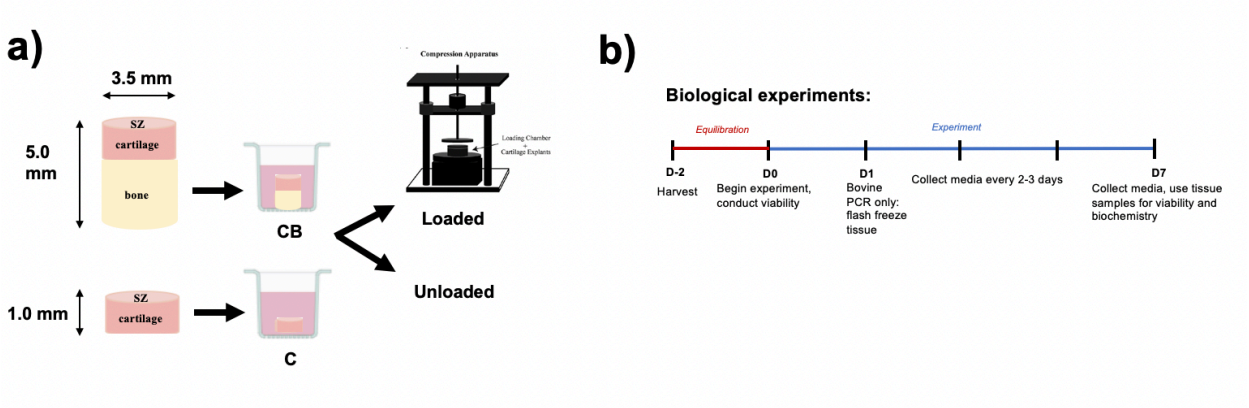

Figure 18. Experimental Setup for Biological Studies. SZ: superficial zone; CB: cartilage-bone explant; C: cartilage-only explant. Cartilage-only explants were used for bovine studies, while cartilage-bone explants were used for human studies (a). In both cases, cartilage was loaded or unloaded for 7 days (one human experiment was 13 days) with different treatment conditions, and media was collected every 2-3 days (b). On the last day of the experiment, tissue samples were collected to test for cell viability, wet weight, DNA content, GAG loss, GAG biosynthesis, collagen content, and media cytokine/NO levels. One day studies were also conducted with bovine tissue to better understand gene expression with Dex and IGF-1 after loading.

4.2.1 *Bovine Knee*

Studies with bovine cartilage-only explants were conducted prior to analyzing human tissue, and three donors were studied over the course of 7 days each. Loading for all groups consisted of a 25 kPa contact and 25 kPa dynamic load as determined in the loading optimization studies outlined in 4.1. With this protocol, total loading strain was within the 20-35% for all plugs, with donors 2 and 3 at the higher end of this range (Figure S3). In the unloaded condition, live/dead cell staining at 7 days demonstrated slightly increased cell death in the cytokine group for all donors (Figure 19). Dexamethasone on cartilage alone did not change cell viability from baseline, though with cytokines it appeared to rescue cell viability for donors 1 and 3, but not donor 2. Under loading, cell viability was greatly increased with cytokines as compared to the same condition without loading for donors 1 and 2 (Figure 20). Additionally, under loading, Dex alone appeared to increase cell viability slightly from the baseline condition for donors 1 and 2. Dex with cytokines improved cell viability as compared to cytokines alone for donors 1

and 3 under loading, which appeared to rescue viability to a greater extent than the unloaded equivalent conditions. For donor 2, the addition of Dex with cytokines decreased cell viability as compared to cytokines alone.

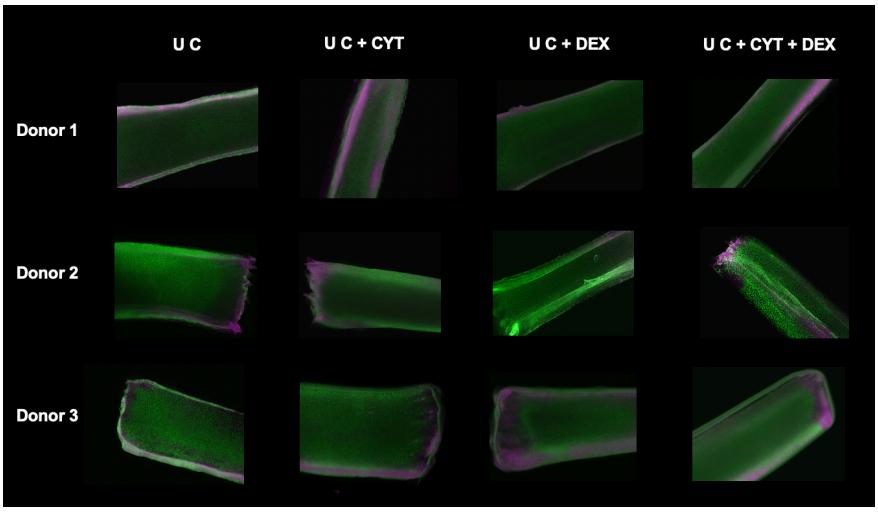

Figure 19. Bovine Biologic Study: Unloaded Cell Viability. Green: live cells; magenta: dead cells; U: unloaded; L: loaded; C: cartilage-only explant; CYT: cytokines; DEX: dexamethasone. Cell viability decreased slightly after 7 days with the addition of cytokines. Dex alone did not change viability, though Dex with cytokines did rescue cell viability for donors 1 and 3 at the macroscale. There were N=2 plugs taken for staining from each condition, and figure is a representative image taken from each group.

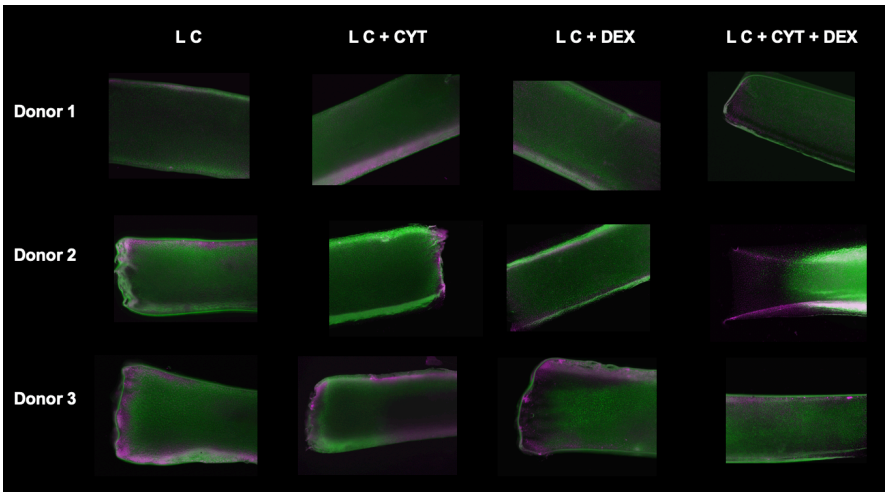

Figure 20. Bovine Biologic Study: Loaded Cell Viability. Green: live cells; magenta: dead cells; U: unloaded; L: loaded; C: cartilage-only explant; CYT: cytokines; DEX: dexamethasone. Cell viability decreased slightly after the addition of cytokines after 7 days. Viability was increased for donors 1 and 2 with the addition of Dex alone as compared to baseline conditions. For donors 1 and 3, cell viability was increased with cytokines and Dex as compared to cytokines alone. There were

N=2 plugs taken for staining from each condition, and figure is a representative image taken from each group.

There were significant differences in DNA content for donor 1 between two groups: 1) unloaded cartilage alone and with Dex, with lower DNA content, and 2) loaded cartilage alone and unloaded cartilage with cytokines, with higher DNA content (Figure S4). These changes were not seen for the other donors, and there were no notable differences in wet weight between groups after 7 days. [S^{35}] incorporation demonstrated a decrease in GAG biosynthesis with addition of cytokines in both the loaded and unloaded conditions, to a more significant extent in donor 1 (Figure 21). Dex alone increased biosynthesis in the unloaded condition for donors 1 and 3. However, in the loaded condition this increase with Dex alone was not seen. For all donors, Dex did not rescue the decrease in biosynthesis seen in cytokine-charged cartilage, both with and without loading. The addition of Dex did not affect GAG loss as compared to cartilage alone, for both unloaded and loaded conditions (Figure 22). GAG loss was increased with cytokines for all donors, with and without loading. Dex was able to rescue some GAG loss in cytokine-charged cartilage for donor 3 and the unloaded condition, and donors 1 and 3 in the loaded condition.

There were no significant differences in cartilage collagen content for donors 1 and 2 (Figure 23). For donor 3, Dex alone in the unloaded condition, as well as all loaded conditions, increased collagen content as compared to unloaded cartilage alone. Media NO concentration was increased with the addition of cytokines for all donors in loaded and unloaded conditions, which was unchanged by the addition of Dex. The addition of Dex alone did not change NO levels from baseline, with and without loading. Loading did not affect NO levels in any treatment condition for all donors.

Reverse transcription PCR was used to quantify gene expression after one day of loading with both Dex and IGF-1 treatment conditions. There were no significant differences in levels due to a low number of animal donors (3), though trends were

apparent. Genes of extracellular matrix proteins aggrecan and collagen II were downregulated in the presence of cytokines, though loading increased these slightly. Loading also increased gene expression of these proteins without cytokines. Dex and IGF-1 treatments with cytokines did not affect aggrecan expression but Dex in the unloaded condition only did increase collagen II expression, as compared to cytokines alone. Dex and IGF-1 treatments to cartilage alone slightly increased expression of these proteins in the unloaded condition, though loading inhibited these increases.

Expression of the MMPs ADAMTS5 and ADAMTS4 was increased in the presence of cytokines as compared to cartilage alone, and this was slightly decreased when Dex (both loaded and unloaded) and IGF-1 (loaded only) was added to cytokines. When both drugs were added to cartilage alone, or cartilage alone was loaded, expression was greatly decreased from that of unloaded cartilage alone.

Expression of the pro-apoptotic protein caspase-3 was increased in the presence of cytokines, and this value was decreased when loading was added, and when Dex and IGF-1 (both unloaded and loaded) were added as treatments. When both drugs were added to cartilage alone, or cartilage alone was loaded, expression was decreased from that of unloaded cartilage alone.

Genes for proteins involved in inflammation, NFkB and iNOS were upregulated in all cytokine-treated conditions, with and without loading. Neither loading nor Dex or IGF-1 had an effect on expression when added to cytokines. There were no trends demonstrating differences in gene expression between treatment groups for genes MAPK1 and COX2.

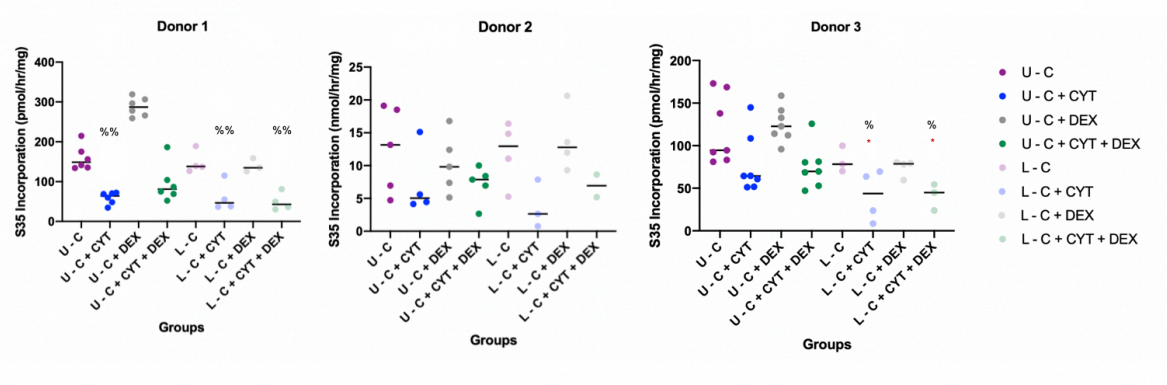

Figure 21. Bovine Biologic Study: GAG Biosynthesis. U: unloaded; L: loaded; C: cartilage-only explant; CYT: cytokines; DEX: dexamethasone. %/%% $p<0.05/0.01$ as compared to U C + DEX; * $p<0.05$ as compared to U C using Kruskal-Wallis test. GAG biosynthesis was decreased in the C + CYT group for all donors in the unloaded condition. Dex alone increased biosynthesis for donors 1 and 3, though this increase was not seen in its loaded equivalent. Dex did not rescue the decrease in biosynthesis for all donors, both in the unloaded and loaded conditions.

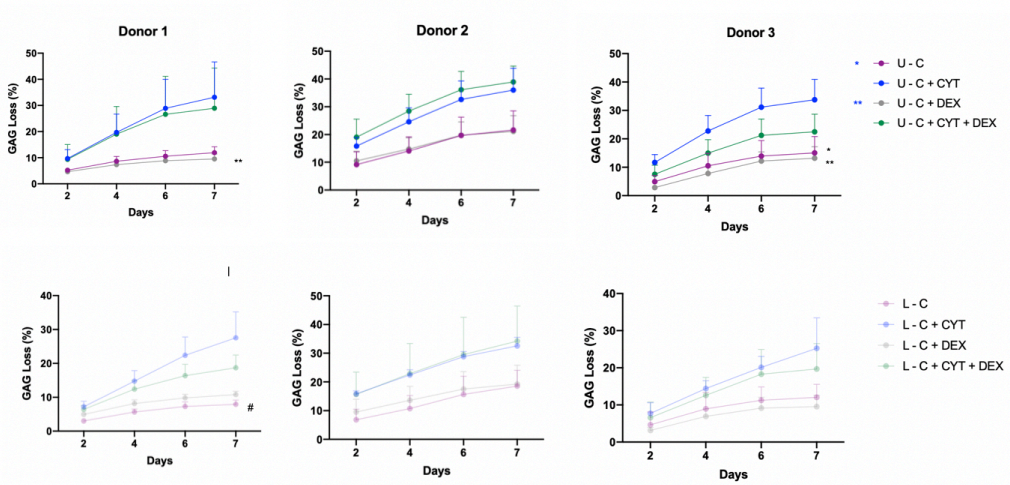

Figure 22. Bovine Biologic Study: GAG Loss. U: unloaded; L: loaded; C: cartilage-only explant; CYT: cytokines; DEX: dexamethasone. */** $p<0.05/0.01$ as compared to U C + CYT; # $p<0.05$ as compared to L C + CYT using Kruskal-Wallis test. The addition of Dex did not affect GAG loss as compared to cartilage alone, for both unloaded and loaded conditions. GAG loss was increased with cytokines for all donors, with and without loading. Dex was able to rescue some GAG loss in cytokine-charged cartilage for donor 3 and the unloaded condition, and donors 1 and 3 in the loaded condition.

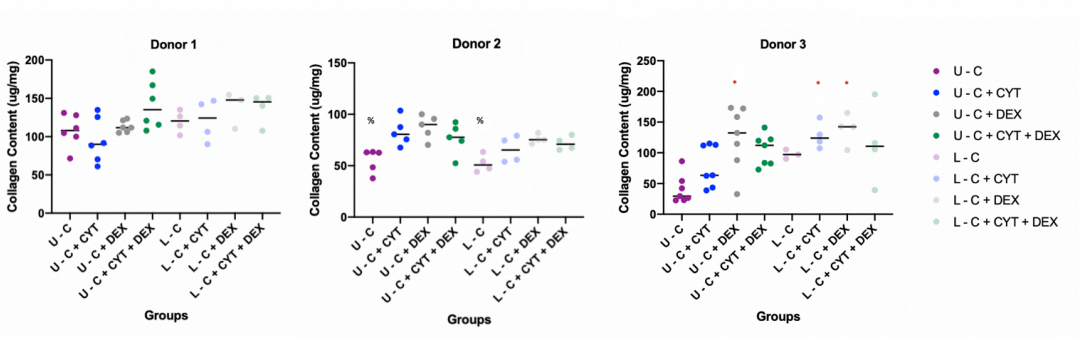

Figure 23. Bovine Biologic Study: Collagen Content. U: unloaded; L: loaded; C: cartilage-only explant; CYT: cytokines; DEX: dexamethasone. % $p<0.05$ as compared to U C + DEX; * $p<0.05$ as compared to U C using Kruskal-Wallis test. There were no significant differences in cartilage collagen content for donors 1 and 2. For donor 3, Dex alone in the unloaded condition, as well as all loaded conditions, increased collagen content as compared to unloaded cartilage alone.

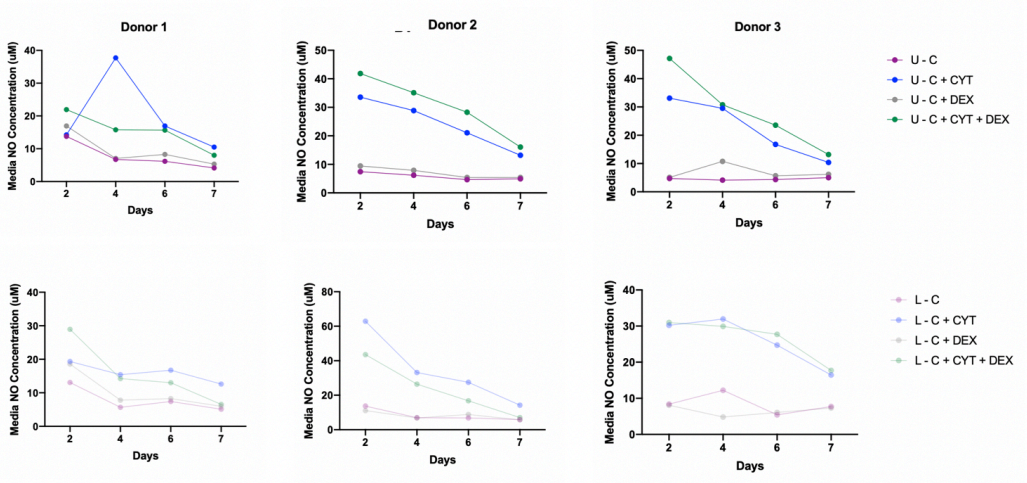

Figure 24. Bovine Biologic Study: Media NO Concentration. U: unloaded; L: loaded; C: cartilage-only explant; CYT: cytokines; DEX: dexamethasone. Pooled media for all plugs in each group at each time point created an inability to perform statistical testing on results. Media NO concentration was increased with the addition of cytokines for all donors in loaded and unloaded conditions, which was unchanged by the addition of Dex. The addition of Dex alone did not change NO levels from baseline, with and without loading. Loading did not affect NO levels for any treatment condition.

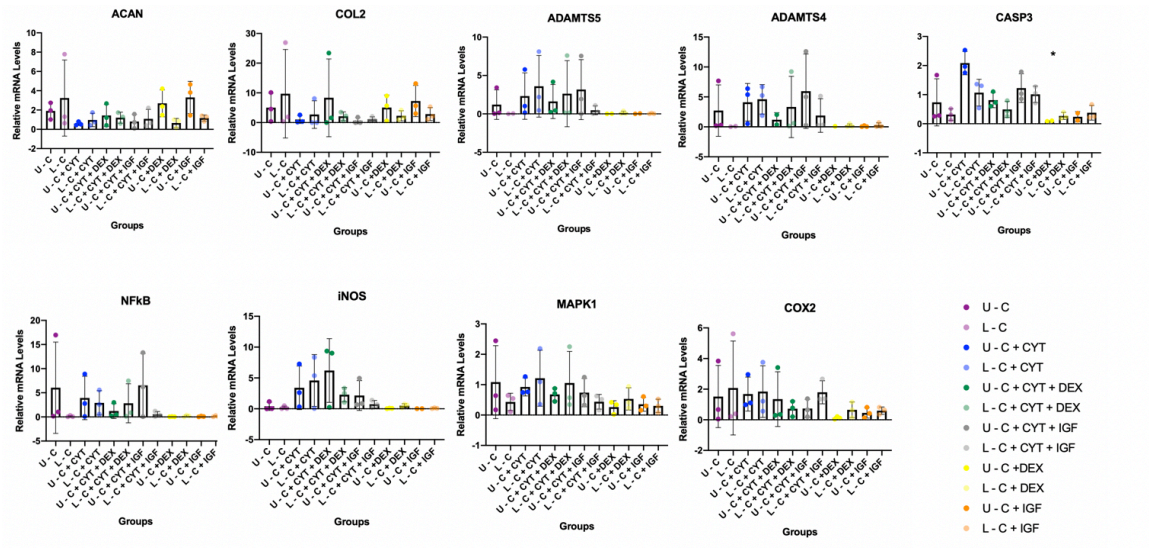

Figure 25. Bovine Biologic Study: Gene Expression. U: unloaded; L: loaded; C: cartilage-only explant; CYT: cytokines; DEX: dexamethasone; IGF: Insulin-like growth factor-1. Cartilage plugs in each condition were pooled for mRNA extraction. Gene expression levels were normalized to beta-actin within each treatment group, and then normalized to day 0 cartilage controls for each animal which have an expression level = 1. * $p<0.05$ as compared to U C + CYT using Kruskal-Wallis test.

4.2.2 *Human Ankle*

Studies with human cartilage-bone explants were conducted using three ankle donors, studied over the course of 7 days for two donors and 13 days for one donor. Loading for all groups consisted of a 10% contact strain and 100 kPa dynamic load as determined in the loading optimization studies outlined in 4.1. With this protocol, total loading strain was within the 15-30% for all plugs, with donors 1 and 2 at the higher end of this range (Figure S5). In the unloaded condition, live/dead cell staining demonstrated increased cell death for donors 2/3 and slightly increased cell death for donor 1 in the cytokine group (Figure 26). Both Dex and IGF-1 rescued some cell viability on cytokine-charged cartilage. Notably however, donor 3 had decreased cell viability at baseline. Under loading, cell viability was decreased with cytokines, but was not as extensive as compared to the unloaded equivalent (Figure 27). Cytokines particularly had a negative impact on viability for donor 3 under loading, but viability was still improved from the unloaded condition. Dex and IGF-1 were used for the 13 day study only with donor 3 – these showed a rescue in viability compared to the cytokine condition.

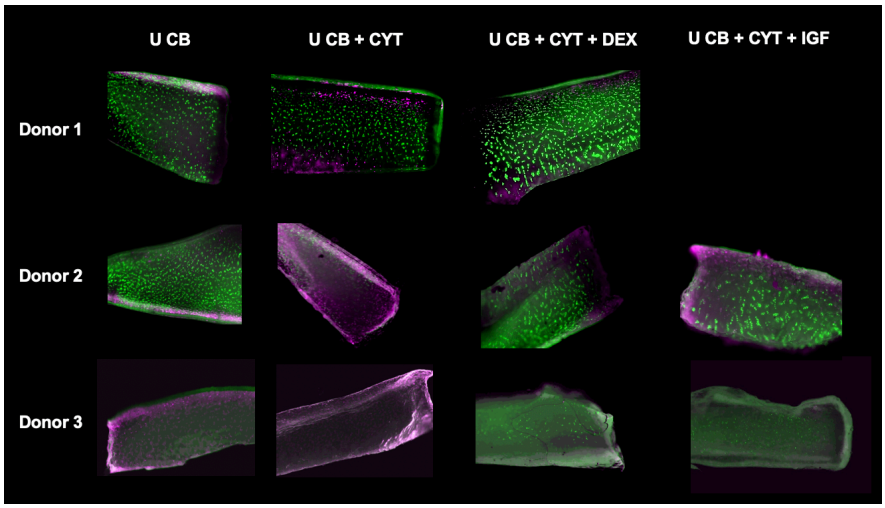

Figure 26. Human Biologic Study: Unloaded Cell Viability. Green: live cells; magenta: dead cells; U: unloaded; L: loaded; CB: cartilage-bone explant; CYT: cytokines; DEX: dexamethasone; IGF: Insulin-like growth factor-1. There was increased cell death for donors 2/3 and slightly increased cell death for donor 1 in the cytokine group. Both Dex and IGF-1 rescued some cell viability on cytokine-charged cartilage. Donor 3 had decreased cell viability at baseline. There were N=2 plugs taken for staining from each condition, and figure is a representative image taken from each group.

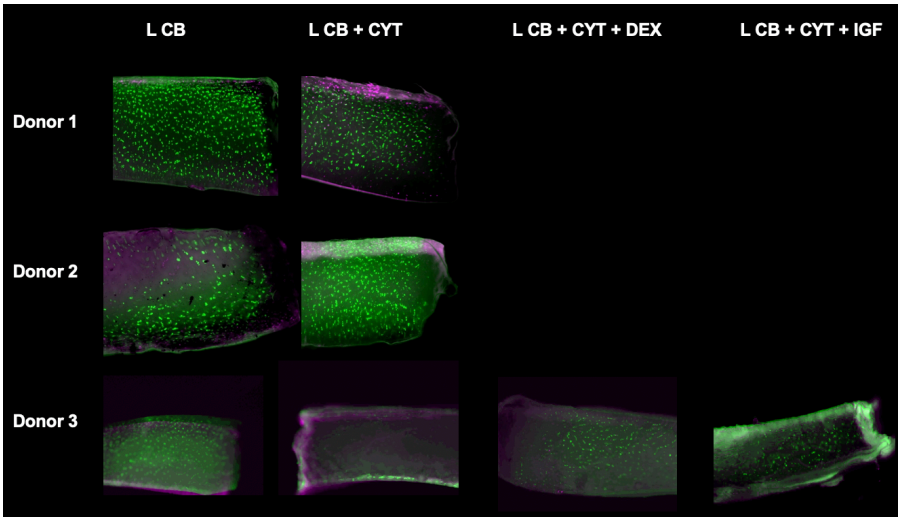

Figure 27. Human Biologic Study: Loaded Cell Viability. Green: live cells; magenta: dead cells; U: unloaded; L: loaded; CB: cartilage-bone explant; CYT: cytokines; DEX: dexamethasone; IGF: Insulin-like growth factor-1. Cell viability was decreased with cytokines, but was not as extensive as compared to the unloaded equivalent. Cytokines particularly had a negative impact on viability for donor 3 under loading, but viability was still improved from the unloaded condition. Dex and IGF-1 were used for the 13 day study only with donor 3 – these showed a rescue in viability compared to the cytokine condition. There were N=2 plugs taken for staining from each condition, and figure is a representative image taken from each group.

There were no significant differences in DNA content for all donors. For donor 1, there was a significantly higher wet weight in the loaded CB groups as compared to its unloaded equivalent (Figure S6), but no other notable differences. [S^{35}] incorporation demonstrated a decrease in GAG biosynthesis with addition of cytokines in the unloaded condition for all donors (Figure 28). Biosynthesis was increased with the addition of Dex for donor 1 only – for donors 2 and 3, the addition of Dex and IGF-1 did not rescue biosynthesis in the disease model. Under loading, cartilage-bone plugs alone experienced an increase in biosynthesis for donors 2 and 3 to that above its unloaded equivalent. Under loading, the addition of cytokines, as well as cytokines with Dex and IGF-1, did not alter biosynthesis levels from the disease model condition in the unloaded state. GAG loss was increased with cytokines in the unloaded condition for all donors, and in the loaded condition for donors 2/3 (Figure 29). In the unloaded condition, the addition of Dex to cytokines lowered GAG loss levels to that of cartilage-bone alone for all donors, and the addition of IGF-1 did not alter GAG loss from that of the cytokine-charged cartilage. Under loading, studied for donor 3, GAG loss was further decreased with the addition of Dex to cytokines from its unloaded equivalent, while GAG loss was further increased with the addition of IGF-1.

In the unloaded condition, the addition of Dex with cytokines increased bone collagen content to a significant extent in donor 1, and Dex also significantly increased cartilage collagen content in donor 2 (Figure 30). Media NO concentration was increased with the addition of cytokines on days 2-6 for donors 1/2, and on days 3-12 for donor 3, for both the unloaded and loaded conditions (Figure 31). Loading did not alter NO concentration levels for each treatment group. The addition of Dex to cytokines in the unloaded condition decreased NO release from the cytokine-alone group for donors 1/2 on days 2-6, and the addition of IGF-1 did not alter NO levels. Under loading for donor 3, both Dex and IGF-1 decreased NO levels from the cytokine-alone group on days 3 and 6.

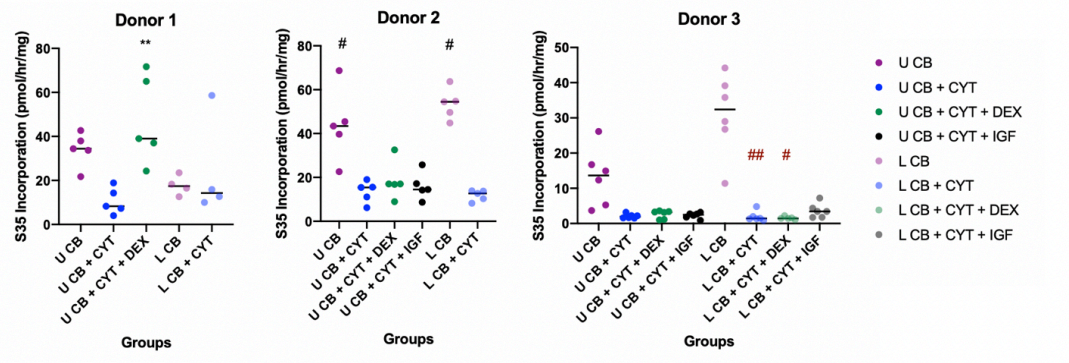

Figure 28. Human Biologic Study: GAG Biosynthesis. U: unloaded; L: loaded; CB: cartilage-bone explant; CYT: cytokines; DEX: dexamethasone; IGF: Insulin-like growth factor-1. ** $p<0.01$ as compared to U CB + CYT; # $p<0.05$ as compared to L CB + CYT; #/## $p<0.05/0.01$ as compared to L CB using Kruskal-Wallis test. Biosynthesis was decreased with cytokines in the unloaded condition for all donors. It was further increased with the addition of Dex for donor 1 only – for donors 2 and 3, the addition of Dex and IGF-1 did not rescue biosynthesis in the disease model. Under loading, cartilage-bone plugs alone experienced an increase in biosynthesis for donors 2 and 3 to that above its unloaded equivalent. Under loading, the addition of cytokines, as well as cytokines with Dex and IGF-1, did not alter biosynthesis levels from the disease model condition in the unloaded state.

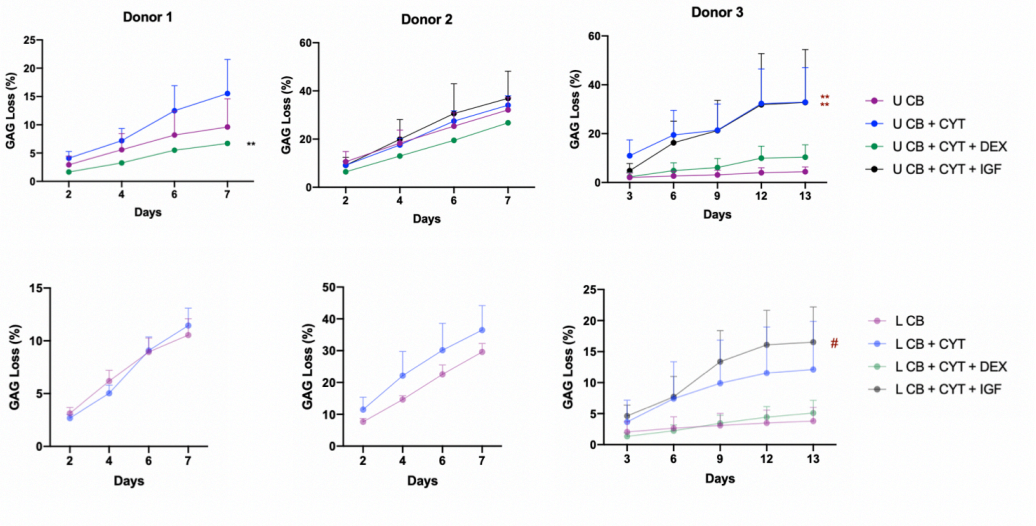

Figure 29. Human Biologic Study: GAG Loss. U: unloaded; L: loaded; CB: cartilage-bone explant; CYT: cytokines; DEX: dexamethasone; IGF: Insulin-like growth factor-1. ** $p<0.01$ as compared to U CB + CYT; # $p<0.05$ as compared to L CB; ** $p<0.01$ as compared to U CB using Kruskal-Wallis test. GAG loss was increased with cytokines in the unloaded condition for all donors, and in the loaded condition for donors 2/3. In the unloaded condition, the addition of Dex to cytokines lowered GAG loss levels to that of cartilage-bone alone for all donors, and the addition of IGF-1 did not alter GAG loss from that of the cytokine-charged cartilage. Under loading, studied for donor 3, GAG loss was further decreased with the addition of Dex to cytokines from its unloaded equivalent, while GAG loss was further increased with the addition of IGF-1.

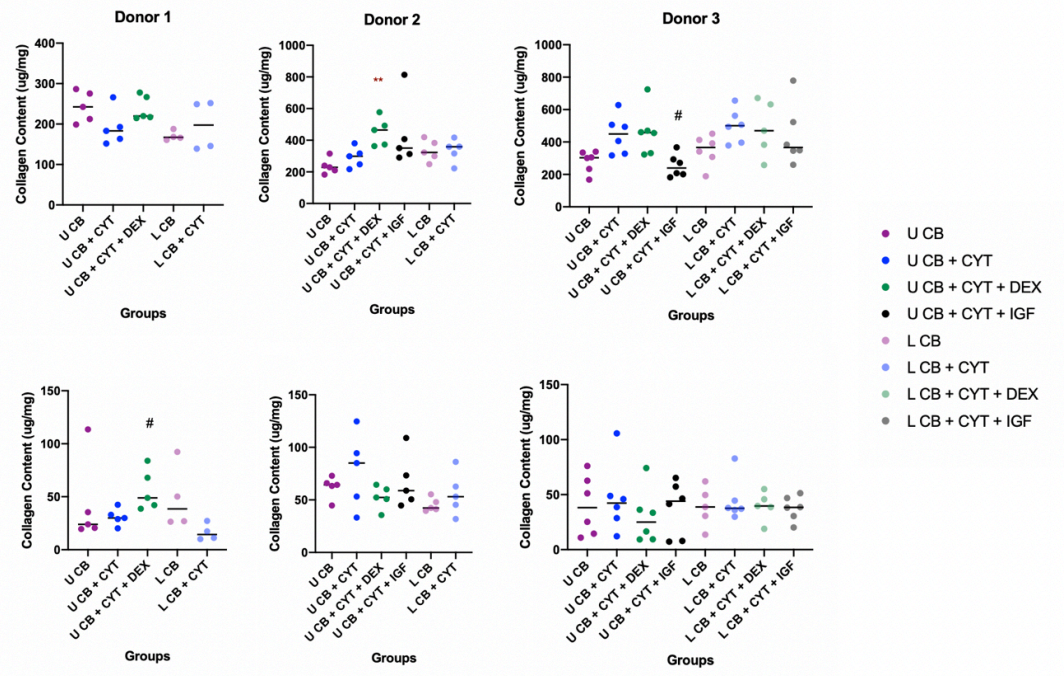

Figure 30. Human Biologic Study: Collagen Content. U: unloaded; L: loaded; CB: cartilage-bone explant; CYT: cytokines; DEX: dexamethasone; IGF: Insulin-like growth factor-1. # $p<0.05$ as compared to L CB + CYT; ** $p<0.01$ as compared to U CB using Kruskal-Wallis test. In the unloaded condition, the addition of Dex with cytokines increased bone collagen content to a significant extent in donor 1, and Dex also significantly increased cartilage collagen content in donor 2.

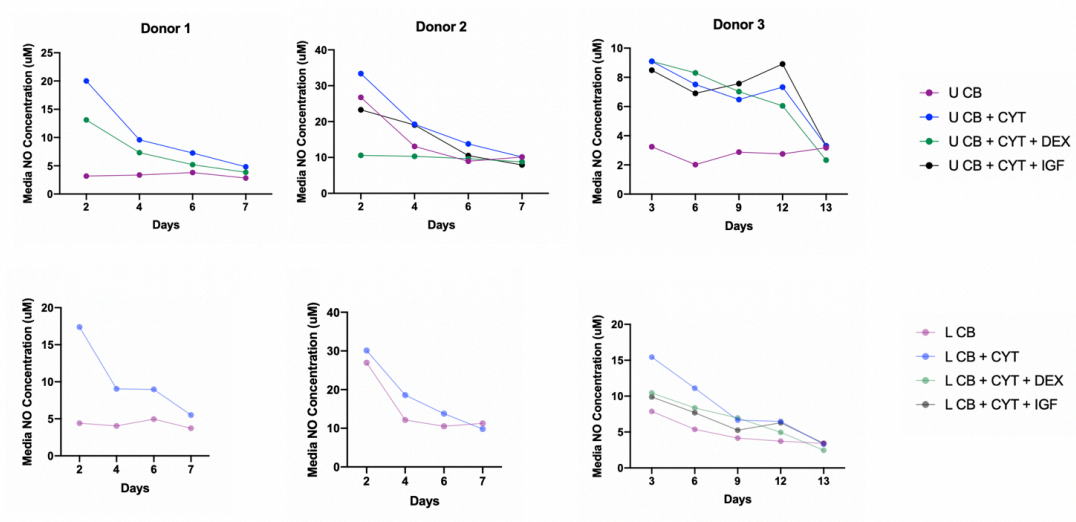

Figure 31. Human Biologic Study: Media NO Concentration. U: unloaded; L: loaded; C: cartilage-only explant; CYT: cytokines; DEX: dexamethasone; IGF: Insulin-like growth factor-1. Pooled media for all plugs in each group at each time point created an inability to perform statistical testing on results. Media NO concentration was increased with the addition of cytokines on days 2-6 for donors 1/2, and on days 3-12 for donor 3, for both the unloaded and loaded conditions (Figure 31). Loading did not alter NO concentration levels for each treatment group. The addition of Dex to

cytokines in the unloaded condition decreased NO release from the cytokine-alone group for donors 1/2 on days 2-6, and the addition of IGF-1 did not alter NO levels. Under loading for donor 3, both Dex and IGF-1 decreased NO levels from the cytokine-alone group on days 3 and 6.

For the 13 day study in donor 3, pooled media samples at four time points (days 3, 6, 9, 12) were collected to determine the concentrations of the pro-inflammatory cytokines using a sandwich ELISA (Figure 32). Both the unloaded and loaded cartilage-bone plugs alone had lower concentrations of all cytokines (except IL-8) as compared to all other groups, which were treated with exogenous cytokines. There was no clear difference in cytokine levels between explants treated with cytokines alone, and those treated with both cytokines and Dex or IGF-1.

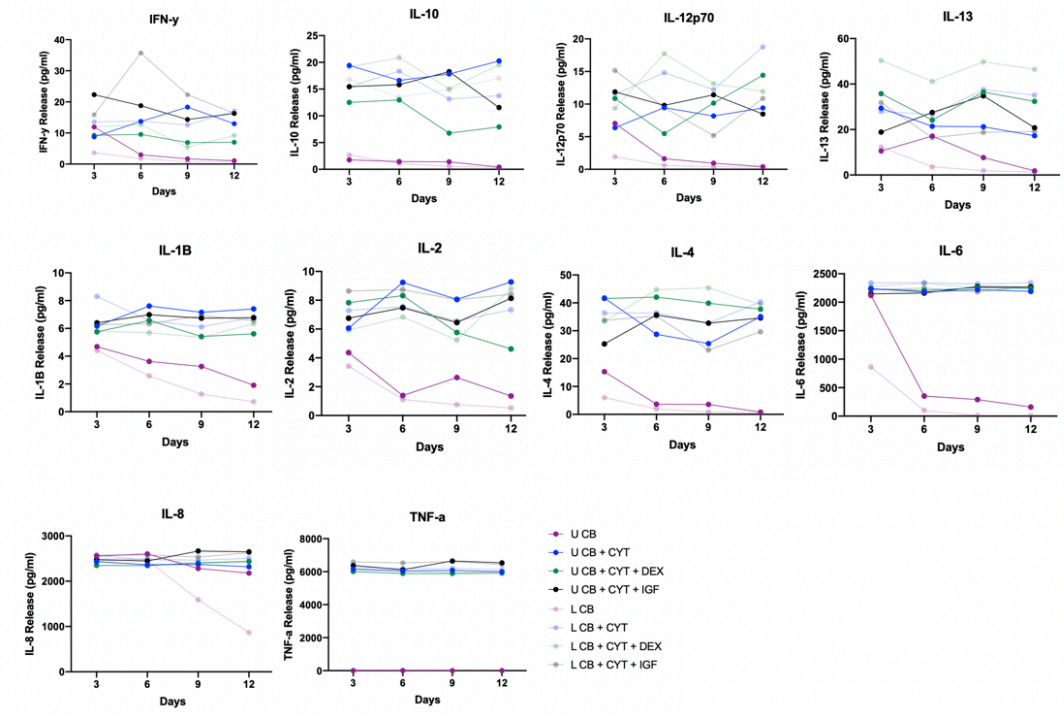

Figure 32. Human Biologic Study: Single-Donor Cytokine Profile. U: unloaded; L: loaded; C: cartilage-only explant; CYT: cytokines; DEX: dexamethasone; IGF: Insulin-like growth factor-1. Pooled media for all plugs in each group at each time point created an inability to perform statistical testing on results. Both the unloaded and loaded cartilage-bone plugs alone had lower concentrations of all cytokines (except IL-8) as compared to all other groups, which were treated with exogenous cytokines. There was no clear difference in cytokine levels between explants treated with cytokines alone, and those treated with both cytokines and Dex or IGF-1.

Studying the biologic impacts of cyclic loading on both bovine (cartilage only) and human (cartilage-bone) explants using similar strains revealed a significant amount

of donor variability in a cellular response to Dex and IGF-1, even though the addition of cytokines caused a consist disease-model effect. In those donors that responded to the molecules, as compared to the disease condition, Dex and IGF-1 both increased cell viability, and Dex increased GAG biosynthesis, decreased GAG loss, increased cartilage and bone collagen content, and decreased media NO release. These treatments also tended to increase expression of pro-anabolic genes (for collagen II) and decrease expression of pro-catabolic genes (for MMPs) as well as the pro-apoptotic gene for caspase-3. Loading alone did not have an effect on the disease model besides slightly rescuing cell viability, and increasing expression of genes for aggrecan and collagen II while decreasing expression of the gene for caspase-3. Loading increased Dex and IGF-1's effect on cell viability, and further increased GAG biosynthesis and decreased GAG loss seen with Dex, though there was also donor variability in this response to loading. Notably, donors that responded to loading also tended to respond to Dex and IGF-1. With these results, further insight was needed to better explain variability between donors. One possibility was that the donors differed in cartilage stiffness and permeability – those that were more stiff and less permeable would have decreased drug penetration into cartilage, decreasing the drugs cellular impact. Additionally, these properties would cause lowered strains and mechanotransduction for a given load amplitude, thus diminishing responses to loading. Thus, human cartilage-bone explants were used to test the differences in mechanical properties between donors at baseline, as well as after treatment with cytokines, and cytokines with Dex, both before and after loading.

4.3 Mechanical Effect of Loading with Dexamethasone

Human cartilage-bone explants were used to test the effects of dexamethasone on mechanical properties in response to loading, correlated with biological changes in an OA disease model using exogenous cytokines. Human cartilage came from the ankle joint, each from three donors (Table 3). Experiments for biochemistry and cell viability lasted 10 days, and tissue was used for mechanical testing before and after a 1 hour session of loading on day 0 and day 10 (Figure 33). Based on previous

studies, the cytokine concentrations used for the for the human disease model were that used in 4.2 (100 ng/mL TNFα, 50 ng/mL IL-6, and 250 ng/mL sIL-6R). The concentration of Dex used also remained the same at 100 nM.[17,137,180] Studies with human cartilage-bone explants were conducted using five ankle donors, studied over the course of 10 days. Loading for all groups consisted of a 10% contact strain and 100 kPa dynamic load as determined in the loading optimization studies outlined in 4.1. With this protocol, total loading strain was within the 15-25% for all plugs, with donor 3 at the higher end and donors 1 and 2 at the lower end of the range (Figure S7). The results below demonstrate the differences between donors at baseline and the effect of Dex of cartilage compressive equilibrium modulus, dynamic stiffness and hydraulic permeability, before and after loading. They also highlight changes in cell viability, wet weight, DNA content, GAG loss, GAG biosynthesis, collagen content, and media NO levels that occur with these mechanical changes

Animal	ID	Tissue	Date of arrival	Sex/Age	Collin's Grade	BMI	Experiment Length (Days)
Human	Donor 1	Ankle	08/26/21	M/53	1	41.8	10
Human	Donor 2	Ankle	08/26/21	M/73	0	31.6	10
Human	Donor 3	Ankle	11/03/21	M/47	1	41.4	10
Human	Donor 4	Ankle	01/15/22	M/47	1	30.0	10
Human	Donor 5	Ankle	01/28/22	M/70	0/1	37.9	10

Table 3. Human Donor Characteristics for Mechanical Studies. Cartilage-bone explants were taken from five human donor ankle pairs. This table outlines the sex, age, BMI and Collin's grade of each joint.

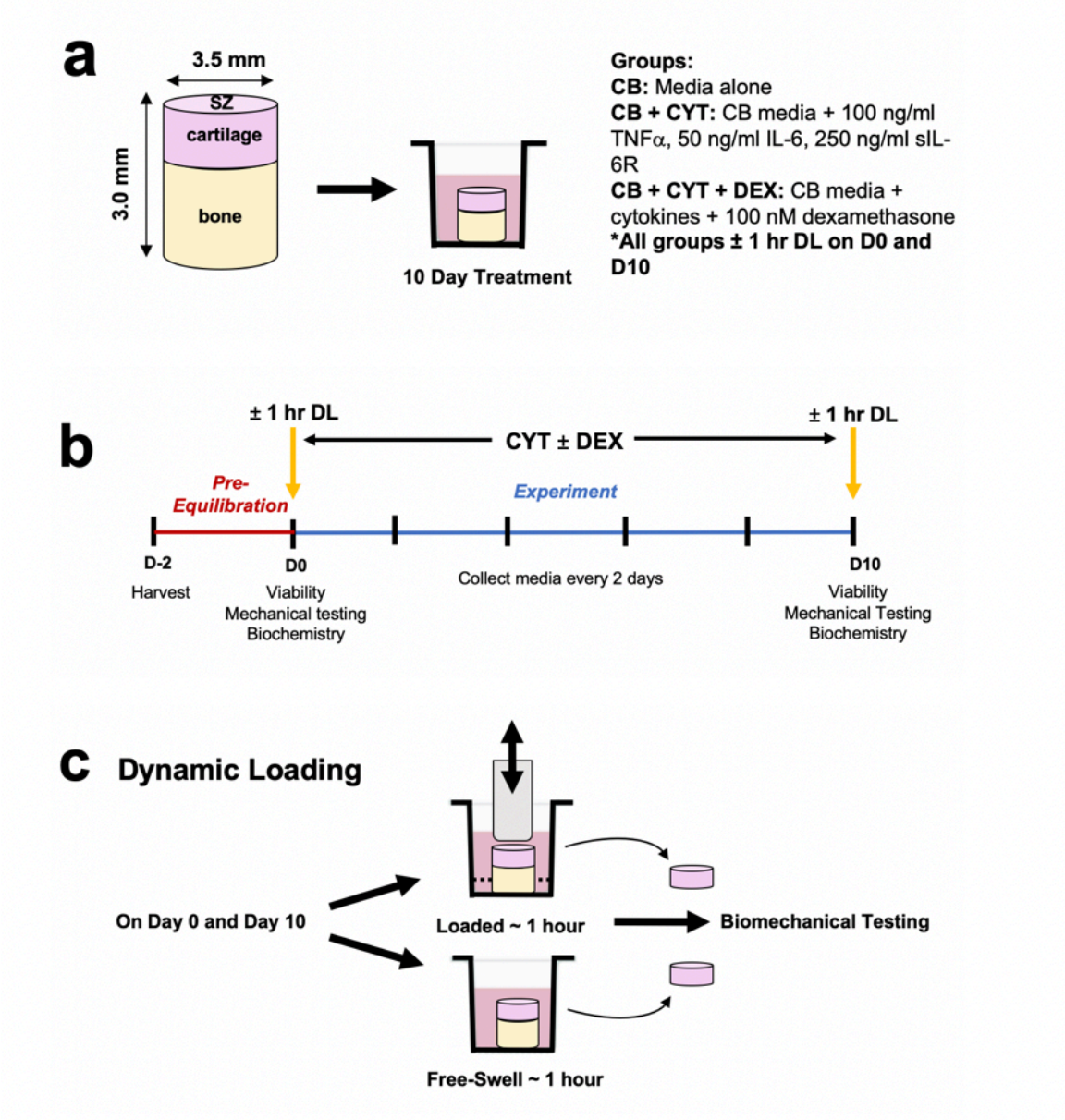

Figure 33. Experimental Setup for Mechanical Studies. (a) Cylindrical osteochondral plugs were taken from human ankle tissue and cut on the bone end for a final height of ~ 3.0 mm and diameter of ~3.5 mm. Explants were placed in media for 10 days and assigned to one of three treatment groups. (b) Experiments for each human donor included a 2 day equilibration period after harvest, followed by a 10 day experiment. Media was collected every two days. Cartilage tissue viability, biochemistry and mechanical stress-relaxation were conducted on days 0 and 10. (c) On the first and final day of experiments, some cartilage tissue samples were taken for ~1 hour of dynamic loading before mechanical testing. This occurred in an unconfined compression chamber to allow media to flow freely through both cartilage and bone tissues. Part of (a) and (c) were made with BioRender. SZ: superficial zone; CB: cartilage-bone; CYT: cytokines (100 ng/mL TNF α, 50 ng/mL IL-6, 250 ng/mL sIL-6R); DEX: 100 nM dexamethasone; DL: dynamic loading.

4.3.1 *Baseline Biomechanical and Biochemical Analysis*

On day zero, cartilage plugs from each donor were removed from the underlying bone and taken for mechanical testing. Parameters calculated from stress-relaxation data included compressive equilibrium modulus (Ey), dynamic stiffness at 1 Hz (E_d), and hydraulic permeability (k_p). There were no distinctions between E_y, E_d and k_p values among all donors at baseline (Fig. 34a-34c). After 1 hour of loading at baseline, there were no differences in E_y, E_d and k_p values for each donor between loaded versus unloaded conditions (Fig. S8). When combining donors based on age, there was a lower E_d value in older (≥70) donors as compared to younger (≤55) donors (Fig. 34e, $p<0.05$). There were no differences in E_y and k_p values demonstrated between age groups (Fig. 34d, 34f). GAG and collagen content demonstrated no difference between donors (Fig. 34g, 34h). However, donors 4 (M/47) and 5 (M/70) were found to have a lower DNA content as compared to donor 2 (Fig. 34i, $p<0.01$, $p<0.05$).

Correlative analysis with across all donors at baseline demonstrated that the compressive equilibrium modulus and dynamic stiffness increased with increasing GAG content ($R=0.6185$, $p=0.0003$; $R=0.7389$, $p<0.0001$), while hydraulic permeability decreased ($R=-0.5323$, $p=0.003$, Fig. 35a-35c). With increasing collagen content, there was a decrease in compressive equilibrium modulus and dynamic stiffness and an increase in hydraulic permeability, though this was a much weaker correlation ($R=-0.4764$, $p=0.0090$; $R=-0.4688$, $p=0.0103$; $R=0.4458$, $p=0.0154$, Fig. 35d-35f).

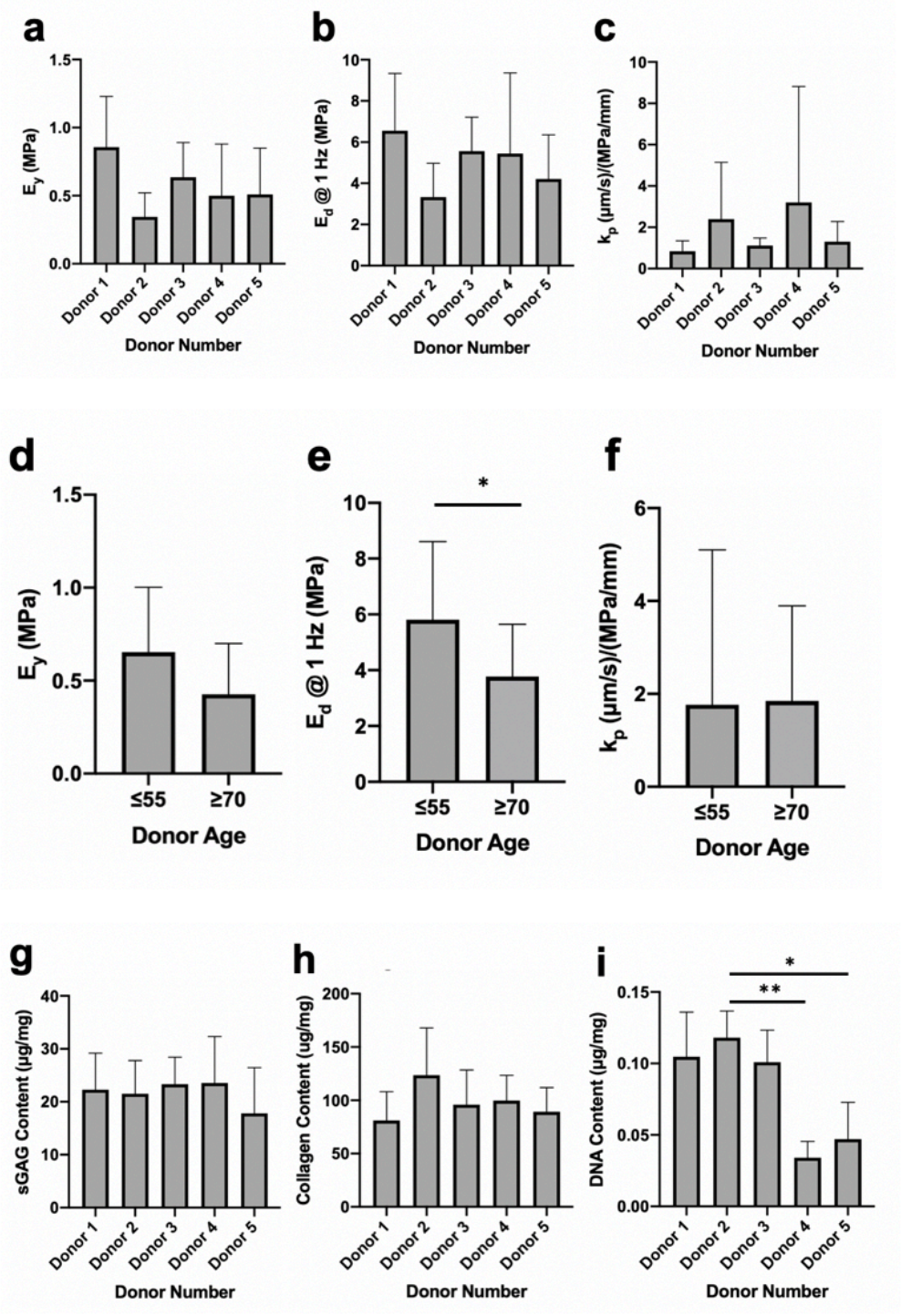

Figure 34. Human Mechanical Study: Biomechanical and Biochemical Baseline Properties of Human Ankle Cartilage. The (a) compressive equilibrium modulus (E_y), (b) dynamic stiffness at 1 Hz (E_d), and (c) hydraulic permeability (k_p) of cartilage at day zero (prior to starting treatments). N=5-6 explants from each of n=5 donors. (d) Ey, (e) E_d and (f) k_p values for the same explants in (a-c), divided by age (≤55 and ≥70). (g) GAG, (h) collagen and (i) DNA content for the same explants in (a-c). For (a-i), data are presented as mean with 95% confidence interval (CI) for each donor with */**$p<0.05/0.01$ between donors or groups.

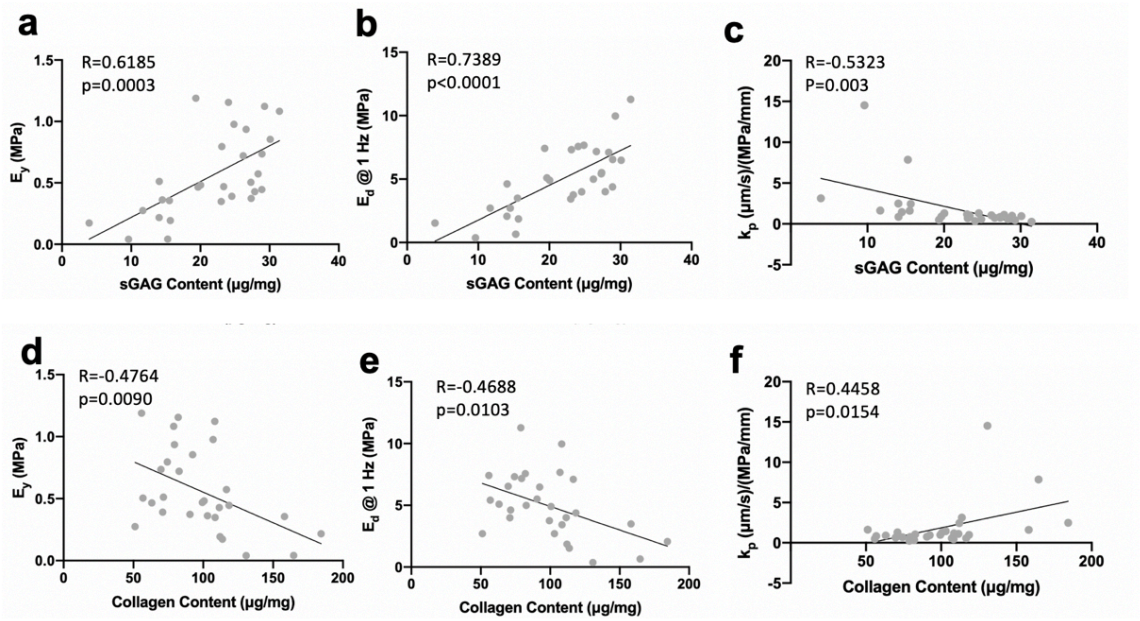

Figure 35. Human Mechanical Study: Variation of Baseline Biomechanical Properties with GAG and Collagen Content. Correlation between GAG content and (a) E_y, (b) E_d, and (c) k_p for cartilage at day zero (prior to starting treatments). N=5-6 explants from each of n=5 donors. Correlation between collagen content and (d) E_y, (e) E_d, and (f) Kk_p for the same explants in (a-c). Data are presented with Pearson's R and associated p-value.

4.3.2 *Biochemical Responses to Cytokines and Dexamethasone*

Intact cartilage-bone explants were cultured for 10 days to study the effects of cytokines, as well as cytokines with 100 nM dexamethasone, on biochemical alterations of cartilage. Increased cell death was observed after 10 days of culture with 100 ng/mL TNFα, 50 ng/mL IL-6, and 250 ng/mL sIL-6R (CB + CYT), at a depth of up to ~75% of plug thickness from the superficial zone (Figure 36a). With the addition of Dex (CB + CYT + DEX), cell death was greatly reduced to nearly that of explants cultured in control medium (CB), though this was donor-dependent. CB explants at day 10 did not experience a change in cell viability from day 0 controls at the macroscopic level.

Over the course of the 10 day treatments, GAG loss to the medium was significantly increased in explants treated with cytokines as compared to CB explants (Figure 36b). At days 2 and 4, GAG loss in CB + CYT and CB + CYT + DEX explants were both increased from that of the CB group ($p<0.05$, $p<0.01$ at day 4), but Dex had no alleviating effect. By day 6, Dex began to rescue GAG loss, and at day 10, average CB + CYT GAG loss reached 44.8%, while that of Dex treated explants was 17.3% ($p<0.001$). The concentration of nitric oxide (NO) released to the media was also measured over the experiment course (Figure 36c). The highest levels of NO concentration occurred on day 2 of treatment, which were markedly increased in CB + CYT explants to 11.8 μM ($p<0.001$). NO release decreased by day 10 for this group, though was still elevated as compared to CB controls ($p<0.001$). The addition of Dex reduced NO concentration from the CB + CYT group to 9.88 μM ($p<0.01$) on day 2, as well as to 5.64μM ($p<0.01$) on day 6.

Next, we examined changes in cartilage tissue composition with cytokines and Dex (Figure 36d-f). By day 10, the CB + CYT explants experienced significantly decreased GAG content compared to controls ($p<0.001$), an effect that was ameliorated with Dex ($p<0.001$). In contrast, there were no differences in both cartilage collagen content and DNA content between day 0 controls and all explants at day 10.

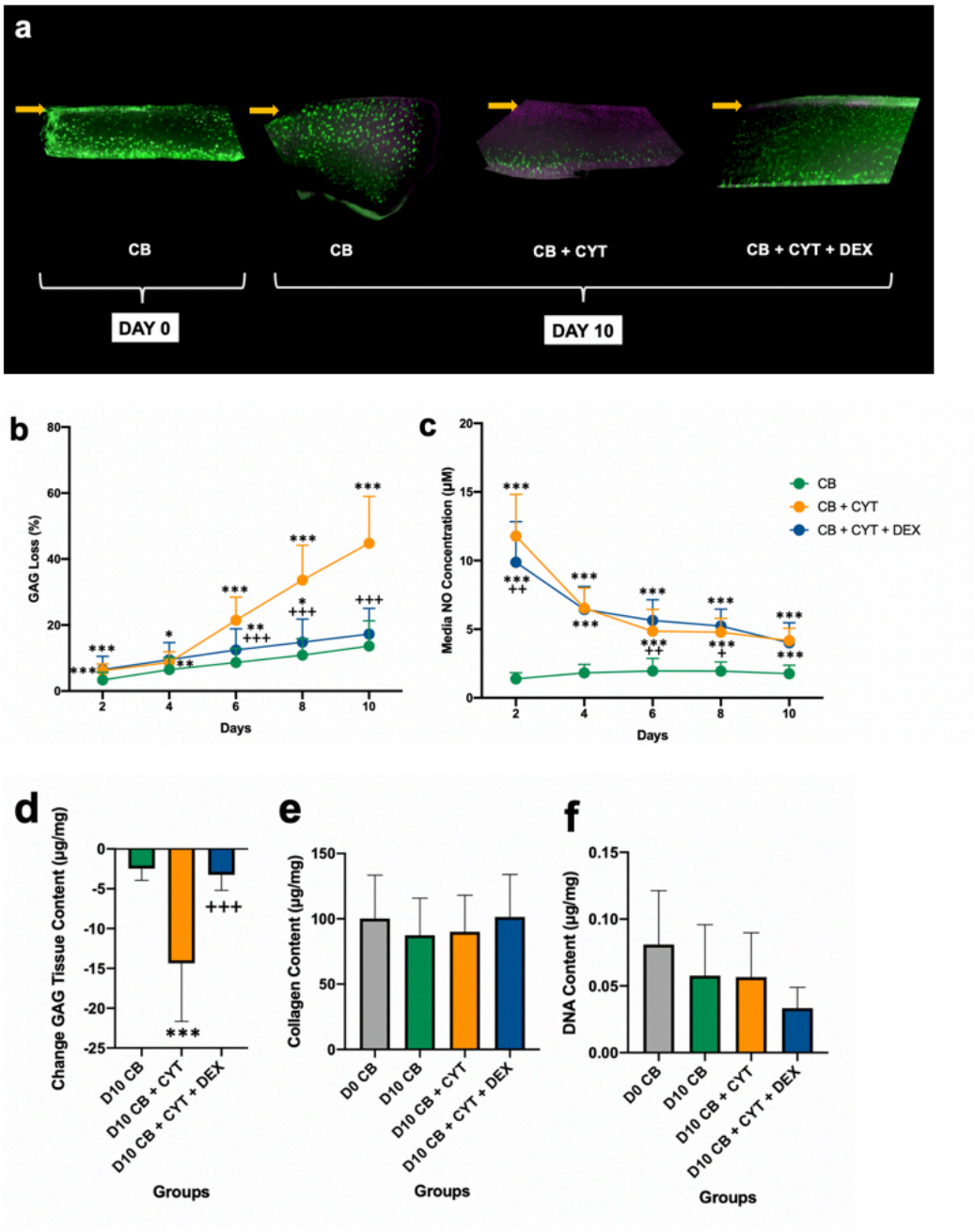

Figure 36. Human Mechanical Study: Biochemical Responses to Cytokines and Dexamethasone. (a) Representative images from donor 2 of fluorescently stained cartilage tissue on day 0 and day 10 of culture. Green (fluorescein diacetate) identifies live cells and magenta (propidium iodide) identifies dead cells. Yellow arrow: intact superficial zone. (b) Percent GAG loss to cartilage over 10 days in culture. N=30 explants from n=5 donors in each treatment group. (c) Amount of NO released into the media by same explants in (b) over 10 days in culture. (d) Percent decrease in GAG tissue content after 10 days in culture, and (e) day 10 collagen and (f) DNA tissue content for the same explants in (b). Data are presented as mean with 95% CI at each time point. */**/*** vs. CB control group, $p<0.05/0.01/0.001$. +/++/+++ vs. CB + CYT group, $p<0.05/0.01/0.001$.

4.3.3 *Biomechanical Responses to Cytokines and Dexamethasone*

At the end of 10 days of treatment, stress-relaxation testing was conducted on all cartilage plugs from cartilage-bone explants. Half of the plugs from each treatment group were subjected to one hour of loading before testing, while the other half were allowed to free-swell. There were no differences in E_y, E_d, and k_p between treatment groups, both unloaded and loaded (Figure 37, Figure S9).

Correlative analysis for day 10 cultures across all donors for unloaded plugs only demonstrated that the compressive equilibrium modulus increased with increasing GAG content for cytokine and cytokine with Dex treated explants (CB + CYT: R=0.4774, p=0.0118; CB + CYT + DEX: R=0.4016, p=0.0420), as did dynamic stiffness for these two groups (CB + CYT: R=0.3812, p=0.0498; CB + CYT + DEX: R=0.6209, p=0.0007, Figure 38a-b). However, hydraulic permeability decreased with increasing GAG content for the Dex treated group only (R=-0.4737, p=0.0145, Figure 38c). With increasing collagen content, there was a decrease in compressive equilibrium modulus for the Dex treated group (R=-0.4008, p=0.0425, Figure 38d-f). Changes in treatment group did not significantly alter the slope of the linear model relating Ey, Ed, and kp to both GAG and collagen content (Table S2, S3).

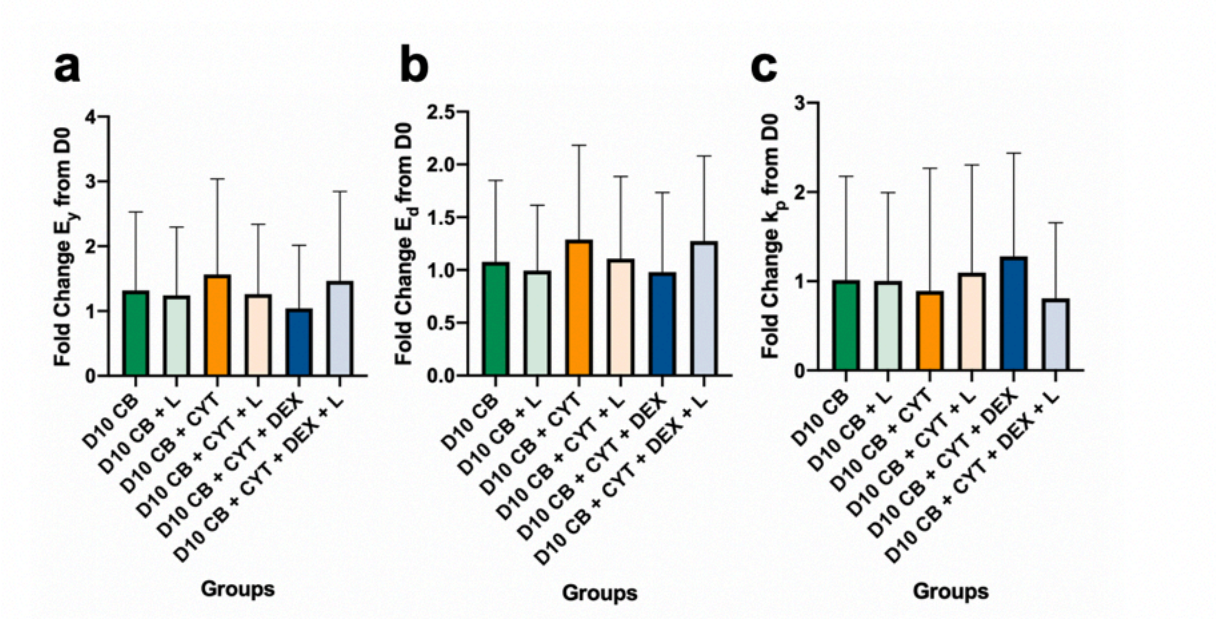

Figure 37. Human Mechanical Study: Biomechanical Changes with Addition of Cytokines and Dexamethasone and Response to Loading. The fold change in (a) E_y, (b) E_d, and (c) k_p for cartilage at day 10 of treatment with control media, cytokines, and cytokines with Dex, as compared to day 0 controls. For each treatment group, explants were either unloaded or underwent one hour of loading before mechanical testing. The E_y, E_d, and k_p values for each explant were normalized to the day 0 average for its respective donor. N=26-29 explants from a total of n=5 donors in each treatment group. Data are presented as mean with 95% CI for each treatment condition. L: loaded explant.

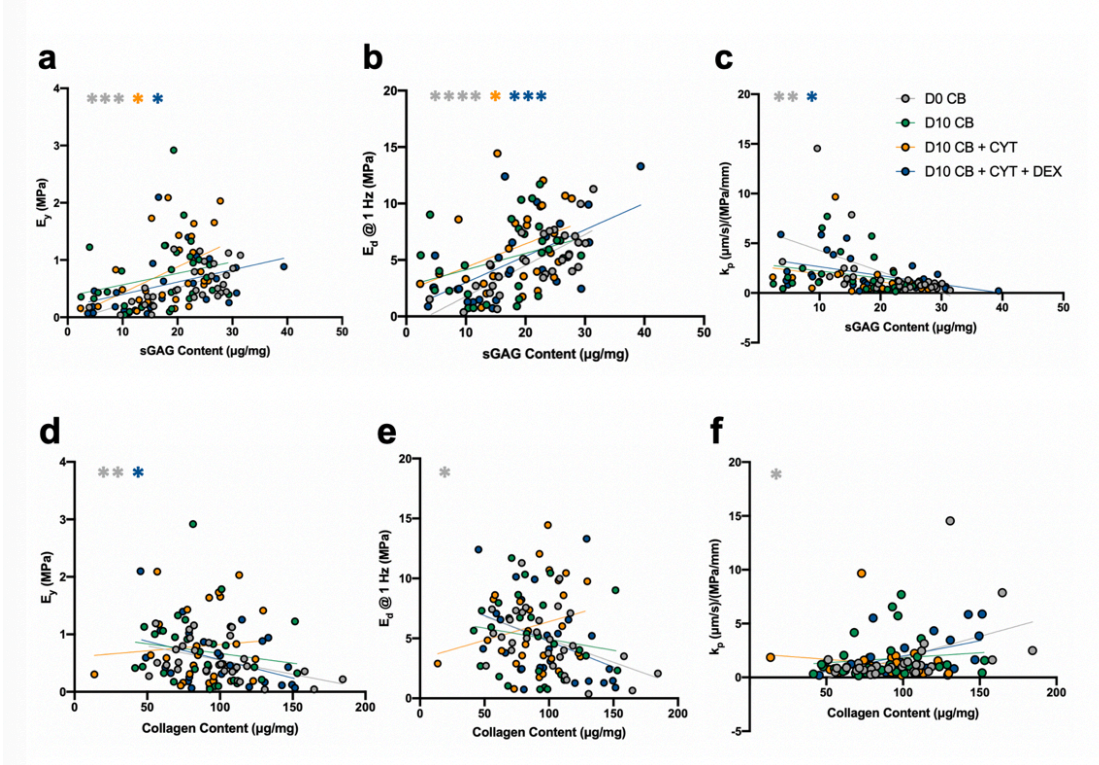

Figure 38. Human Mechanical Study: Variation of Biomechanical Properties with GAG and

Collagen Content. Correlation between GAG content and (a) E_y, (b) E_d, and (c) k_p. N=26-29 explants from a total of n=5 donors in each treatment group. Correlation between collagen content and (d) E_y, (e) E_d, and (f) k_p for the same explants in (a-c). For (a-f) data are presented with fit line, for which the slope with 95% CI, as well as Pearson's R and associated p-values are in Supplementary Table 2 and 3, with */**/***/**** $p<0.05/0.01/0.001/0.0001$.

5 DISCUSSION

5.1 Loading Optimization

Previous work in the lab has demonstrated that loading under displacement control alleviates catabolic responses to inflammatory cytokines in cartilage explant cultures and enhance matrix biosynthesis in normal bovine cartilage explants.[18,29] Particularly, the use of displacement control was found to mechanically distinguish the biologic effects of static versus dynamic loading, due to the added creep displacement that occurs during load-controlled dynamic loading.[29] However, few studies have used load-controlled compression regimens, which more realistically describes rehabilitation/exercise environments.[34] Motivated by this, the first part of this thesis work sought to design and implement a dynamic loading protocol for explants under load-control that modeled a 1 hour daily loading routine for exercise/rehabilitative use. The loading protocol consisted of an initial static compression for 5 minutes to ensure contact, followed by dynamic compression with a load-controlled haversine waveform (0.33 Hz, 40% duty cycle), with 8 waveform repetitions in each of 4 sets, in each of 6 exercises (Figure 9). In both bovine and human models, we aimed to determine which loading amplitudes maximized cell viability while keeping strain within a physiologically relevant range, around 20-30%, which has also been shown to optimize anti-catabolic action against cytokines.[29] Using predetermined Young's modulus values for bovine and human cartilage[34], it was hypothesized that this total strain value would occur for a dynamic load amplitude between 25-200 kPa for bovine cartilage plugs and 100 kPa - 1 MPa for human cartilage-bone explants. Additionally, with human explants we investigated the effect of loading session frequency on tissue mechanics and health in the presence of cytokines, proposing that an increased amount of time undergoing loading might amplify any beneficial effects (increased cell viability, decreased GAG loss, increased biosynthesis) seen with loading in

a disease model, given that the cartilage has enough time to reswell in between loading sessions.

Bovine experiments demonstrated no changes in chondrocyte cell viability at the macroscale level between different dynamic loading amplitudes tested after 7 days, but that creep compressive strain increased non-linearly with increases in dynamic loading amplitude. Total strain was optimized in the 20-30% range with a contact load and dynamic load each of 25 kPa. This was at the lower end, but nevertheless within the stress ranges found with prior studies examining physiologic strains in bovine cartilage.[29,34]

Human tissue studies utilized a cartilage-bone system, which required the design of a new polysulfone chamber in which metal rings could hold bone perpendicularly to the chamber surface. This ensured that all cartilage surfaces were in contact with platens for dynamic loading. Because bone tended to crumble after multiple days in media, thus causing varying heights of each explant, a displacement-controlled contact strain was fixed at 10%. Experiments testing dynamic loading amplitudes demonstrated that a 100 kPa dynamic load optimized total strain in the 20-30% range, while maintaining cell viability. There are not currently any studies in the literature conducting load-controlled dynamic loading on human osteochondral tissues, but displacement controlled loading on chrondrocyte-seeded cartilage tissue constructs have recorded stresses of the same order of magnitude for a fixed strain of 10%.[181] Cell viability decreased with increased dynamic load amplitude, seen likely due to the decreased chondrocyte density in human cartilage as compared to bovine cartilage, which did not demonstrate these changes at the macroscale.[182] The study looking at the effect of loading session frequency with the addition of cytokines to human ankle tissue demonstrated no differences in between loading tissue once vs. twice a day. Further, cytokines caused decreases in cell viability and GAG biosynthesis, as well as increases in GAG loss and NO release. Loading (regardless of frequency) had an effect on explants without cytokines only, increasing GAG biosynthesis, but otherwise loading caused no biochemical changes in treatment groups from their unloaded counterparts.

Overall, loading optimization experiments confirmed the proposition that a load-controlled protocol designed to mimic a physiologically relevant physical rehabilitation program could produce a total strain in the optimum range discovered in previous studies. The dynamic loading amplitude was at the lower end of the hypothesized ranges for both bovine and human tissue. This could potentially be due to an older average age of human donors, which causes a decrease in elastic compressive modulus,[183] or changes to cartilage's modulus after co-culture with subchondral bone, as cartilage-bone systems have been shown to have different poro-viscoelastic properties as compared to the isolated tissues alone.[184] Additionally, the expected result that increasing the duration of time under loading (two sessions per day) would amplify any biochemical effects seen with a single loading session was not seen - doubling the amount of time did not alter the changes seen with the one hour session. Though this experiment would benefit from more donors studied, the findings indicate a plateau in biochemical effects with respect to loading duration, and may be a result of activated mechanotransduction pathways that have not had time to become deactivated before another loading stimulus is added, as activation duration can last on the order of hours.[185] Future studies should test the effects of multiple loading sessions with an increased time between them, or sessions with different dynamic stress amplitudes. The results from this work demonstrated a successful modeling of a one hour daily loading routine at physiologically relevant strains using a load-controlled protocol, applied to both bovine cartilage and human cartilage-bone specimens. Having optimized this protocol, it could then be applied for future experiments to better understand the effects of cyclic loading on the action of the drugs dexamethasone and IGF-1 in an OA disease model.

5.2 Biologic Effect of Loading with Dexamethasone and IGF-1

Both the potent synthetic glucocorticoid dexamethasone, and the polypeptide hormone Insulin-like growth factor-1, have shown promise as a preventative therapy for PTOA when administered in low doses. Previous work has demonstrated that Dex can be chondroprotective in animal and in vitro models of PTOA with anti-catabolic effects which inhibit cytokine-induced matrix loss and cell death via glucocorticoid receptor pathways.[13,14,16] Further, IGF-1 has been shown to prevent chondrocyte apoptosis induced

by mechanical injury and inflammatory cytokines, and upregulate cartilage matrix biosynthesis in both human and animal models.[29,135-137] Dynamic loading has also been studied as a potential modulator of chondrocyte metabolic activity as a function of frequency, amplitude and duty cycle of compressions. Loading studies under displacement control have been shown to alleviate catabolic responses to inflammatory cytokines in cartilage explant cultures and enhance matrix biosynthesis in normal bovine cartilage explants.[18,29]. However, little is known about the combined effect of these therapies at physiologically relevant compression rates and durations that represents realistic rehabilitative regimens. In this regard, few studies have used load-controlled compression regimens, which more realistically describes rehabilitation/exercise environments.[34] We aimed to apply a combination of load-controlled dynamic loading and Dex/IGF-1 to both bovine and human cartilage explants treated with exogenous cytokines, with the ultimate aim to investigate whether loading within a rehabilitative range could maximize the therapeutic actions of Dex/IGF-1 in preventing cartilage degradation and preserving chondrocyte viability associated with PTOA. It was hypothesized that dynamic loading in a physiologic range would enhance the anti-catabolic and pro-anabolic actions of IGF-1 and Dex, respectively, in both bovine cartilage explant and human cartilage-bone explant models.

Using similar strains on bovine (cartilage only) and human (cartilage-bone) explants, the addition of cytokines created a consistent disease-model effect in both models, causing decreases in cell viability and GAG biosynthesis, and increases in GAG loss. However, there was a significant amount of donor variability seen in biologic responses to both Dex and IGF-1, as well as the addition of loading. For donors that responded to these therapeutics, as compared to the disease condition, Dex and IGF-1 both increased cell viability, and Dex increased GAG biosynthesis, decreased GAG loss, increased cartilage and bone collagen content, and decreased media NO release. These findings for Dex are consistent with previous studies looking at cartilage alone in animal[13-15] and human models,[36] and are novel for osteochondral explants, for which biologic outcomes have not been studied after treatment with Dex. However, IGF-1 had an effect on cell viability only, which is surprising given the large amount of evidence that IGF-1 also has pro-anabolic

effects in non-human animal models and human chondrocyte cell culture.[186] This may suggest that there are differences in IGF-1 penetration and diffusion into cartilage tissue that is attached to bone in culture. On the mRNA level, Dex tended to increase expression for collagen II and decrease expression for the MMP ADAMTS-5 from that seen with cytokines. Both Dex and IGF-1 decreased expression for the pro-apoptotic gene caspase-3. These findings are consistent with the ECM outcome measures tested – namely that Dex has biochemical protective effects, while IGF-1 only affected cell viability. However, no absolute conclusions can be made due to the large variability in gene expression values with a small animal number (N=3).

Loading alone slightly rescued cell viability in the disease model, and increased expression of genes for aggrecan and collagen II while decreasing expression of the gene for caspase-3 – these chondroprotective affects are consistent with the effects seen in bovine cartilage by Li et al.,[29] and demonstrate that loading alone may have pro-anabolic effects on human osteochondral tissue. Loading also amplified effects seen with both treatment molecules with cytokines, as compared to the disease model alone, in donors that were responders: it appeared to increase Dex and IGF-1's effect on cell viability, and further increased GAG biosynthesis and decreased GAG loss seen with Dex. Gene expression studies did not reveal significant alterations in gene expression between loaded treatment groups and their unloaded equivalents. Notably, donors that responded to Dex/IGF-1 were the same as those that responded to loading, in both bovine and human explants.

The results of these studies suggest that dynamic loading of cartilage may have different effects on the multiple molecular pathways underlying Dex/IGF-1 therapy, with the potential to amplify some beneficial outcomes of the drugs. However, they also highlight the high degree of donor variability in biochemical responses to physiologically relevant load-controlled dynamic loading on both bovine and human articular cartilage in the presence of inflammatory cytokines. However, loading caused a more consistent rescue in cell viability for the disease model across donors, suggesting that the variability may lie within the pathways underlying extracellular matrix production that are affected by the presence of inflammation. Previous work has suggested that Dex can have varying

protective effects on cartilage in different disease model systems,[187] and here we demonstrate donor-to-donor variability in disease rescue with both Dex in the unloaded condition and with loading at a fixed stress amplitude. In human tissue, these varying protective anti-catabolic and pro-anabolic responses may be due to differing mechanical properties of cartilage and supportive subchondral bone based on age, sex and BMI, causing different strains between donors for a set dynamic stress, as well as mechanobiological signaling affecting intracellular processes. Our results suggest that a rehabilitative loading therapy in combination with Dex/IGF-1 could enhance certain disease-modifying effects of each of the two drugs while reducing others. They also indicate that a given load may not affect individuals in the same way, and thus to maximize protective disease-modifying effects, rehabilitation exercises must be personalized. Ongoing studies must focus on better understanding these biological variations in response to dynamic compression, utilizing other outcome measures assessed here (such as proteomics and metabolomics) to strengthen the understanding of the role of loading. The findings suggest that a rehabilitative loading therapy could have protective effects against human cartilage inflammation, and provide insight into utilizing the combination of moderate dynamic loading and drug treatment when developing treatment strategies for OA intervention.

5.3 Mechanical Effect of Loading with Dexamethasone

In this study, we aimed to investigate how the biomechanical properties of human articular differ at baseline, and whether these change in an inflammatory state mimicking the disease-like environment of OA, as well as with the potent chondroprotective corticosteroid dexamethasone. We used a combination of TNFα, IL-6, and sIL-6R as a cytokine challenge to adult human ankle osteochondral tissue *in vitro*, with and without lose-dose Dex for 10 days duration. We also subjected cartilage to 1 hour of a physiologically relevant loading session at day 0 and 10, to study the effects of treatments on protection against mechanical stress. It was hypothesized that there would be differences in mechanical properties at baseline between donors, and that Dex might rescue any function properties that were degraded in the presence of cytokines.

We demonstrated that at baseline, variation existed in ankle articular cartilage biomechanical properties between human donor age groups. Notability, the older donors (≥70) were found to have change in dynamic stiffness that suggest a decreased ability to resist oscillatory loading, as compared to the younger donors (≤55), with no differences in compressive equilibrium modulus and hydraulic permeability between age groups. This is consistent with a prior report finding a decrease in dynamic stiffness in the proximal phalanx of mature horses as compared to those at birth.[188] In human tissue, dynamic stiffness has not been completely studied, and results on other biomechanical properties are not consistent - one study found a marginal decrease in equilibrium modulus with age without changes in permeability in the human patella,[183] while another identified increases in permeability with aging in the human nasal septum.[189] Though our findings suggest that older age could have an effect on biomechanical properties in the human ankle, possibly through a decreased ability of cells to maintain the ECM over time,[190] a larger sample size of donors will be necessarily to fully understand what other characteristics (such as sex, BMI, etc.) can cause innate variability in these properties.

While there was some variation in biomechanical properties at baseline, there were notably no differences in GAG and collagen content between donors, while donors 4 and 5 had decreased cartilage cellularity. GAG content appeared to have a much stronger correlation with compressive equilibrium modulus and dynamic stiffness as compared to collagen content with these parameters. Studies investigating these relationships in human cartilage have demonstrated mixed results: Franz et al.[191] found no correlation between GAG and collagen content and compressive stiffness of human knee cartilage, while Treppo et al.[176] found a strong correlation between GAG content and equilibrium modulus for the talus, femur, and tibial plateau. Our findings support a strong relationship between GAG and biomechanical structure in human talus cartilage, suggesting that proteoglycans, rather than collagen, contribute prominently to these properties. However, given similar tissue composition between donors, individual variability may come from other determinants of biomechanical properties, such as extracellular matrix structure or biochemical constituents not studied here.

Treating osteochondral explants with TNFα, IL-6, and sIL-6R, we demonstrated that cytokines successfully created an inflammatory environment to study degradative changes associated with OA. On the biochemical level, cytokines greatly decreased cell viability, while increasing GAG loss by day 10 and elevating NO release, most prominently on day 2 of culture. The disease-like effects of cytokines and anti-catabolic actions of low dose Dex are consistent with prior studies on human ankle[17] and knee tissue.[192] Established mechanisms behind the effects of Dex include downregulation of caspase-3,[17] matrix metalloproteases (MMPs),[193] and NO synthase,[194] though proteomics techniques are currently being employed to investigate this further.[195,196] Notably, neither cytokines nor Dex had an effect on cartilage collagen content on day 10 of culture. This is expected, given previous work demonstrating that collagen loss with cytokine challenge does not occur until after day 10 in bovine cartilage, most likely due to aggrecan protection from proteolytic cleavage by MMPs until enough aggrecan has been released from the ECM.[17,197] Given this observation with cytokines, it is probable that no changes would be seen with cytokines with Dex treatment either.

Mechanical testing on day 10 of experiments strikingly revealed no changes with cytokines or cytokines with Dex in the compressive equilibrium modulus, dynamic stiffness, or hydraulic permeability of cartilage from donor-normalized baseline values. There were also no differences in these values after one hour of loading on day 10. These findings are especially interesting given that the equilibrium and dynamic moduli of juvenile bovine cartilage have been demonstrated to decrease with GAG loss at a similar percentage (30-40%) seen in this study.[198] There are a few possible explanations for our results in human ankle tissue. First, juvenile bovine cartilage, on which many biomechanics studies have been conducted, is less variable in biochemical composition and biomechanical properties as compared to human cartilage, which can exhibit differences within a single joint (based on location), between left and right joints in a donor, and between donors.[199,200] Explants within a donor can also respond differently to cytokines and Dex treatments biochemically, and thus this variability statistically makes it more difficult to identify differences between treatment groups with a low explant and donor number. Second, there may be a threshold amount at which GAG loss leads to changes in ECM structure that cause changes in

biomechanical properties, which may be different from juvenile bovine cartilage. Alternatively, there may be a time delay between microscopic biochemical changes and their resulting structural changes. In either of these cases, changes in properties may not be seen for any treatment group unless a longer term culture were conducted. Future studies may also incorporate nanomechanical analysis such as atomic force microscopy, which has been successfully employed to study property changes at the nanoscale, before macroscopic changes have occurred.[170,201] Third, with the addition of cytokines and Dex, there may be other biochemical factors not studied here that determine a cartilage plug's biomechanical properties. Both the cytokine and cytokine with Dex groups were correlated to compressive equilibrium modulus and dynamic stiffness less strongly than seen with baseline tissue. These relationships suggest that other consequences of inflammation (such as changes in fiber orientation/microstructure and signaling between cartilage and bone), which may not consistently occur among all treated explants, may be necessary to produce functional alterations. Finally, Bian et al[202] demonstrated that the properties in mature bovine and canine cartilage were not significantly affected by Dex alone after 4 weeks in culture, suggesting that age may play a role in the structural response to Dex. Given that all the donors studied here were between 47-73 years old, our findings may indicate a discrepancy in the microscopic biochemical and macroscopic structural effects of cytokines and Dex in aged human cartilage tissue. Studying the impacts of these treatments on immature human cartilage would give a better understanding of whether this difference is age-related as seen in bovine cartilage, though this type of tissue is often times not available. With these explanations in mind, it would be expected that one hour of loading would not further effect these biomechanical properties, if the structural integrity of cartilage tissue was not altered from baseline.

In summary, this study provides insight into how cytokines and Dex impact biomechanical properties of human ankle cartilage cultured with subchondral bone, and how these relate to changes on the biochemical level. The glucocorticoid had a protective effect on chondrocyte viability after 10 days but did not appear to change the functional properties of cartilage and its response to loading. Future studies might utilize a larger, more diverse sample size, as well as analyze biomechanical and biochemical alterations in bone to

capture a more complete picture regarding donor variability in functional properties at baseline and in response to cytokines and Dex. A longer treatment duration may also be helpful in determining the time point at which properties begin to break down with cytokines. The relationships found between treatment conditions, tissue composition, and biomechanical properties may help to form a better clinical understanding of the impacts of Dex when used as a therapeutic for OA.

6 SUMMARY AND CONCLUSIONS

Osteoarthritis, a debilitating disease affecting millions worldwide, is characterized by cartilage degradation due to a variety of causes including inflammation, and can eventually lead to alterations in the mechanical properties of articular cartilage. The glucocorticoid dexamethasone and peptide hormone Insulin-like growth factor 1 have been shown to have chondroprotective effects when administered at low doses in the presence of inflammatory cytokines. Additionally, though OA can be caused by excessive mechanical stress, moderate exercise has also been demonstrated as an alleviating therapy. There is significant potential for these therapeutics to be synergistic in preventing disease initiation and progression in OA - however, most work has been conducted on pharmacologic and physical treatments and their effects separately, in bovine (or other animal) cartilage tissues. Further, dynamic loading modalities that have focused previously on mechanistic studies of mechanobiology, have often been studied with protocols that do not reflect human-physiologically relevant movement.

The work of this thesis aimed to first create and test a loading protocol with a stress and frequency that accurately mimicked a physiologically relevant rehabilitation program in healthy cartilage that utilizes native human osteochondral explants. It then aimed to test this protocol with potential therapeutics Dex and IGF-1 in a cytokine-challenged PTOA disease model to evaluate the biological efficacy of such a combination therapy. Finally, given that there is little known about the structural response of human cartilage to Dex in a diseased state, this work sought to examine cartilage biomechanical properties in the context of biochemical and mechanical changes observed with human osteochondral tissues when treated with exogenous cytokines and Dex.

Experiments first optimized a loading protocol by testing different physiologically relevant dynamic loading amplitudes on both bovine cartilage and human osteochondral explants. The effects of loading duration (1 vs. 2 one-hour sessions per day) on human tissue was also examined. Additional experiments subjected bovine and human tissue to a combination of the cytokines, TNFα, IL-6 and sIL-6R to mimic an OA/PTOA disease initiation, and to examine the effects of Dex and IGF-1 with and without dynamic loading for 7 days. The protocol optimized in the first set of experiments (at 0.33 Hz for 1 hour per day) was then utilized for these explants. Metrics were obtained at the end of 7 days to assess cell viability, and biochemical changes, on the protein and gene expression levels. It was found that a load-controlled protocol could mimic exercise with total creep compressive strain (by the end of 1-hour) that remained within the physiologically relevant range. Loading also increased Dex and IGF-1's effect on cell viability, and further increased GAG biosynthesis and decreased GAG loss seen with Dex. Notably, in human tissue there was marked donor-to-donor variability in the response to both loading (on its own) and to Dex/IGF-1 with and without loading.

Biomechanical testing was used to determine cartilage material properties (i.e., the compressive equilibrium modulus (E_y), dynamic stiffness (E_d) and hydraulic permeability (k_p), both before and after a 1-hour loading session, for human tissue at baseline and after treatment with cytokines and Dex. It was found that while Dex preserved cell viability and decreased GAG loss and NO release from cartilage treated with cytokines, it did not alter E_y, E_d and k_p values (before or after loading) after 10 days, though there was variation in E_d values between donor age groups at baseline. In the two treated groups, GAG content exhibited a correlation with E_y and E_d that was weaker than that seen at baseline.

Overall, the results of this thesis include a load-controlled compression protocol for osteochondral tissue, that lays a foundation for future studies testing dynamic loading either on its own for with therapeutic pharmacologic molecules. They also suggest that a rehabilitative loading therapy in combination with Dex/IGF-1 could enhance certain disease-modifying effects of each of the two drugs while reducing others. However,

consistent with the variation in responses to Dex/IGF-1 alone on cartilage seen in studies conducted by other members in the lab (Garima Dwivedi, Rebecca Black et al., unpublished), these results indicate that not all human donors respond to a given loading amplitude in the same way. Mechanical results demonstrated an inherent biomechanical variability that could contribute to these different responses to loading over time. They also indicate an important role for structural rather than biochemical changes in producing functional property alterations in response to cytokines and Dex. Future studies may focus on identifying the molecular pathways underlying the variations in response to loading, Dex and IGF-1, as well as the role of bone in these responses, utilizing technology such as proteomics and metabolomics. Testing dynamic loading with other disease-modifying drug candidates may also prove beneficial in pursuit of forming better treatment strategies for OA intervention.

7 REFERENCES

1. Le Graverand-Gastineau, M. P. Disease modifying osteoarthritis drugs: facing development challenges and choosing molecular targets. *Current Drug Targets* 11, 528-535 (2010).
2. Felson, D. T., Neogi, T. Osteoarthritis: is it a disease of cartilage or of bone? *Arthritis Rheumatology* 50, 341-344 (2004).
3. Wieland, H. A., Michaelis, M., Kirshbaum, B. J., et. al. Osteoarthritis – an untreatable disease? *Nature Reviews Drug Discovery* 4, 331-344 (2005).
4. Bay-Jensen, A. C., Hoegh-Madsen, S., Dam, E., et. al. Which elements are involved in reversible and irreversible cartilage degradation in osteoarthritis? *Rheumatology International* 30, 435-442 (2010).
5. Carbone, A., Rodeo, S. Review of current understanding of post-traumatic osteoarthritis resulting from sports injuries. *Journal of Orthopedic Research* 35, 397-405 (2017).
6. Brown, T. D., Johnston, R. C., Saltzman, C. L., et. al. Posttraumatic osteoarthritis: a first estimate of incidence, prevalence, and burden of disease. *Journal of Orthopedic Trauma* 20, 739-744 (2006).
7. Anderson, D. D., Chubinskaya, S., Guilak, F., et. al. Post-traumatic osteoarthritis: Improved understanding and opportunities for early intervention. *Journal of Orthopedic Research* 29, 802-809 (2011).
8. Lohmander, L. S., Englund, P. M., Dahl, L. L., et. al. The long-term consequence of anterior cruciate ligament and meniscus injuries: osteoarthritis. *American Journal of Sports Medicine* 35, 1756-1769 (2007).
9. Irie, K., Uchiyama, E., Iwaso, H. Intraarticular inflammatory cytokines in acute anterior cruciate ligament injured knee. *Knee* 10, 93-96 (2003).

10. Kapoor, M., Martel-Pelletier, J., Lajeunesse, D., et. al. Role of proinflammatory cytokines in the pathophysiology of osteoarthritis. *Nature Reviews Rheumatology* 7, 33-42 (2011).
11. Hunter, D. J. Pharmacologic therapy for osteoarthritis – the era of disease modification. *Nature Review Rheumatology* 7, 13-22 (2011).
12. Osteoarthritis Treatment. Arthritis Foundation. Available at: http://www.arthritis.org/aboutarthritis/types/osteoarthritis/treatment.php. (Accessed: March 18th 2020).
13. Lu, Y., Evans, C. H., Grodzinsky, A. J. Effects of short-term glucocorticoid treatment on changes in cartilage matrix degradation and chondrocyte gene expression induced by mechanical injury and inflammatory cytokines. *Arthritis Research & Therapy* 13, R142 (2011).
14. Huebner, K. D., Shrive, N. G., Frank, C. B.. Dexamethasone inhibits inflammation and cartilage damage in a new model of post-traumatic osteoarthritis. *Journal of Orthopedic Research* 32, 566-572 (2014).
15. Heard, B., Barton,, K., Chung, M., et. al. Single intra-articular dexamethasone injection immediately post-surgery in a rabbit model mitigates early inflammatory responses and post-traumatic osteoarthritis-like alterations. *Journal of Orthopedic Research* 33, 1826-1834 (2015).
16. Grodzinsky, A. J., Wang, Y., Kakar, S., et. al. Intra-articular dexamethasone to inhibit the development of post-traumatic osteoarthritis. *Journal of Orthopedic Research* 35, 406-411 (2017).
17. Li, Y., Wang, Y., Chubinskaya, S., et. al. Effects of insulin-like growth factor-1 and dexamethasone on cytokine-challenged cartilage: relevance to post-traumatic osteoarthritis. *Osteoarthritis and Cartilage* 23, 266-274 (2015).
18. Sah, R. L., Kim, Y. J., Doong, J. Y., et.al. Biosynthetic response of cartilage explants to dynamic compression. *Journal of Orthopedic Research* 7, 619-636 (1989).
19. Ackermann, B., Steinmeyer, J. Collagen biosynthesis of mechanically loaded articular cartilage explants. *Osteoarthritis and Cartilage* 13, 906-914 (2005).
20. Kim, Y. J., Sah, R. L., Grodzinsky, A. J., et. al. Mechanical regulation of cartilage biosynthetic behavior: physical stimuli. *Archives of Biochemistry and Biophysics* 311, 1-12 (1994).
21. Kisiday, J. D., Jin, M., DiMicco, M. A., et. al. Effects of dynamic compressive loading on chondrocyte biosynthesis in self-assembling peptide scaffolds. *Journal of Biomechanics* 37, 595-604 (2004).
22. Chowdhury, T. T., Arghandawi, S., Brand, J., et. al. Dynamic compression counteracts IL-1beta induced inducible nitric oxide synthase and cyclo-oxygenase-2 expression in chondrocyte/agarose constructs. *Arthritis Research & Therapy* 10, R35 (2008).
23. Bonassar, L. J., Grodzinsky, A. J., Frank, E. H., et. al. The effect of dynamic compression on the response of articular cartilage to insulin-like growth factor-I. *Journal of Orthopedic Research* 19, 11-17 (2001).
24. Quinn, T. M., Grodzinsky, A. J., Buschmann, M. D., et. al. Mechanical Compression alters proteoglycan deposition and matrix deformation around individual cells in cartilage explants. *Journal of Cell Science* 111, 573-583 (1998).

25. Buschmann, M. D., Kim, Y. J., Wong, M., et. al. Stimulation of aggrecan synthesis in cartilage explants by cyclic loading is localized to regions of high interstitial fluid flow. *Archives of Biochemistry and Biophysics* 366, 1-7 (1999).
26. Soulhat, J., Buschmann, M. D., Shirazi-Adl, A. A fibril-network-reinforced biphasic model of cartilage in unconfined compression. *Journal of Biomechanical Engineering* 121, 340-347 (1999).
27. Fitzgerald, J. B., Jin, M., Dean, D., et. al. Mechanical compression of cartilage explants induces multiple time-dependent gene expression patterns and involves intracellular calcium and cyclic AMP. *Journal of Biological Chemistry* 279, 19502-19511 (2004).
28. Fitzgerald, J. B., Jin, M., Chai, D. H., et. al. Shear- and compression-induced chondrocyte transcription requires MAPK activation in cartilage explants. *Journal of Biological Chemistry* 283, 6735-6743 (2008).
29. Li, Y., Frank, E. H., Wang, Y., et. al. Moderate dynamic compression inhibits pro-catabolic response of cartilage to mechanical injury, tumor necrosis factor-α and interleukin-6, but accentuates degradation above a strain threshold. *Osteoarthritis and Cartilage* 21, 1933-1941 (2013).
30. Van de Velde, S. K., Gill, T. J., Li, G. Evaluation of kinematics of anterior cruciate ligament-deficient knees with use of advanced imaging techniques, three-dimensional modeling techniques, and robotics. *Journal of Bone and Joint Surgery* 91, 108-114 (2009).
31. Van de Velde, S. K., Bingham, J. T., Hosseini, A., et. al. Increased tibiofemoral cartilage contact deformation in patients with anterior cruciate ligament deficiency. *Arthritis and Rheumatology* 60, 3693-3702 (2009).
32. Barker, M. K., Seedhom, B. B. The relationship of the compressive modulus of articular cartilage with its deformation response to cyclic loading: does cartilage optimize its modulus so as to minimize the strains arising in it due to the prevalent loading regime? *Rheumatology* 40, 274-284 (2001).
33. Ko, F. C., Dragomir, C. L., Plumb, D. A., et. al. Progressive cell-mediated changes in articular cartilage and bone in mice are initiated by a single session of controlled cyclic compressive loading. *Journal of Orthopedic Research* 34, 1941-1949 (2016).
34. Park, S., Hung, C. T., Ateshian, G. A.. Mechanical Response of bovine articular cartilage under dynamic unconfined compression loading at physiological stress levels. *Osteoarthritis and Cartilage* 12, 65-73 (2004).
35. Kaplan, J. T., Neu, C. P., Drissi, H., et. al. Cyclic loading of human articular cartilage: the transition from compaction to fatigue. *Journal of the Mechanical Behavior of Biomedical Materials* 65, 734-742 (2017).
36. Dwivedi, G., Flaman, L., Frank, E., et. al. Human cartilage-bone-synovium microphysiological system to study ptoa pathogenesis and treatment on earth and in space. *Osteoarthritis and Cartilage* 27, S167 (2019).
37. Evans, A. *The Pocket Podiatry Guide: Paediatrics* 32-47 (Churchill Livingstone, 2010).
38. Tamer, T. M. Hyaluronan and synovial joint: function, distribution and healing. *Interdisciplinary Toxicology* 6, 111-125 (2013).
39. Goldring, S. R., Goldring, M. B. in *Kelley and Firestein's Textbook of Rheumatology* 1-19 (Elsevier, 2017).

40. OpenStax. Anatomy and Physiology, Synovial Joints. Available at: https://opentextbc.ca/anatomyandphysiology/chapter/9-4-synovial-joints/ (Accessed: 27th April 2020).
41. Schulz, R. M., Bader, A. Cartilage tissue engineering and bioreactor systems for the cultivation and stimulation of chondrocytes. *European Biophysics Journal* 36, 539-568 (2007).
42. Tarafder, S., Lee, C. H. in *In Situ Tissue Regeneration* 253-273 (Academic Press, 2016).
43. Sophia Fox, A. J., Bedi, A., Rodeo, S. A. The Basic Science of Articular Cartilage. *Sports Health* 1, 461-568 (2009).
44. Buckwalter, J. A., Mow, V. C., Ratcliffe, A. Restoration of Injured or Degenerated Articular Cartilage. *Journal of the American Academy of Orthopaedic Surgeons* 2, 192-201 (1994).
45. Buckwalter, J. A., Rosenberg, L. A., Hunziker, E. B. *Articular Cartilage and Knee Joint Function: Basic Science and Arthroscopy* 319-333 (Raven Press, 1990).
46. Buschmann, M. D., Grodzinsky, A. J. A molecular model of proteoglycan-associated electrostatic forces in cartilage mechanics. *Journal of Biomechanical Engineering* 117, 179-192 (1995).
47. Bhosale, A. M., Richardson, J. B. Articular cartilage: structure, injuries and review of management. *British Medical Bulletin* 87, 77-95 (2008).
48. Orthobullets. Articular Cartilage (2020). Available at: https://www.orthobullets.com/basic-science/9017/articular-cartilage (Accessed: 27th April 2020).
49. Fang, H., Huang, L., Welch, I., et al. Early changes of articular cartilage and subchondral bone in the DMM mouse model of osteoarthritis. *Nature Scientific Reports* 8, 2855 (2018).
50. Heidari, B. Knee osteoarthritis prevalence, risk factors, pathogenesis and features: Part I. *Caspian Journal of Internal Medicine* 2, 205-212 (2011).
51. Zhang, Y., Jordan, J. M. Epidemiology of osteoarthritis. *Clinics in Geriatric Medicine* 26, 355-369 (2010).
52. Grazio, S., Balen, D. Obesity: risk factor and predictor of osteoarthritis. *Lijecnicki vjesnik* 131, 22-26 (2009).
53. Altman, R. D. Early management of osteoarthritis. *American Journal of Managed Care* 16, S41-47 (2010).
54. Altman, R. D., Gold, G. E. Atlas of individual radiographic features in osteoarthritis, revised. *Osteoarthritis and Cartilage* 15, A1-A56 (2007).
55. Kolasinski, S. L., Neogi, T., Hochberg, M. C., et al. 2019 American College of Rheumatology/Arthritis Foundation Guideline for the Management of Osteoarthritis of the Hand, Hip, and Knee. *Arthritis Care & Research* 72, 149-162 (2020).
56. Spector, T. D., MacGregor, A. J. Risk factors for osteoarthritis: genetics. *Osteoarthritis and Cartilage* 12, S39-44 (2004).
57. Yucesoy, B., Charles, L. E., Baker, B., et al. Occupational and genetic risk factors of osteoarthritis: a review. *Work* 50, 261-273 (2015).
58. Sandell, L. Etiology of osteoarthritis: genetics and synovial joint development. *Nature Reviews Rheumatology* 8, 77-89 (2012).

59. Sandmark, H., Hogstedt, C., Vingard, E. Primary osteoarthrosis of the knee in men and women as a result of lifelong physical load from work. *Scandinavian Journal of Work, Environment & Health* 26, 20-25 (2000).
60. Muraki, S., Akune, T., Oka, H., et al. Association of occupational activity with radiographic knee osteoarthritis and lumbar spondylosis in elderly patients of population-based cohorts: a large-scale population-based study. *Arthritis & Rheumatology* 61, 779-796 (2009).
61. Murphy, G., Lee, M. H. What are the roles of metalloproteinases in cartilage and bone damage? *Annals of Rheumatic Diseases* 64, S4iv44-7 (2005).
62. Aigner, T., Kurz, B., Fukui, N., et al. Roles of chondrocytes in the pathogenesis of osteoarthritis. *Current Opinion in Rheumatology* 14, 578-584 (2002).
63. Sandiford, N., Kendoff, D., Muirhead-Allwood, S. Osteoarthritis of the hip: aetiology, pathophysiology and current aspects of management. *Annals of Joint* 5, 8 (2020).
64. Goldring, M. B., Goldring, S. R. Osteoarthritis. *Journal of Cell Physiology* 213, 626-634 (2007).
65. Suri, S., Walsh, D. A. Osteochondral alterations in osteoarthritis. *Bone* 51, 204-211 (2012).
66. Thomas, A. C., Hubbard-Turner, T., Wikstrom, E. A., et al. Epidemiology, of Posttraumatic Osteoarthritis. *Journal of Athletic Training* 52, 491-496 (2017).
67. Carbone, A., Rodeo, S. Review of current understanding of post-traumatic osteoarthritis resulting from sports injuries. *Journal of Orthopedic Research* 35, 397-405 (2016).
68. Segawa, H., Omori, G., Koga, Y. Long-term results of non-operative treatment of anterior cruciate ligament injury. *Knee* 8, 5-11 (2001).
69. Daniel, D. M., Stone, M. L., Dobson, B. E., et al. Fate of the ACL-injured patient. American *Journal of Sports Medicine* 22, 632-644 (1993).
70. Kessler, M., Behrend, H., Henz, S., et al. Function, osteoarthritis and activity after ACL-rupture: 11 years follow-up results of conservative versus reconstructive treatment. *Knee Surgery, Sports Traumatology, Arthroscopy* 16, 442-448 (2008).
71. Delco, M. L., Kennedy, J. G., Bonassar, L. J., et al. Post-traumatic osteoarthritis of the ankle: a distinct clinical entity requiring new research approaches. *Journal of Orthopedic Research* 35, 440-453 (2017).
72. Falah, M., Nierenberg, G., Soudry, M., et al. Treatment of articular cartilage lesions of the knee. *International Orthopaedics* 34, 621-630 (2010).
73. Irie, K., Uchiyama, E., Iwaso, H. Intraarticular inflammatory cytokines in acute anterior cruciate ligament injured knee. *Knee* 10, 93-96 (2003).
74. Haslauer C. M., Elsaid K. A., Fleming B. C., et al. Loss of extracellular matrix from articular cartilage is mediated by the synovium and ligament after anterior cruciate ligament injury. *Osteoarthritis and Cartilage* 21, 1950-1957 (2013).
75. Kramer, W. C., Hendricks, K. J., Wang, J. Pathogenic mechanisms of posttraumatic osteoarthritis: opportunities of early intervention. *International Journal of Clinical and Experimental Medicine* 4, 285-298 (2011).
76. Lima, D. D. D., Hashimoto, S., Chen, P. C., et al. Human chondrocyte apoptosis in response to mechanical injury. *Osteoarthritis and Cartilage* 9, 712-719 (2001).
77. Liu-Bryan, R., Terkeltaub, R. Emerging regulators of the inflammatory process in osteoarthritis. *Nature Reviews Rheumatology* 11, 35-44 (2014).

78. Ziskoven, C., Jager, M., Zilkens, C., et al. Oxidative stress in secondary osteoarthritis: from cartilage destruction to clinical presentation? *Orthopedic Reviews* 2, e23 (2010).
79. Riegger, J., Brenner, R. E. Pathomechanisms of Posttraumatic Osteoarhtritis: Chondrocyte Behavior and Fate in a Precarious Environment. *International Journal of Molecular Sciences* 21, 1560 (2020).
80. Scanlan, S. F., Chaudhari, A. M. W., Dyrby, C. O., et al. Differences in tibial rotation during walking in ACL reconstructed and healthy contralateral knees. *Journal of Biomechanics* 43, 1817-1822 (2011).
81. Jordan, J. M., Helmick, C. G., Renner, J. B., et al. Prevalence of knee symptoms and radiographic and symptomatic knee osteoarthritis in African Americans and Caucasians: the johnston county prevalence of knee symptoms and radiographic and symptomatic knee osteoarthritis in African Americans and Caucasians. *Rheumatology* 34, 172-180 (2007).
82. Dillon, C. F., Rasch, E. K., Gu, Q., et al. Prevalence of knee osteoarthritis in the United States: arthritis data from the third national health and nutrition examination survey. *Rheumatology* 33, 2271-2279 (2006).
83. Tourville, T. W., Johnson, R. J., Slauterbeck, J. R., et al. Relationship between markers of type II collagen metabolism and tibiofemoral joint space width changes after ACL injury and reconstruction. *American Journal of Sports Medicine* 41, 779-787 (2013).
84. Harkey, M. S., Luc, B. A., Golightly, Y. M., et al. Osteoarthritis-related biomarkers following anterior cruciate ligament injury and reconstruction: a systematic review. *Osteoarthritis and Cartilage* 23, 1-12 (2015).
85. Huang, Z., Ding, C., Li, T., et al. Current status and future prospects for disease modification in osteoarthritis. *Rheumatology* 57, iv108-123 (2018).
86. McAlindon, T. E., Bannuru, R. R., Sullivan, M. C., et al. OARSI guidelines for the non-surgical management of knee osteoarthritis. *Osteoarthritis & Cartilage* 22, 363-388 (2014).
87. Uhlig, T., Slatkowsky-Christensen, B., Moe, R. H., et al. The burden of osteoarthritis: the societal and the patient perspective. *Therapy* 7, 605-619 (2010).
88. Pelletier, J., Martel-Pelletier, J. The DMOAD Dream: a Generation Later. *Rheumatologist* 5, 18-20 (2011).
89. Lundblad, H., Kreicbergs, A., Jansson, K. A. Predication of persistent pain after total knee replacement for osteoarthritis. *Journal of Bone and Joint Surgery B* 90, 166-171 (2008).
90. Ronn, K., Reischul, N., Gautier, E., et al. Current Surgical Treatment of Knee Osteoarthritis. *Arthritis* 454873 (2011).
91. Krzeski, P., Bucklandwright, C., Bálint, G., et al. Development of musculoskeletal toxicity without clear benefit after administration of PG-116800, a matrix metalloproteinase inhibitor, to patients with knee osteoarthritis: a randomized, 12-month, double-blind, placebo-controlled study. *Arthritis Research & Therapy* 9, R109 (2007).
92. Brandt, K. D., Mazzuca, S. A., Katz, B. P., et al. Effects of doxycycline on progression of osteoarthritis: results of a randomized, placebo-controlled, double-blind trial. *Arthritis & Rheumatology* 52, 2015–2025 (2005).
93. Lohmander, L. S., Hellot, S., Dreher, D., et al. Intraarticular sprifermin (recombinant human fibroblast growth factor 18) in knee osteoarthritis: a randomized, double-blind, placebo-controlled trial. *Arthritis & Rheumatology* 66, 1820-1831 (2014).

94. Dahlberg, L. E., Aydemir, A., Muurahainen, N., et al. A first-in-human, double-blind, randomised, placebo-controlled, dose ascending study of intra-articular rhFGF18 (sprifermin) in patients with advanced knee osteoarthritis. *Clinical and Experimental Rheumatology* 34, 445-450 (2016).
95. Jo, C. H., Lee, Y. G., Shin, W. H., et al. Intra-articular injection of mesenchymal stem cells for the treatment of osteoarthritis of the knee: a proof-of-concept clinical trial. *Stem Cells* 32, 1254-1266 (2014).
96. Vega, A., Martín-Ferrero, M. A., Del, C. F., et al. Treatment of knee osteoarthritis with allogeneic bone marrow mesenchymal stem cells: a randomized controlled trial. *Transplantation* 99, 1681-1690 (2015).
97. Yves-Marie, P., Lars, R., Rosanna, F., et al. Adipose mesenchymal stromal cell-based therapy for severe osteoarthritis of the knee: a phase I dose-escalation trial. *Stem Cells Translational Medicine* 5, 847 (2016).
98. Manicourt, D., Beaulieu, A., Garnero, P., et al. Effect of treatment with the cathepsin-K inhibitor, balicatib, on cartilage volume and biochemical markers of bone and cartilage degradation in patients with painful knee osteoarthritis. *Osteoarthritis & Cartilage* 15, C130 (2007).
99. Lindstrom, E., Grabowska, U., Jerling, M., et al. MIV-711, a highly selective cathepsin K inhibitor, reduces biomarkers of bone resorption and cartilage degradation in healthy subjects. *Osteoarthritis & Cartilage* 22, S197 (2014).
100. Laslett, L. L., Kingsbury, S. R., Hensor, E. M., et al. Effect of bisphosphonate use in patients with symptomatic and radiographic knee osteoarthritis: data from the Osteoarthritis Initiative. *Annals of Rheumatic Diseases* 73, 824–830 (2014)
101. Bingham, C. O., Buckland-Wright, J. C., Garnero, P., et al. Risedronate decreases biochemical markers of cartilage degradation but does not decrease symptoms or slow radiographic progression in patients with medial compartment osteoarthritis of the knee: results of the two-year multinational knee osteoarthritis structural arthritis study. *Arthritis & Rheumatology* 54, 3494–3507 (2006).
102. Karsdal, M. A., Byrjalsen, I., Alexandersen, P., et al. Treatment of symptomatic knee osteoarthritis with oral salmon calcitonin: results from two phase 3 trials. *Osteoarthritis & Cartilage* 23, 532–543 (2015).
103. Reginster, J. Y., Badurski, J., Bellamy, N., et al. Extended report: efficacy and safety of strontium ranelate in the treatment of knee osteoarthritis: results of a double-blind, randomised placebo-controlled trial. *Annals of Rheumatic Diseases* 72, e13 (2013).
104. Pelletier, J. P., Roubille, C., Raynauld, J. P., et al. Disease-modifying effect of strontium ranelate in a subset of patients from the Phase III knee osteoarthritis study SEKOIA using quantitative MRI: reduction in bone marrow lesions protects against cartilage loss. *Annals of Rheumatic Diseases* 74, 422–429 (2013).
105. Cook, A. D., Pobjoy, J., Steidl, S., et al. Granulocyte-macrophage colony-stimulating factor is a key mediator in experimental osteoarthritis pain and disease development. *Arthritis Research & Therapy* 14, R199 (2012).
106. Matthews, G. L., Hunter, D. J. Emerging drugs for osteoarthritis. *Expert Opinion on Emerging Drugs* 16, 479–491 (2011).
107. Hellio le Graverand, M. P., Clemmer, R. S., Redifer, P., et al. A 2-year randomised, double-blind, placebo-controlled, multicentre study of oral selective iNOS inhibitor,

cindunistat (SD-6010), in patients with symptomatic osteoarthritis of the knee. *Annals of Rheumatic Diseases* 72, 187–195 (2013).
108. Jotanovic, Z., Mihelic, R., Sestan, B., et al. Role of interleukin-1 inhibitors in osteoarthritis: an evidence-based review. *Drugs & Aging* 29, 343–358 (2012).
109. Chevalier, X., Giraudeau, B., Conrozier, T., et al. Safety study of intraarticular injection of interleukin 1 receptor antagonist in patients with painful knee osteoarthritis: a multicenter study. *The Journal of Rheumatology* 32, 1317–1323 (2005).
110. Verbruggen, G., Wittoek, R., Cruyssen, B. V., et al. Tumour necrosis factor blockade for the treatment of erosive osteoarthritis of the interphalangeal finger joints: a double blind, randomised trial on structure modification. *Annals of Rheumatic Diseases* 71, 891–898 (2012).
111. Chevalier, X., Ravaud, P., Maheu, E., et al. Adalimumab in patients with hand osteoarthritis refractory to analgesics and NSAIDs: a randomised, multicentre, double-blind, placebo-controlled trial. *Annals of Rheumatic Diseases* 74, 1697–1705 (2015).
112. Evans, C. H., Kraus, V. B., Setton, L. A. Progress in intra-articular therapy. *Nature Reviews Rheumatology* 10, 11-22 (2014).
113. Wernecke, C., Braun, H. J., Dragoo, J. L. The effect of intra-articular corticosteroids on articular cartilage: a systematic review. *Orthopaedic Journal of Sports Medicine* 5, 2325967115581163 (2015).
114. Syed, H. M., Green, L., Bianski, B., et al. Bupivacaine and triamcinolone may be toxic to human chondrocytes: a pilot study. *Clinical Orthopaedics and Related Research* 469, 2941-2947 (2011).
115. Dragoo, J. L., Danial, C. M., Braun, H. J., et al. The chondrotoxicity of single-dose corticosteroids. *Knee Surgery, Sports Traumatology, Arthroscopy* 9, 1809-1814 (2012).
116. Wallis, W. J., Simkin, P. A., Nelp, W. B. Protein traffic in human synovial effusions. *Arthritis & Rheumatology* 30, 57-63 (1987).
117. Larsen, C., Ostergaard, J., Larsen, S. W., et al. Intra-articular depot formulation principles: role in the management of postoperative pain and arthritic disorders. *Journal of Pharmaceutical Sciences* 97, 4622-4654 (2008).
118. Bajapayee, A. G., Wong, C. R., Bawendi, M. G., et al. Avidin as a model for charge driven transport into cartilage and rug delivery for treating early stage post-traumatic osteoarthritis. *Biomaterials* 35, 538-549 (2014).
119. Hollander, J. L. Clinical use of dexamethasone: role in treatment of patients with arthritis. *JAMA* 172, 306-310 (1960).
120. Asadullah, K., Schacke, H., Cato, A. C. Dichotomy of glucocorticoid action in the immune system. *Trends in Immunology* 23, 120-122 (2002).
121. Vanden Berghe, W., Vermeulen, L., De Wilde, G., et al. Signal transduction by tumor necrosis factor and gene regulation of the inflammatory cytokine interleukin-6. *Biochemical Pharmacology* 60, 1185–1195 (2000).
122. Grewe, M., Gausling, R., Gyufko, K., et al. Hoffmann R, Decker K. Regulation of the mRNA expression for tumor necrosis factor-alpha in rat liver macrophages. *Journal of Hepatology* 20, 811–818 (1994).
123. Bendrups, A., Hilton, A., Meager, A., et al. Reduction of tumor necrosis factor alpha and interleukin-1 beta levels in human synovial tissue by interleukin-4 and glucocorticoid. *Rheumatology International* 12, 217–220 (1993).

124. Lukiw, W. J., Pelaez, R. P., Martinez, J., et al. Budesonide epimer R or dexamethasone selectively inhibit platelet-activating factor-induced or interleukin 1beta-induced DNA binding activity of cis-acting transcription factors and cyclooxygenase-2 gene expression in human epidermal keratinocytes. *Proceedings of the National Academy of Sciences USA* 95, 3914–3919 (1998).
125. DiBattista, J. A., Martel-Pelletier, J., Wosu, L. O., et al. Glucocorticoid receptor mediated inhibition of interleukin-1 stimulated neutral metalloprotease synthesis in normal human chondrocytes. *The Journal of Clinical Endocrinology & Metabolism* 72, 316-326 (1991).
126. Makrygiannakis, D., Revu, S., Engstrom, M., et al. Local administration of glucocorticoids decreases synovial citrullination in rheumatoid arthritis. *Arthritis Research & Therapy* 14, R20 (2012).
127. Fernandez-Palazzi, F., Caviglia, H. A., Salazar, J. R., et al. Intraarticular dexamethasone in advanced chronic synovitis in hemophilia. *Clinical Orthopaedics and Related Research* 343, 25–29 (1997).
128. Mollmann, H., Balbach, S., Hochhaus, G., et al in *Handbook of Pharmacokinetic/Pharmacodynamic Correlation* 323-362 (CRC Press, 1995).
129. PubChem (NIH National Library of Medicine). Dexamethasone (2020). Available at: https://pubchem.ncbi.nlm.nih.gov/compound/Dexamethasone (Accessed: 4th May 2020).
130. Aguirre, A. G., Rodriguez De Ita, J., de la Garza, R. G., et al. Insulin-like growth factor-1 deficiency and metabolic syndrome. *Journal of Translational Medicine* 14, 3 (2016).
131. Yin, W., Park, J. I., Loeser, R. F. Oxidative stress inhibits insulin-like growth factor-I induction of chondrocyte proteoglycan synthesis through differential regulation of phosphatidylinositol 3-Kinase-Akt and MEK-ERK MAPK signaling pathways. *Journal of Biological Chemistry* 284, 31972-31981 (2009).
132. Perez, R., Garcia-Fernandez, M., Diaz-Sanchez, M., et al. Mitochondrial protection by low doses of insulin-like growth factor-I in experimental cirrhosis. *World Journal of Gastroenterology* 14, 2731–2739 (2008).
133. Puche, J. E., Garcia-Fernandez, M., Muntane, J., et al. Low doses of insulin-like growth factor-I induce mitochondrial protection in aging rats. *Endocrinology* 149, 2620–2627 (2008).
134. Garcia-Fernandez, M., Delgado, G., Puche, J. E., et al. Low doses of insulin-like growth factor I improve insulin resistance, lipid metabolism, and oxidative damage in aging rats. *Endocrinology* 149, 2433–2442 (2008).
135. Lo, M. Y., Kim, H. T.. Chondrocyte apoptosis induced by collagen degradation: inhibition by caspase inhibitors and IGF-1. *Journal of Orthopedic Research* 22, 140-144 (2004).
136. D'Lima, D. D., Hashimoto, S., Chen, P. C., et al. Prevention of chondrocyte apoptosis. *Journal of Bone and Joint Surgery* 83-A, 25-26 (2001).
137. Tyler, J. A. Insulin-like growth factor 1 can decrease degradation and promote synthesis of proteoglycan in cartilage exposed to cytokines. *Biochemical Journal* 260, 543-548 (1989).
138. Protein Data Bank. Insulin Like Growth Factor 1 (2020). Available at: https://www.rcsb.org/structure/1b9g (Accessed: 4th May 2020).
139. Ahmed, A. M., Burke, D. L. In-vitro measurement of static pressure distribution in synovial joints – part I: tibial surface of the knee. *Journal of Biomechanical Engineering* 105, 216-225 (1983).

140. Brown, T. D., Shaw, D. T. In vitro contact stress distributions in the natural human hip. *Journal of Biomechanics* 16, 373-384 (1983).
141. Matthews, L. S., Sonstegard, D. A. Hanke, J. A. Load bearing characteristics of the patella-femoral joint. *Acta Orthopaedica* 48, 511-516 (1977).
142. Armstrong, C. G., Bahrani, A. S., Gardner, D. L. In vitro measurement of articular cartilage deformations in the intact human hip joint under load. *Journal of Bone and Joint Surgery* 61, 744-755 (1979).
143. Kaab, M. J., Ito, K., Clark, J. M., et al. Deformation of articular cartilage collagen structure under static and cyclic loading. *Journal of Orthopedic Research* 16, 743-751 (1998).
144. Cross, R. Standing, walking, running, and jumping on a force plate. *American Journal of Physics* 67, 304-309 (1999).
145. Dickinson, J. A., Cook, S. D., Leinhardt, T. M. The measurement of shock waves following heel strike while running. *Journal of Biomechanics* 18, 415-422 (1985).
146. Hoshino, A., Wallace, W. A. Impact-absorbing properties of the human knee. *Journal of Bone and Joint Surgery* 69, 807-811 (1987).
147. Iqbal, S. M., Leonard, C., Regmi, S. C., et al. Lubricin/Proteoglycan 4 binds to and regulates the activity of Toll-like receptors *in vitro*. *Nature Scientific Reports* 6, 18910 (2016).
148. Musumeci, G., Loreto, C., Leonardi, R., et al. The effects of physical activity on apoptosis and lubricin expression in articular cartilage in rats with glucocorticoid-induced osteoporosis. *Journal of Bone and Mineral Metabolism* 31, 274-284 (2013).
149. Eckstein, F., Hudelmaier, M., Putz, R. The effects of exercise on human articular cartilage. *Journal of Anatomy* 208, 491-512 (2006).
150. Mow, V. C., Holmes, M. H., Lai, W. M. Fluid transport and mechanical properties of articular cartilage: a review. *Journal of Biomechanics* 17, 377-394 (1984).
151. Miller, G. J., Morgan, E. F. Use of microindentation to characterize the mechanical properties of articular cartilage: comparison of biphasic material properties across length scales. *Osteoarthritis & Cartilage* 18, 1051-1057 (2010).
152. Simon, B. R., Coats, R. S., Woo, S. L. Y. Relaxation and creep quasi linear viscoelastic models for normal articular cartilage. *Journal of Biomechanical Engineering* 106, 159-164 (1984).
153. Woo, S. L. Y., Mow, V. C., Lai, W. M. in *Handbook of Bioengineering* 4.1-4.44 (McGraw-Hill Book Co, 1987).
154. Lee, R. C., Frank, E. H., Grodzinsky, A. J., et al. Oscillatory compressional behavior of articular-cartilage and its associated electro-mechanical properties. *Journal of Biomechanical Engineering- Transactions of the ASME* 103, 280-292 (1981).
155. Frank, E. H., Grodzinsky, A. J. Cartilage electromechanics 1 electrokinetic transduction and the effects of electrolyte Ph and ionic-strength. *Journal of Biomechanics* 20, 615-627 (1987).
156. Grodzinsky, A. J., Frank, E. H. *Fields, Forces, and Flows in Biological Systems* 239-286 (Garland Science, 2011).
157. Li, L. P., Soulhat, J., Buschmann, M. D., et al. Nonlinear analysis of cartilage in unconfined ramp compression using a fibril reinforced poroelastic model. *Clinical Biomechanics* 14, 673-682 (1999).

158. Musumeci, G. The Effect of Mechanical Loading on Articular Cartilage. *Journal of Functional Morphology and Kinesiology* 1, 154-161 (2016).
159. Nejati, P., Farzinmehr, A., Moradi-Lakeh, M. The effect of exercise therapy on knee osteoarthritis: a randomized clinical trial. *Medical Journal of the Islamic Republic of Iran* 29, 186 (2015).
160. NIH Clinical Trials. Early Regenerative Intervention for Post-Traumatic Osteoarthritis (ERIPTO). Available at: https://clinicaltrials.gov/ct2/show/NCT04222140 (Accessed: 9th May 2020).
161. NIH Clinical Trials. Prevention of Post-Traumatic Osteoarthritis (OA). Available at: https://clinicaltrials.gov/ct2/show/results/NCT00054821 (Accessed: 9th May 2020).
162. Akeson, W. H., Woo, S. L., Amiel, D., et al. The Connective Tissue Response to Immobility: Biochemical Changes in Periarticular Connective Tissue of the Immobilized Rabbit Knee. *Clinical Orthopaedics and Related Research* 93, 356-362 (1973).
163. Kiviranta, I., Jurvelin, J., Tammi, M., at al. Weight bearing controls glycosaminoglycan concentration and articular cartilage thickness in the knee joints of young beagle dogs. *Arthritis & Rheumatism* 30, 801-809 (1987).
164. Gray, M. L., Pizzanelli, A. M., Grodzinsky, A. J., et al. Mechanical and physicochemical determinants of the chondrocyte biosynthetic response. *Journal of Orthopaedic Research* 6, 777-792 (1988).
165. Palmoski, M. J., Brandt, K. D. Effects of static and cyclic compressive loading on articular cartilage plugs in vitro. *Arthritis & Rheumatism* 27, 675-681 (1984).
166. Larsson, T., Aspden, R. M., Heinegard, D. Effects of mechanical load on cartilage matrix biosynthesis in vitro. *Matrix* 11, 388-394 (1991).
167. Parkkinen, J. J., Lammi, M. J., Helminen, H. J., et al. Local stimulation of proteoglycan synthesis in articular cartilage explants by dynamic compression in vitro. *Journal of Orthopedic Research* 10, 610-620 (1992).
168. Salinas, D., Mumey, B. M., June, R. K. Physiological dynamic compression regulates central energy metabolism in primary human chondrocytes. *Biomechanics and Modeling in Mechanobiology* 18, 69-77 (2019).
169. Fu, S., Thompson, C. L., Ali, A., et al. Mechanical loading inhibits cartilage inflammatory signaling via an HDAC6 and IFT-dependent mechanism regulating primary cilia elongation. *Osteoarthritis & Cartilage* 27, 1064-1074 (2019).
170. Nia, H. T., Bozchalooi, I. S., Li, Y., et. al. High-bandwidth AFM-based rheology reveals that cartilage is most sensitive to high loading rates in early stages of impairment. *Biophysical Journal* 104, 1529-1530 (2013).
171. Frank, E. H., Jin, M., Loening, A. M., et. al. A versatile shear and compression apparatus for mechanical stimulation of tissue culture explants. *Journal of Biomechanics* 33, 1523-1527 (2000).
172. Farndale, R. W., Buttle, D. J., Barrett, A. J. Improved quantitation and discrimination of silphated glycosaminoglycans by use of dimethymethylene blue. *Biochemical and Biophysical Acta* 833, 178-177 (1986).
173. Kim, Y. J., Sah, R. L., Doong, J. Y., et. al. Fluorometric assay of DNA in cartilage explants using Hoechst 33258. *Archives of Biochemistry and Biophysics* 174, 168-176 (1988).
174. Stegemann, H., Stalder, K. Determination of hydroxyproline. *Clinica Chimica Acta* 18, 267-273 (1967).

175. Woessner, J. F. The determination of hydroxyproline in tissue and protein samples containing small proportions of this imino acid. *Archives of Biochemistry and Biophysics* 93, 440-447 (1961).
176. Treppo, S., Koepp, H., Quan, E. C., et. al. Comparison of biomechanical and biochemical properties of cartilage from human knee and ankle pairs. *Journal of Orthopedic Research* 18, 739-748 (2000).
177. Downs, M. E. *ARED Example Exercise Days* (Sent by email December 18th, 2019).
178. Sundberg, C. W., Bundle, M. W. Influence of duty cycle on the time course of muscle fatigue and the onset of neuromuscular compensation during exhaustive dynamic isolated limb exercise. *American Journal of Physiology – Regulatory, Integrative and Comparative Physiology* 309, R51-R61 (2015).
179. Temple, D. K., Cederlund, A. A., Lawless, B. M., et. al. Viscoelastic properties of human and bovine articular cartilage: a comparison of frequency-dependent trends. *BMC Musculoskeletal Disorders* 17, 419 (2016).
180. Bonassar, L. J., Grodzinsky, A. J., Srinivasan, A., et. al. Mechanical and physiochemical regulation of the action of insulin-like growth factor-I on articular cartilage. *Archives of Biochemistry and Biophysics* 379, 57-63 (2000).
181. Mauck, R. L., Wang, C. C., Oswald, E. S., et. al. The role of cell seeding density and nutrient supply for articular cartilage tissue engineering with deformational loading. *Osteoarthritis and Cartilage* 11, 879–890 (2003).
182. Bobacz, K., Erlacher, L., Smolen, J., et. al. Chondrocyte number and proteoglycan synthesis in the aging and osteoarthritic human articular cartilage. *Annals of the Rheumatic Diseases* 63, 1618–1622 (2004).
183. Armstrong, C. G., & Mow, V. C. Variations in the intrinsic mechanical properties of human articular cartilage with age, degeneration, and water content. *The Journal of Bone and Joint Surgery* 64, 88–94 (1982).
184. Mountcastle, S. E., Allen, P., Mellors, B., et. al. Dynamic viscoelastic characterisation of human osteochondral tissue: understanding the effect of the cartilage-bone interface. *BMC Musculoskeletal Disorders* 20, 575 (2019).
185. Shuaib, A., Motan, D., Bhattacharya, P., et. al. Heterogeneity in The Mechanical Properties of Integrins Determines Mechanotransduction Dynamics in Bone Osteoblasts. *Scientific Reports* 9, 13113 (2019).
186. Wen, C., Xu, L., Xu, X., et. al. Insulin-like growth factor-1 in articular cartilage repair for osteoarthritis treatment. *Arthritis Research & Therapy* 23, 277 (2021).
187. Black, R., & Grodzinsky, A. J. Dexamethasone: chondroprotective corticosteroid or catabolic killer?. *European Cells & Materials* 38, 246–263 (2019).
188. Brommer, H., Brama, P. A., Laasanen, M. S., et. al. Functional adaptation of articular cartilage from birth to maturity under the influence of loading: a biomechanical analysis. *Equine Veterinary Journal* 37, 148–154 (2005).
189. Rotter, N., Tobias, G., Lebl, M., et. al. Age-related changes in the composition and mechanical properties of human nasal cartilage. *Archives of Biochemistry and Biophysics* 403, 132–140 (2002).
190. Martin, J. A., Buckwalter, J. A., Articular cartilage aging and degeneration. *Sports Medicine and Arthroscopy Review* 4, 263–275 (1996).

191. Franz, T., Hasler, E. M., Hagg, R., et. al. In situ compressive stiffness, biochemical composition, and structural integrity of articular cartilage of the human knee joint. *Osteoarthritis and Cartilage* 9, 582–592 (2001).
192. Wang, Y., Lorenzo, P., Chubinskaya, S., et. al. Dexamethasone treatment alters the response of human cartilage explants to inflammatory cytokines and mechanical injury as revealed by discovery proteomics. *Osteoarthritis and Cartilage* 25, S76-S444 (2017).
193. Sadowski, T., Steinmeyer, J., 2001. Effects of non-steroidal antiinflammatory drugs and dexamethasone on the activity and expression of matrix metalloproteinase-1, matrix metalloproteinase-3 and tissue inhibitor of metalloproteinases-1 by bovine articular chondrocytes. Osteoarthritis and Cartilage 9, 407–415.
194. Palmer, R. M., Hickery, M. S., Charles, I. G., et. al. Induction of nitric oxide synthase in human chondrocytes. *Biochemical and Biophysical Research Communications* 193, 398–405 (1993).
195. Black, R. M., Wang, Y., Struglics, A., et. al. Proteomic analysis reveals dexamethasone rescues matrix breakdown but not anabolic dysregulation in a cartilage injury model. *Osteoarthritis and Cartilage Open* 2, 100099 (2020).
196. Black, R. M., Wang, Y., Struglics, A., et. al. Proteomic clustering reveals the kinetics of disease biomarkers in bovine and human models of post-traumatic osteoarthritis. *Osteoarthritis and Cartilage Open* 3, 100191 (2021).
197. Pratta, M. A., Yao, W., Decicco, C., et. al. Aggrecan protects cartilage collagen from proteolytic cleavage. *The Journal of Biological Chemistry* 278, 45539–45545 (2003).
198. Bian, L., Lima, E. G., Angione, S. L., et. al. Mechanical and biochemical characterization of cartilage explants in serum-free culture. *Journal of Biomechanics* 41, 1153–1159 (2008).
199. Guo, J. B., Liang, T., Che, Y. J., et. al. Structure and mechanical properties of high-weight-bearing and low-weight-bearing areas of hip cartilage at the micro- and nano-levels. *BMC Musculoskeletal Disorders* 21, 425 (2020).
200. Sanchez-Adams, J., Wilusz, R. E., Guilak, F. Atomic force microscopy reveals regional variations in the micromechanical properties of the pericellular and extracellular matrices of the meniscus. *Journal of Orthopaedic Research* 31, 1218–1225 (2013).
201. Wang, M., Peng, Z., Watson, J. A., et. al. Nanoscale study of cartilage surfaces using atomic force microscopy. *Proceedings of the Institution of Mechanical Engineers. Part H, Journal of Engineering in Medicine* 226, 899–910 (2012).
202. Bian, L., Stoker, A. M., Marberry, K. M., et. al. Effects of dexamethasone on the functional properties of cartilage explants during long-term culture. *The American Journal of Sports Medicine* 38, 78–85 (2010).
203. Zhao, H., Liu, J., Li, Y., et. al. Validation of Reference Genes for Quantitative Real-Time PCR in Bovine PBMCs Transformed and Non-transformed by Theileria annulata. *The Korean Journal of Parasitology 54*, 39–46 (2016).
204. Fitzgerald, J. B., Jin, M., Grodzinsky, A. J. Shear and compression differentially regulate clusters of functionally related temporal transcription patterns in cartilage tissue. *The Journal of Biological Chemistry* 281, 24095–24103 (2006).

8 APPENDICIES

8.1 Commonly Used Recipes and Protocols

1. HG/LGCCM (High glucose/low glucose complete control medium)
For 50 mL of medium:
-47.6 mL Dulbecco's modified eagle medium (DMEM), low glucose (1 g/L) or high glucose (4.5 g/L)
-500 uL HEPES
-500 ul Non-essential amino acids (NEAA)
-500 ul Penicillin G, Streptomycin, Amphotericin B (PSA)
-500 ul Insulin, transferrin, selenium (ITS)
-200 ul Ascorbic acid
-200 ul Proline

2. Proteinase K
For stock solution of 2 mg/ml for human tissue:
-dissolve 100 mg proteinase K in 50 mL Tris Buffer (50 mM Tris-HCl, 1 mM $CaCl_2$, pH 8.0)
For solution of 0.1 mg/ml for bovine tissue:
-1:20 dilution of stock in Tris buffer

3. *Detailed Dynastat Protocol*
Preparation:
1. Separate the cartilage plug from the bone. The height of each individual plug needs to be determined first since it is required to run the program.
2. Prepare PBS with Protease inhibitor (PBS-PI) to be used in the chamber while the compression analysis is being carried out to prevent drying and proteolysis of the samples during the procedure which typically takes 45 minutes. Dissolve one pill in 50 ml PBS. The pills are stored in a small bright blue bottle (just like the Pro-K bottle) on RHS in the walk-in refrigerator.

Procedure:
1. Thaw cartilage in PBS-PI.
2. Choose correct protocol (Biomech.pro).
3. Lower platen to -50g and tighten parts.
4. Configure 10g Hi-R balance so that load reads around -10g.
5. Add the parameters pertinent to the sample – sample name and height and area. The area will remain same for all the plugs 9.62 m^2.
7. Save output file.
8. Begin program: "Prompt – Insert sample."
9. Only at this point, put the plug into the chamber, trying to place it at the center. DO NOT add fluid (PBS-PI) at this point as the plug may float away since it is not secured in any way.
10. Continue program so that "Prompt – "Put in Fluid" appears.
11. Now add, 2 ml of PBS-PI to the chamber slowly.

12. Continue program so that “Prompt – “Make LO-R = HI-R” appears.
13. Look at the “difference” in voltage field on the right hand side in the program.
14. Try to adjust the difference to near 0 using the wheel on the loading component, on the left side of the sample/loading chamber by turning clockwise or anticlockwise.
15. Then adjust using the small attached screw driver through the “LOW R BAL” on the console. Turn clockwise or anticlockwise until the difference starts to move between + 0.00xy and -0.00xy, essentially meaning 0. It will not be an exact zero.
16. Then switch Hi-R to Lo-R. There is a button on the console for this. Pull the plug out and push downwards to switch from Hi-R to Lo-R.
17. Continue program so that stress-relaxation and dynamic testing will begin.
18. After about 40-45 minutes, the program will end.
19. There will be a “Prompt – Sample unloaded” message.
20. Continue program so that “Prompt – Set Lo-R to Hi-R” appears.
21. Set Lo-R to Hi-R by pushing the plug upwards.
22. Continue program, and platen will move upwards.
23. Take the sample out of the sample chamber.
24. Remove the fluid from the chamber before adding the next sample.

8.2 Supplemental Data

Gene Name	Forward (5’ → 3’)	Reverse (5’ → 3’)
beta-Actin[203]	GATCTGGCACCACACCTTCTAC	AGGCATACAGGGACAGCACA
18S rRNA[203]	TTCGATGGTAGTCGCTGTGC	TTGGATGTGGTAGCCGTTTCT
ACAN[13]	CCTGAACGACAAGACCATCGA	TGGCAAAGAAGTTGTCAGGCT
iNOS[13]	AGGAGATAGAAACAACAGGAACC	TGCCATCTGGCATCTGGTAGC
COX2[204]	AAAAGCTGGGAAGCCTTTTC	GCTCTTTCCTCCCTTTCACA
NFkB[29]	CGGGTGAATCGGAACTCTGG	TCGATGTCCTCTTTCTGCACC
MAPK1[204]	TCCAAGGGCTACACCAAGTC	GTGGTTCAGCTGGTCAAGGT
COL2[204]	AAGAAGGCTCTGCTCATCCAGG	TAGTCTTGCCCCACTTACCGGT
CASP3[17]	GAAGTCTGACTGGAAAACCC	GAAGTCTGCCTCAACTGGTA
ADAMTS4[204]	AACTCGAAGCAATGCACTGGT	TGCCCGAAGCCATTGTCTA
ADAMTS5[204]	CTCCCATGACGATTCCAA	AATGCTGGTGAGGATGGAAG

Table S1. Primer Pairs and Sequences. List of primers used for bovine gene expression study with gene name (cited with a previous study using the primer), as well as forward and reverse sequences.

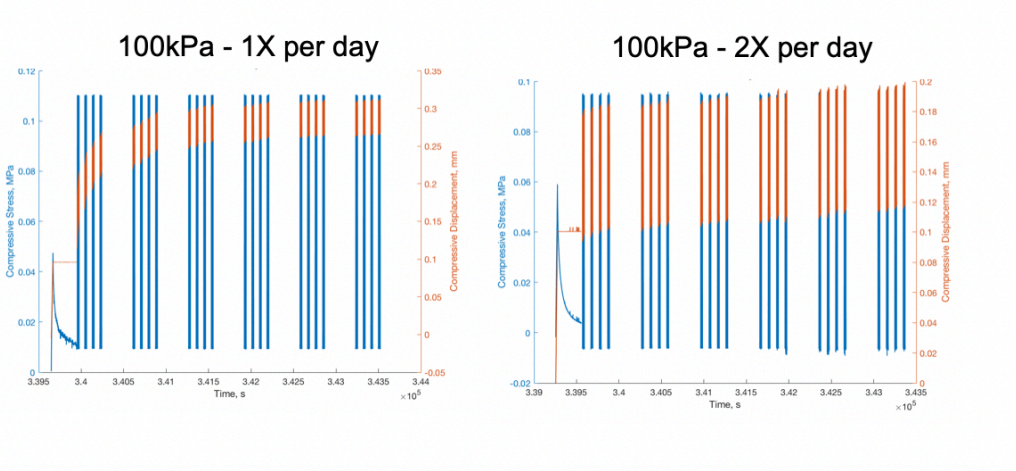

Figure S1. Loading Frequency Study: Representative Stress/Strain Curves. Loading occurred in two compression apparatus chambers, with the same contact strain (10%) and dynamic load (100 kPa). Total strain for both once and twice per day groups fell within the optimal 20-30% strain range.

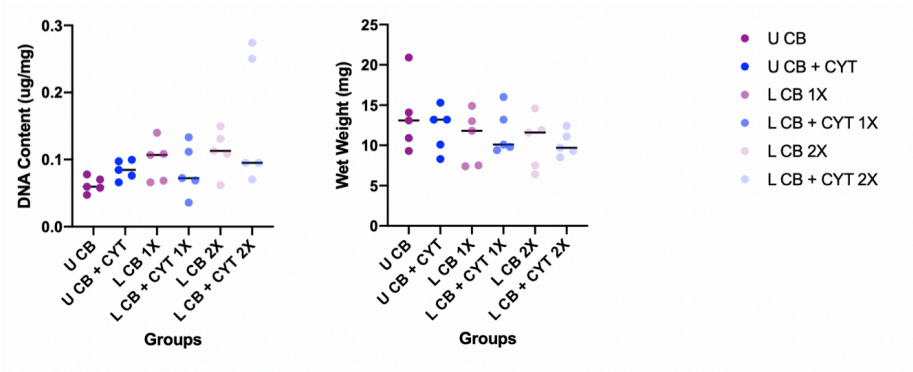

Figure S2. Loading Frequency Study: DNA and Wet Weight. DNA content was measured with PicoGreen and weights were measured on the final experimental day immediately after removal from media. There were no significant differences in DNA content and wet weight between all groups after 7 days.

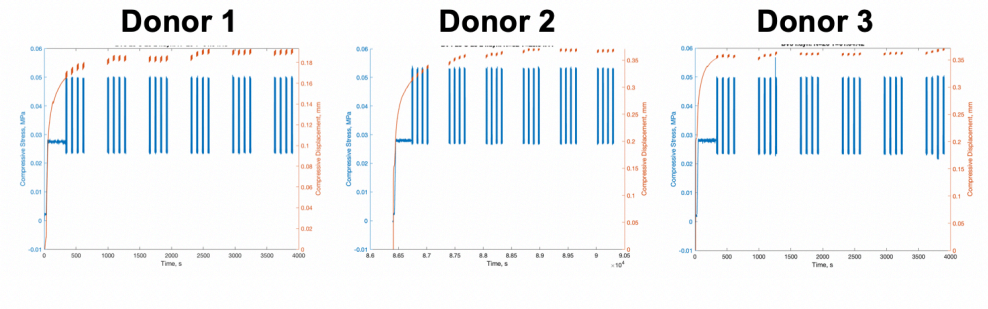

Figure S3. Bovine Biologic Study: Representative Stress/Strain Curves. Loading occurred in a single compression apparatus chamber, which was used for all three donors with the same contact load (25 kPa) and dynamic load (25 kPa). Total strain for all groups fell between the 20-35% range, with donors 2 and 3 at the higher end of this range compared to donor 1.

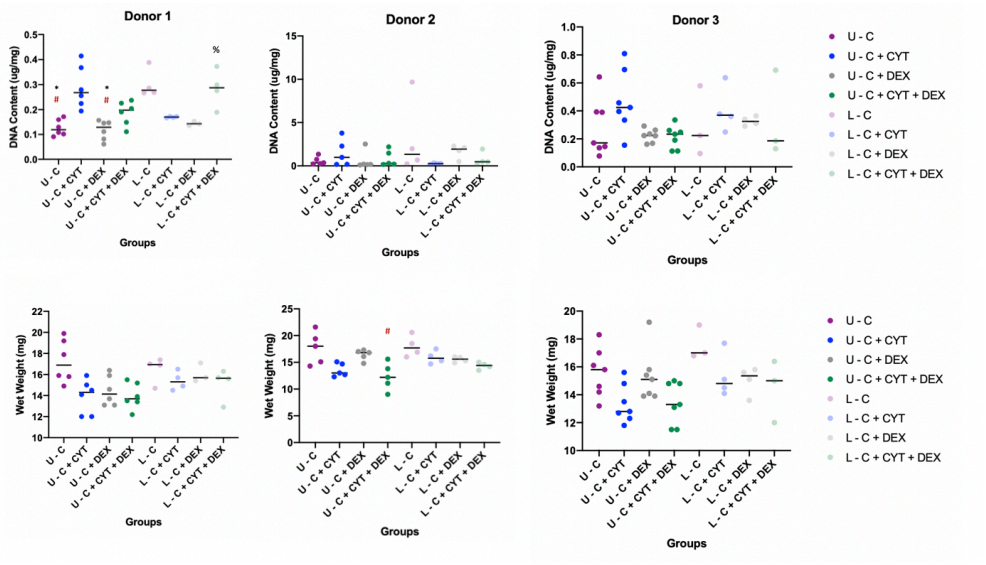

Figure S4. Bovine Biologic Study: DNA Content and Wet Weight. DNA content was measured with the Hoechst assay and weights were measured on the final experimental day immediately after removal from media. # $p<0.05$ as compared to L C; * $p<0.05$ as compared to U C+CYT; % $p<0.05$ as compared to U C+DEX using Kruskal-Wallis test. There were significant differences in DNA content for donor 1 between two groups: 1) unloaded cartilage alone and with Dex, with lower DNA content, and 2) loaded cartilage alone and unloaded cartilage with cytokines, with higher DNA content. These changes were not seen for the other donors. There were no significant differences in wet weight.

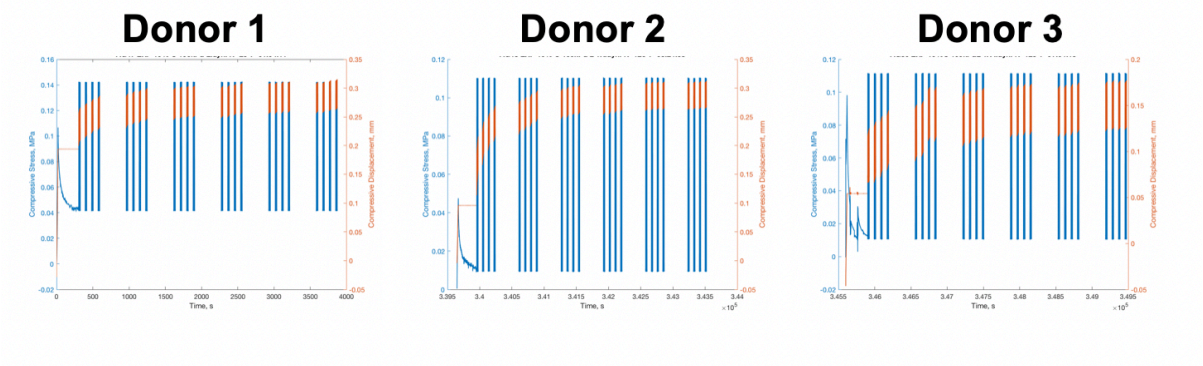

Figure S5. Human Biologic Study: Representative Stress/Strain Curves. Loading occurred in a single compression apparatus chamber, which was used for all three donors with the same contact strain (10%) and dynamic load (100 kPa). Total strain for all groups fell between the 15-30% range, with donors 1 and 2 at the higher end of this range compared to donor 3.

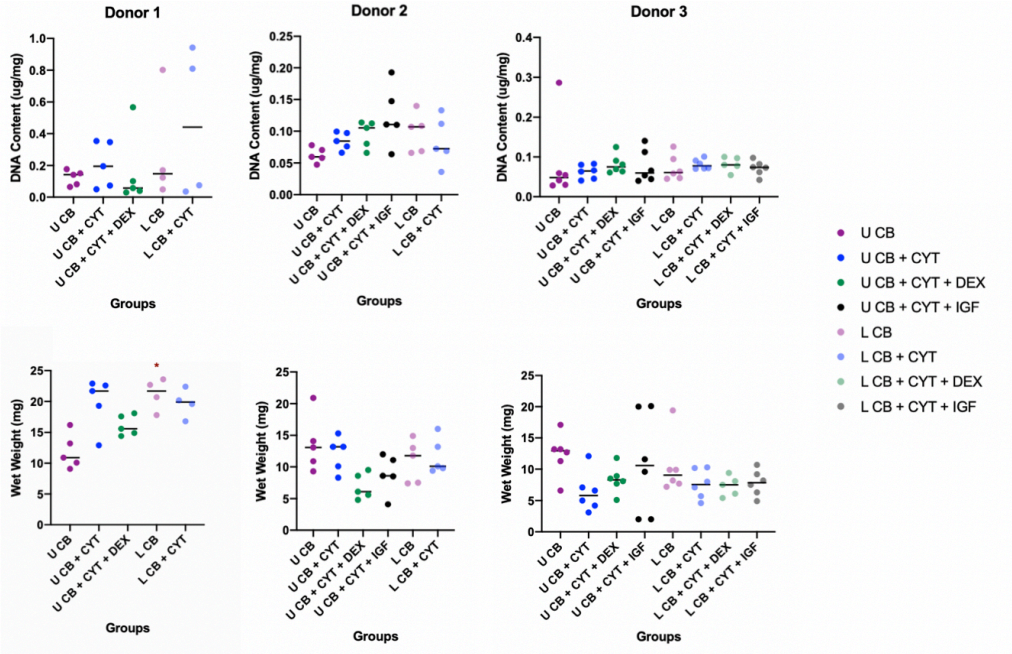

Figure S6. Human Biologic Study: DNA Content and Wet Weight. DNA content was measured with PicoGreen and weights were measured on the final experimental day immediately after removal from media. * $p<0.05$ as compared to U CB using Kruskal-Wallis test. There were no significant differences in DNA content for all donors. For donor 1, there was a significantly higher wet weight in the loaded CB groups as compared to its unloaded equivalent.

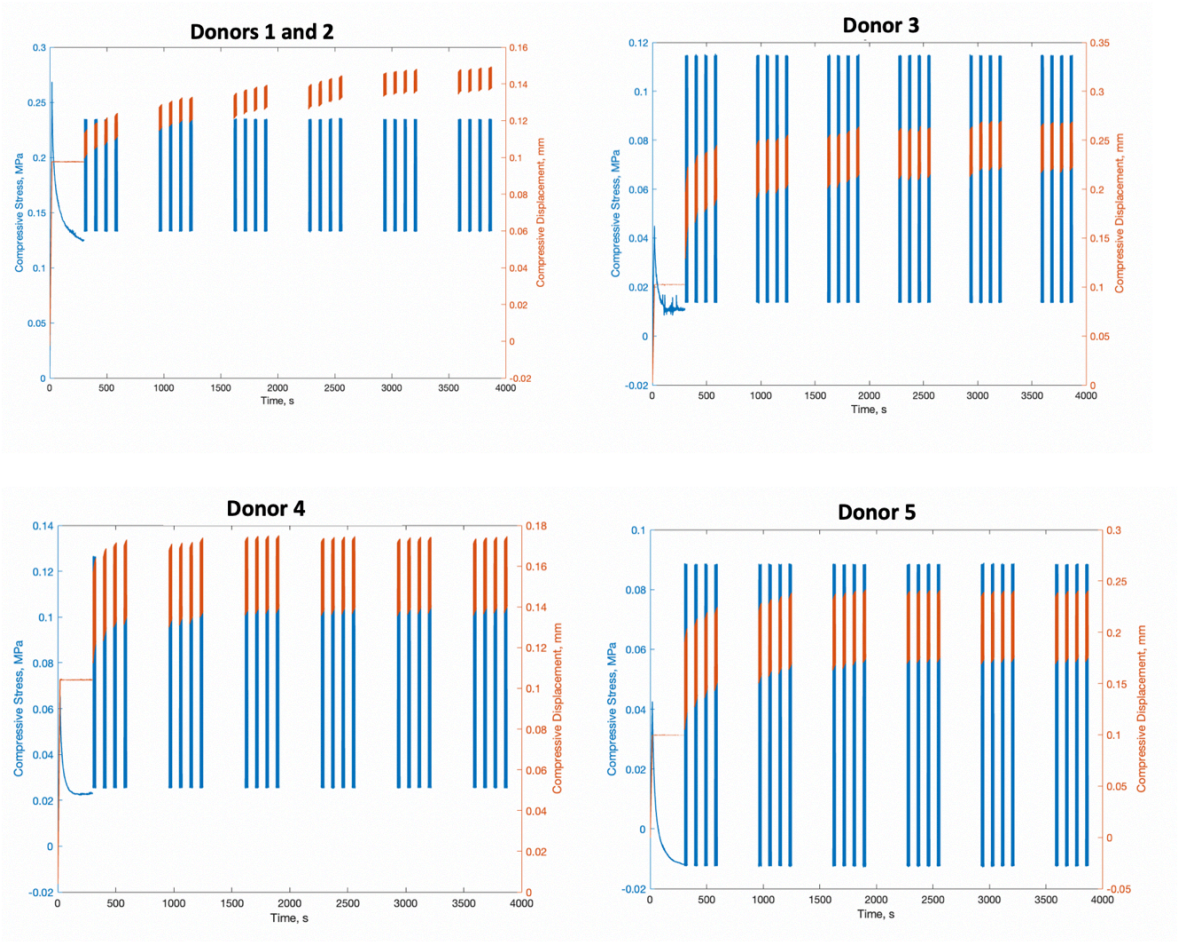

Figure S7. Human Mechanical Study: Representative Stress/Strain Curves. Loading occurred in a single compression apparatus chamber, which was used for all three donors with the same contact strain (10%) and dynamic load (100 kPa). Total strain for all groups fell between the 15-25% range, with donor 3 at the higher end and donors 1 and 2 at the lower end of this range. Experiments for donors 1 and 2 were conducted at the same time.

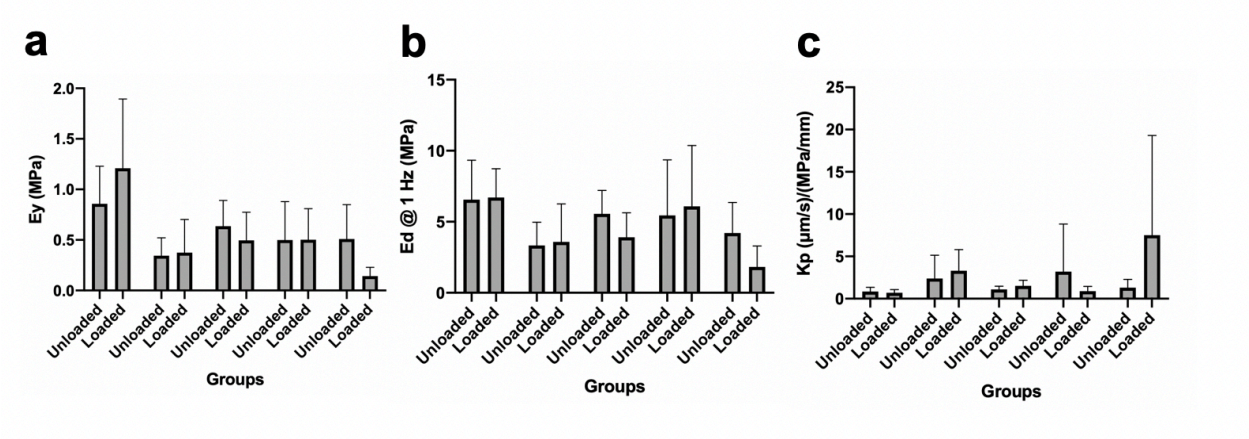

Figure S8. Human Mechanical Study: Biomechanical Properties After Loading at Baseline. The values of (a) E_y, (b) E_d, and (c) K_p for cartilage at day 0 for each donor, both unloaded and after one hour of loading. N=5-6 explants from each of n=5 donors. Data are presented as mean with 95% CI.

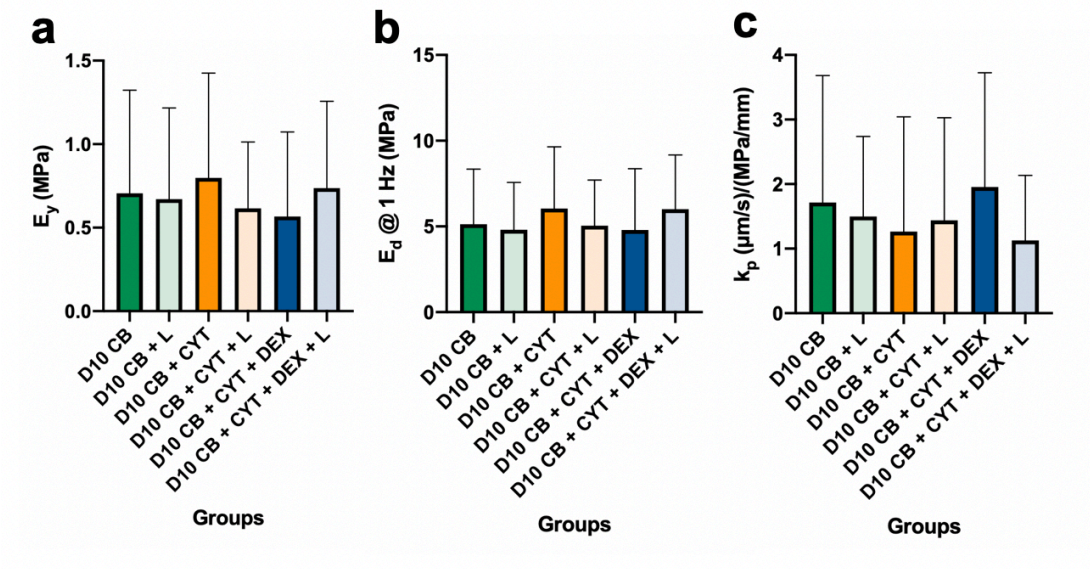

Figure S9. Human Mechanical Study: Biomechanical Changes with Addition of Cytokines and Dexamethasone and Response to Loading, Non-Normalized. Values of (a) E_y, (b) E_d, and (c) k_p for cartilage at day-10 of treatment with control media, cytokines, and cytokines with Dex. For each treatment group, explants were either unloaded or underwent one hour of loading before mechanical testing. N=26-29 explants from a total of n=5 donors in each treatment group. Data are presented as mean with 95% CI for each treatment condition. L: loaded explant.

Group	Ey (β [95% CI], R, *p*)	Ed (β [95% CI], R, *p*)	Kp (β [95% CI], R, *p*)
D0 CB N=29	0.0300 [0.0175, 0.0423], 0.6185, *0.0003*	0.2743 [0.1850, 0.3636], 0.7389, *<0.0001*	-2.274e-4 [-3.493e-4, -9.058e-5], -0.5323, *0.0030*
D10 CB N=29	0.0293 [-0.0020, 0.0586], 0.2432, *0.2036*	0.1745 [0.0318, 0.3126], 0.3391, *0.0719*	-9.290e-5 [-1.872e-4, -6.700e-6], -0.2718, *0.1538*
D10 CB + CYT N=27	0.0298 [-3.613e-4, 0.0655], 0.4774, *0.0118*	0.1322 [-0.0598, 0.3736], 0.3812, *0.0498*	-6.720e-5 [-1.791e-4, -2.179e-5], -0.2928, *0.1383*
D10 CB + CYT + DEX N=26	0.0170 [-0.0036, 0.0387], 0.4016, *0.0420*	0.2125 [0.0841, 0.3513], 0.6209, *0.0007*	-8.059e-5 [-1.535e-4, -1.045e-5], -0.4737, *0.0145*

Table S2. Human Mechanical Study: Parameters From Correlational Analysis Between Biomechanical Properties and GAG Content. Data are presented with linear mixed effects model slope [95% CI], and Pearson's R with associated p-value for each treatment group with E_y, E_d, and K_p. All p values less than 0.05 are highlighted in red.

Group	Ey (β [95% CI], R, *p*)	Ed (β [95% CI], R, *p*)	Kp (β [95% CI], R, *p*)
D0 CB N=29	-0.0049 [-0.0083, -0.0015], -0.4764, *0.0090*	-0.0381 [-0.0651, -0.0111], -0.4688, *0.0103*	3.902e-5 [9.533e-6, 6.581e-5], 0.4458, *0.0154*
D10 CB N=29	-0.0030 [-0.0110, 0.0049], -0.1541, *0.4248*	-0.0158 [-0.0545, 0.0224], -0.1632, *0.3977*	7.391e-6 [-1.796e-5, 3.341e-4], 0.1130, *0.4915*
D10 CB + CYT N=27	0.0012 [-0.0068, 0.0094], 0.08958, *0.6568*	0.0270 [-0.0211, 0.0766], 0.2222, *0.2652*	-6.016e-6 [-3.6444e-5, 1.989e-5], -0.1550, *0.4400*
D10 CB + CYT + DEX N=26	-0.0071 [-0.0117, -0.0023], -0.4008, *0.0425*	-0.0368 [-0.0743, 8.565e-4], -0.3803, *0.0553*	2.547e-5 [7.774e-6, 4.454e-5], 0.5078, *0.081*

Table S3: Human Mechanical Study: Parameters From Correlational Analysis Between Biomechanical Properties and Collagen Content. Data are presented with linear mixed effects model slope [95% CI], and Pearson's R with associated p-value for each treatment group with E_y, E_d, and K_p. All p values less than 0.05 are highlighted in red.

8.3 Experimental Lessons Learned

8.3.1 *Loading Optimization*

-The incudynes may not operate similarly and cause different strains for a given load amplitude input – make sure to vary tissue treatment groups among both incudynes.

-For human cartilage-bone explants, cartilage thickness will vary between plugs. Make sure to cut bone with a bone cutter so that plugs are as close in height as possible, so that the load and displacement readouts are accurate and apply to all plugs in a chamber.

8.3.2 *Biologic Effect of Loading with Dexamethasone and IGF-1*

-Make sure to continue to fill water trays with sterilized water in the incudynes, as they tend to become dry in a week's time and can cause excessive evaporation of media for tissue cultures in this environment.

-The incudyne is not sterile, and thus is extremely prone to microbe contamination. Use of 1.0 g/L of copper sulfate in the water bath, as well as frequent cleaning with 70% ethanol can help prevent against this.

8.3.3 *Mechanical Effect of Loading with Dexamethasone*

-The dynastat is particularly sensitive to any movement near it, so while stress-relaxation tests are occurring it is best to leave the room if possible.

-The micrometer may not be calibrated perfectly, so before measuring tissue thickness check where the "zero" point is for the system.

-Divide protease inhibitor pills into quarters to reduce waste when preparing PBS-PI, as 50 mL is too large an amount for the number of plugs tested in the dynastat per day.